# IMPROVED VIABILITY OF LACTOBACILLUS RHAMNOSUS GG DURING STORAGE AND SIMULATED GASTROINTESTINAL DIGESTION BY ENCAPSULATION

A Dissertation
Submitted to the Graduate Faculty
of the
North Dakota State University
of Agriculture and Applied Science

By

Xiaoxi Qi

In Partial Fulfillment of the Requirements
for the Degree of
DOCTOR OF PHILOSOPHY

Major Program:
Cereal Science

May 2021

Fargo, North Dakota

# North Dakota State University
Graduate School

**Title**

IMPROVED VIABILITY OF LACTOBACILLUS RHAMNOSUS GG DURING STORAGE AND SIMULATED GASTROINTESTINAL DIGESTION BY ENCAPSULATION

**By**

Xiaoxi Qi

The Supervisory Committee certifies that this ***disquisition*** complies with North Dakota State University's regulations and meets the accepted standards for the degree of

**DOCTOR OF PHILOSOPHY**

SUPERVISORY COMMITTEE:

Dr. Jiajia Rao
Chair

Dr. Jane Schuh

Dr. Manthey Frank

Dr. Senay Simsek

Approved:

June 17, 2021
Date

Richard Horsley
Department Chair

## ABSTRACT

Probiotics are "*live microorganisms which when administered in adequate amounts confer a health benefit on the host*". However, the current techniques are still struggling with delivering enough live probiotics into the designated site of action. This project aimed to improve the viability of the probiotic *Lactobacillus rhamnosus* GG (LGG) under adverse conditions by encapsulation. Properties of the formed microcapsules such as particle size, morphology, mechanical properties, and rheological properties were examined by corresponding methods and equipment, and the viability of LGG under storage and simulated gastrointestinal (GI) digestion was evaluated.

First, two modified alginate-based hydrogel bead systems were established on the basis of the reaction between sodium alginate (ALG) and $Ca^{2+}$ by 1) adding an additional layer of chitosan with three different molecular weights was formed on the surface of alginate particles; 2) partially substituting ALG with low methoxyl pectin (LMP) or κ-carrageenan (KC) to form a double-network since pectin and carrageenan can interact with $Ca^{2+}$ as well. In the first system, I found that the chitosan oligosaccharide (COS) improved the viability of LGG during storage by reinforcing the mechanical properties. However, no significant improvement on the viability of LGG during GI digestion was observed. In the second hydrogel bead systems, the ALG to LMP ratio of 8:2 in hydrogel provided the stronger inner structure and showed a better protective effect on the viability of LGG during GI digestion.

Furthermore, I studied the complex coacervates formed from sugar beet pectin (SBP) and sodium caseinate (SC) or pea protein isolates (PPI) to be as encapsulation wall material for improving the viability of LGG during digestion. The impact of protein type, protein to sugar beet pectin mixing ratio (5:1 or 2:1), as well as the finishing technology (freeze-drying and

spray-drying) on the viability of LGG were examined. Spray-dried samples, especially spray-dried PPI–SBP microcapsules, demonstrated superior performance against cell loss and maintained more than 7.5 Log CFU/g viable cells after simulated GI digestion. Overall, the project demonstrated a great potential for improving the viability of probiotics by encapsulation.

## ACKNOWLEDGMENTS

First of all, I want to thank my advisor, Dr. Jiajia Rao, for giving me the opportunity to pursue higher education in the United States and for her patience in instructing me in academia research. I appreciated her scientific training on me including experimental design, experiment organizing, scientific thinking and writing. Without her guidance, I may not have achieved such accomplishments. Dr Rao's passion on scientific study and her positive and uplifting attitude in life inspired me when I encountered some difficulties and setback in my study. I also want to express my gratitude to my committee members: Dr. Clifford Hall, Dr. Jane Schuh, Dr. Frank Manthey and Dr. Senay Simsek, for their great and valuable suggestions on my study. The completement of my project is inseparable from people's generous help. I want to thank Dr. Kalidas Shetty for letting me conduct part of my experiments in his lab. Also, I appreciate the help and cooperation from their lab members, Dr Dipayan Sarkar, Ramnarain Ramakrishna and Pradeepika Chintha. I feel grateful to Kristin Whitney from Dr. Simsek's lab for her assistance in my experiments and to Dr. Jae-Bom Ohm in USDA-ARS wheat quality lab for his assistance in the FTIR study. I am so lucky and grateful that I could work together with so many brilliant researchers.

Moreover, I want to express my deepest gratitude to my family and my friends for their warm, unconditional, and endless support. I would have not come so far without my parents' continuously encouragement and support. I sincerely appreciate everything they did to support my study in the United States. Also, I want to thank all my lab members for their help, and I learned a lot from them. Last, I would thank China Scholarship Council that provided me a scholarship for my doctoral study.

## TABLE OF CONTENTS

## LIST OF TABLES

## LIST OF FIGURES

## LIST OF APPENDIX TABLES

## INTRODUCTION

Probiotics are "*live microorganisms which when administered in adequate amounts confer a health benefit on the host*", as defined by the World Health Organization [1]. Many studies have claimed health benefits of ingesting probiotics as supplements or medical treatments [2-4]. In this project, *Lactobacillus rhamnosus* GG (LGG) was chosen as the research subject due to its well-established properties and being recognized as a probiotic organism for a long time. In the last few decades, probiotic containing foods, beverages, and supplements have drawn increasing attention due to people's awareness of the importance of gut health. However, since the viability of probiotics is impacted by many factors, such as adverse conditions during processing and storage, and especially, harsh environments in human GI system [5], current techniques are still struggling to deliver enough live probiotics into the designated site of action, which becomes the biggest limitation of the incorporation and application of probiotics in the food industry.

Encapsulation is a promising solution that has been widely used in protecting bioactive chemicals, oils, and probiotics against adverse environments by building a physical barrier. Common encapsulation techniques include gelation, spray drying, fluidized bed, and coacervation [6]. Hydrogel particles formed by extruding sodium alginate (ALG) drops into calcium chloride solution is the most extensively used method in protecting probiotics due to its simplicity, low cost, and good gelation properties. However, the drawback of this method is that the natural porous structure of the ALG gel makes it easier for acid to infuse into the cross-linked matrix and deactivate the encapsulated probiotics [7]. To overcome this limitation, some modifications have been proposed.

The first alternative method is to add another layer of biopolymer on the surface of ALG hydrogel particles through physical or chemical interactions. Considering the food safety, this modification is mostly done through electrostatic interaction to avoid usage of chemical reagent. Chitosan derived from various crustaceans and insects lends its positively charged amine groups (pKa~6.5) to enable the electrostatic interaction between chitosan and other anionic biopolymers, including ALG. Based on the molecular weight (MW), chitosan is divided into four types: chitosan oligosaccharide (COS), low–molecular–weight (LMW) chitosan, medium–molecular–weight (MMW) chitosan, and high–molecular–weight (HMW) chitosan. Since the surface charge of each type of chitosan carries varies, the physicochemical properties of chitosan coatings on alginate hydrogel particles can differ from each other. The previous studies were mostly conducted with either LMW or MMW chitosan [8-11]. The effects of molecular weight of chitosan on properties of the ALG hydrogel and the survivability of the encapsulated probiotics have not been fully elucidated. For this project, the additional layer of three kinds of chitosan with different molecular weight were studied.

Next, substituting ALG with other polysaccharides to form a double cross-linking network is another path to strengthen the ALG hydrogel. Low-methoxyl pectin (LMP) is an acidic-tolerant polysaccharide and able to form a strong gel at the presence of $Ca^{2+}$. It has been widely employed in encapsulation of probiotics to protect them against GI digestion and facilitate the release to colon [12, 13]. Singh et al. reported the mixtures of LMP and ALG were capable to improve the controlled delivery of the encapsulated bioactive compounds such as vitamin E, folic acid, and caffeine [14]. Meanwhile, κ-carrageenan, another kind of polysaccharide that is usually used as a stabilizer due to its high viscosity, is recognized as a potential high quality wall material in encapsulation since it not only forms gel with $Ca^{2+}$ but also implants

characteristic viscosity to the system [15]. Dafe et al. indicated that probiotics encapsulated in KC–carboxymethyl cellulose (CMC) hydrogel particles presented a better acid tolerance compared to those encapsulated in CMC alone [16]. The gel strength and other physicochemical properties are usually affected by several factors: 1) the polysaccharide concentration, 2) the ratio between two types of polymer, and 3) the type and concentration of the cross-linking agent etc. [17]. Hence, the properties of the hydrogel and the viability of the encapsulated probiotics were evaluated in this project in terms of the wall material source and the mixing ratios between ALG and LMP or KC.

Additionally, complex coacervation, an associative phase separation phenomenon originated from electrostatic attraction between two oppositely charged biopolymers, is well-studied as a probiotics delivery system. It is valued for its relatively high encapsulation yield and biocompatibility, as well as the good acidic tolerance [18]. The complex coacervates containing probiotics are typically formed by adjusting the pH of the mixed probiotics and protein–polysaccharide solution to a certain pH to induce phase separation between the biopolymers and solution. As previously reported, the physical properties of complex coacervates are dependent on several factors, such as wall material source and compositions, the mass ratio between protein and polysaccharide, and drying methods used in the finish process [19, 20]. These factors also determine the functional performance of complex coacervates as a microencapsulation wall material for protecting the viability of probiotics under harsh conditions. Various proteins are used as wall material in complex coacervation. These are mostly animal-based, such as gelatin, whey protein, and sodium caseinate (SC) [21-23]. SC stands out for having hydrophobic characteristic and better thermal stability [24]. On the other hand, market demand of incorporating plant-based protein in food systems is gaining popularity [25, 26], it has drawn significant interest in constructing a complex coacervates delivery system by using pea protein as wall material.

Therefore, complex coacervates systems formed between SC or pea protein isolate (PPI) and sugar beet pectin (SBP) with varied protein-SBP ratios were established in this project to evaluate their capacity to improve the viability of the encapsulated LGG during simulated GI digestion.

While forming the complex coacervates encapsulated probiotics, drying is the last and critical step to develop commercially available probiotic functional foods. In general, spray-drying and freeze-drying are the two most common methods for drying microcapsules of probiotics, with which different microstructure is formed [27]. Few studies have been done to evaluate the effects caused by different drying methods on the properties of microcapsules and the viability and functionality of probiotics [28]. Hence, both spray- and freeze-drying were applied on the wet complex coacervates to fill the knowledge gaps.

# CHAPTER 1. LITERATURE REVIEW

## Probiotics in Food

### Definition of Probiotics and Their Health Benefits

Human beings started to use natural existing bacteria in fermentation to preserve perishable food for thousands of years, which can be dated back to as early as 10,000 B.C., even before they understood the science behind it [29, 30]. After the word was first used, it took several decades to come a consensus of the definition of probiotics: "*live microorganisms which when administered in adequate amounts confer a health benefit on the host*" in 2001 [1].

After years of research, increasing evidence has been attributed the beneficial effects include improving the intestinal health, boosting the immune status, reducing the serum cholesterol, and preventing cancer to probiotics. Many researchers have proposed that these effects are results from the various activities of the probiotics: 1) anti-pathogenic activity [2, 31], 2) anti-diabetic activity [3], 3) anti-inflammatory activity [32], 4) anti-allergic activity [33, 34] and 5) potential anti-cancer activity [4]. It is worth pointing out that the beneficial effects of a certain strain are affected by various mechanisms and cannot be generalized and attributed to other strains [35].

The mechanism of the healthy benefits of probiotics are not completely elucidated yet. Subjected to numerous studies, hypotheses range from the production of bacteriocin and short chain fatty acid, nutrient competition, production of acid and lowering of gut pH especially for the lactic acid bacteria to stimulation of mucosal barrier function and immunomodulating activity [36]. For example, one mechanism proposed is that orally ingested probiotics are able to attach to the intestinal mucosa to prevent the epithelial attachment of pathogenic bacteria. Mack et al. claimed that the probiotic *L. (Lactobacillus) plantarum* 299v and *Lactobacillus rhamnosus* GG

(LGG) quantitatively declined the adherence of two pathogenic *Escherichia coli* to HT-29 intestinal epithelial cells, but no influence observed to the non-intestinal HEp-2 cells. Their hypothesis was that the inhibition of pathogenic microorganisms of probiotics was achieved by increasing the expression of intestinal mucins (MUC2 and MUC3) [37]. Another proposed mechanism of action is their immunomodulating effects. Perdigón et al. demonstrated the possible mechanism that several strains of lactobacilli could be involved in the interaction at the intestinal level [38]. They found that *L. acidophilus* and *L. rhamnosus* activated the gut mucosal reaction and induced an immune response after ingested orally. Researchers found that probiotic treatment of LGG was able to facilitate and modify the activity of other bacteria and modulate the gut microbiota on healthy individuals [39].

**Strains Used as Probiotics**

After decades of development, numerous studies have been done on probiotics and various strains have been identified as probiotic. In 1910s, Elie Metchnikoff , who is recognized as the father of probiotics, firstly proposed that the bacteria 'Bulgarian bacillus' in fermented milk have beneficial effects on human beings [40]. The strain as recognized as 'Bulgarian bacillus' by Metchnikoff was later proved to be a member of lactobacilli and to this day, lactobacilli still remain the most commonly used probiotics, including *L. rhamnosus*, *L. reuteri*, *L. casei* (first column in **Table 1-1**). Apart from lactobacilli, the other most commonly used genera is *Bifidobacterium*. Representative strains including *B. (Bifidobacterium) adolescentis, B. animalis, B bifidum* etc. [41-43]. Moreover, strains from other species, such as *Streptococci* spp., *Enterococcus* spp., *Bacillus* spp., and *Saccharomyces* spp., are identified as probiotics as well [36]. Although most of the current known probiotics are studied based on their beneficial effects on human beings, some species have been proven beneficial on animals and used as animal feed

additives. Bernardeau and Vernoux stated that yeast, especially *Saccharomyces cerevisiae* is important in ruminants' nutrition system, while *Bacillus* spp., *Enterococcus* spp. and *Lactobacillus* spp. are more effective on pigs and poultry [44]. **Table 1-1** lists the current commonly used probiotics strains in both human and animals.

**Table 1-1**. Microorganisms used as probiotic [45, 46].

| Lactobacillus species | Bifidobacterium species | Other lactic acid bacteria | Non-lactic acid bacteria |
|---|---|---|---|
| *L. acidophilus* | *B. adolescentis* | *Enterococcus faecalis* | *Bacillus cereus (toyoi)*[1,2] |
| *L. bulgaricus* | *B. animalis* | *Enterococcus faecium* | *Escherichia coli (Nissle 1917)*[2] |
| *L. casei* | *B. bifidum* | *Lactococcus lactis* | *Propionibacterium freudenreichii*[1,2] |
| *L. crispatus* | *B. breve* | *Leuconostoc mesenteroides* | *Saccharomyces boulardii*[2] |
| *L. fermentum* | *B. infantis* | *Pediococcus acidilactici* | *Saccharomyces cerevisiae*[2] |
| *L. gallinarum*[1] | *B. lactis* | *Sporolactobacillus inulinus*[1] | |
| *L. gasseri* | *B. longum* | *Streptococcus thermophilus* | |
| *L. johnsonii* | | | |
| *L. lactis* | | | |
| *L. plantarum* | | | |
| *L. rhamnosus* | | | |
| *L. reuteri* | | | |
| *L. salivarius* | | | |

[1] Mainly used on animals.
[2] Mainly used as pharmaceutical treatments.

In recent years, to further widen the range of probiotics, some researchers focus on isolating candidate probiotics from certain sites of healthy human as a novel "next-generation" probiotic for the usage in pharmaceuticals [47-49]. However, to be eligible and qualified as probiotic, a special strain needs to satisfy some important criteria. First of all, the genus, species and strain level need to be accurately identified. Moreover, the organism should be 1) non-pathogenic, non-toxic and considered as GRAS (generally recognized as safe) [50]; 2) able to

survive through the GI tract [51]; 3) able to successfully adhere to the intestinal epithelium and propagate [52]; and 4) have validated beneficial effects on the host [53]. Furthermore, considering the application in food and pharmaceutical industry, the organism should possess good tolerance to the stresses during manufacturing, processing, distribution and storage [51]. The effects caused by processing, distribution, and storage are discussed in next section.

**Impact of Processing Condition and Simulated Human Gastrointestinal Digestion on the Viability of Probiotics**

As stated in the definition, the potential health benefits of probiotics can only be achieved while sufficient number of live cells reach and survive in the gastrointestinal (GI) tract. The common consensus is that the viable cells should be no less than $10^6$ per dose/day for supplement and $10^8$ for therapeutic use [54]. However, de Vos et al. claimed that in traditional dairy foods, the probiotics presented poor viability [55]. The main challenge of adding probiotics into food system is their huge loss of viability during processing, storage and human digestion.

In general, the viability and functionality of probiotics change while cultivated in different food systems. Gitton et al. demonstrated that the *L. lactis* presented different proteomic patterns in milk, milk microfiltrate, or broth [56]. As to the products in liquid form, the loss of viability is normally more problematic during storage than that of powder production. This might be caused by the acidified condition and the existence of antimicrobial component such as organic acids in the system [57, 58]. For instance, the viability loss of *L. acidophilus* and *B. bifidum* in five different commercial yogurts during refrigerated storage was evaluated over a five-week period and counts of live cells of both strains were decreased to an unacceptable level [59]. Huge viability loss was also observed in other food products such as cheddar cheese [60] and fruit juices [61].

Additionally, the extremely low pH conditions and digestive enzymes in the GI system cause tremendous stress on the survival of the probiotics [7, 62]. To assure that enough probiotics is ingested and able to pass through the GI tract and colonize in the intestine, various techniques have been trialed. One research area is to develop molecular tools which allow the application of genetics transformation and selection on bacteria survival. Berger et al. conducted the selection on a heat-shock resistant mutant of bacteria to improve survival of *B. longum* [63]. Moreover, addition of protective agent into the probiotics culture system is another path to improve viability of probiotics during food processing. Corcoran et al. remarkably enhanced the viability of LGG in simulated stomach digestion by adding glucose into the culture [64]. This method was sometimes combined with encapsulation technique to improve probiotics' survival rate in food matrix and in human GI tract [65], which is one of the techniques that drew significant attention in these years. Three widely reported encapsulation technologies used to improve viability of probiotics in literatures are reviewed in next section.

## Current Encapsulation Methods to Improve Probiotics Viability

### Hydrogel Particles Delivery System

The hydrogel or hydrogel particles are usually obtained by the reaction between biopolymer solution and another gelling agent solution such as ions or enzymes. According to this concept, the process can be achieved by either extruding the probiotic live cell containing biopolymer mixture suspension into a gelling agent solution to form hydrogel particles or reversely, adding the gelling agent to the probiotics-biopolymer mixture solution to form hydrogel. The former method is commonly called simple extrusion method and carried out through a syringe needle. The most commonly used approaches to form hydrogel particles are alginate/pectin solution and calcium ions, chitosan solution and a tripolyphosphate solution or

the heat-set/cold-set gelation. The formation of hydrogel particles by using extrusion method is the most widely studied method in laboratory since this method is economical and simple to operate (**Fig. 1-1**).

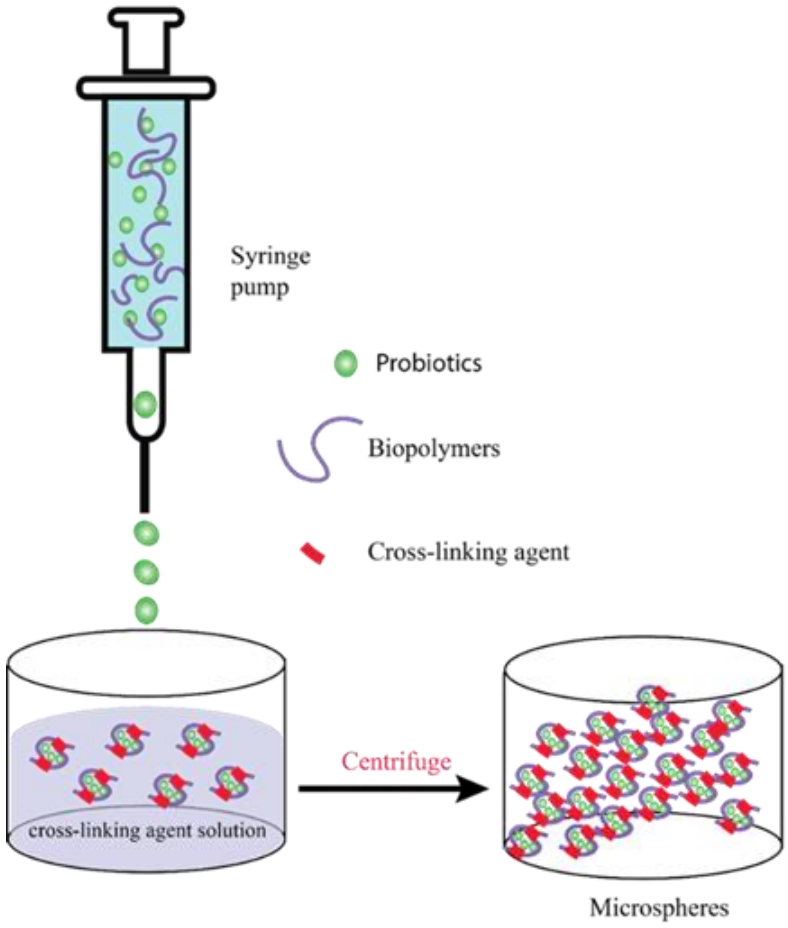


**Fig. 1-1.** Schematic representation of extruded hydrogel particles delivery system for encapsulation of probiotics.

This method was first used in 1980s when the researchers focused on lactic acid bacteria as the main category of probiotics. Steenson et al. employed the alginate-calcium system to immobilize the bacteria during fermentation and they indicated that this system would favor the probiotics in certain dairy fermentations [66]. Similar system and results were observed in other studies as well [67, 68]. Alginate (ALG) is a linear polysaccharide mainly obtained from brown

algae and some bacterial sources, composed of 1-4 linked β-(D)-glucuronic and α-(L)-mannuronic acids [69]. Attributed to its GRAS status, good gelling property, low cost and nontoxicity, alginate can be used alone [70] or companied with other polysaccharide such as starch [71] to improve the survivability and control the release of probiotics. Because of the low tolerance to the harsh digestion conditions of ALG [72], many double-layer reinforced ALG hydrogel particles by means of the electrostatic interaction are developed [73, 74]. Additionally, the interaction between ALG and chitosan are widely studied due to the unique cationic property of chitosan under acidic condition among polysaccharides [73, 75].

While ALG is widely used in research, many other biopolymers have been discovered to be effective to form hydrogel, such as carrageenan and pectin. Pectin is a structural biopolymer existing in land-based plants which plays an important role in reinforcing the cell wall strength. Based on the degree of the esterification (DE) of galacturonic acid residues on the backbone, pectin can be classified into low methoxyl pectin (< 50%, LMP) and high methoxyl pectin (>50%, HMP). The naturally existed pectin is normally HMP and the DE varies depending on the extract method and conditions. The gelling mechanisms of LMP and HMP are different. LMP gels through ionotropic gelation and forms the salt bridge with $Ca^{2+}$ cations which makes it a useful biopolymer wall material in encapsulation, while the HMP gels at high solid concentrations (e.g. sugars) and low pH. Typically, pectin stays intact in the stomach and small intestine, but collapses in the colon. The degradation rate of pectin can be changed by chemical modification which allows pectin to deliver probiotics and drugs to the target area in GI tract. Ribeiro et al. encapsulated *L. acidophilus* LA-5 in hydrogel particles formed by pectin and $CaCl_2$ and then submersed the particles into whey protein concentrate to form complex coacervation, which will be discussed in next section [76].

Apart from polysaccharides, some proteins also have the capacity to encapsulate the probiotic bacteria. Milk proteins, such as casein and whey protein have been used in a water-insoluble matrix to protect bacteria through the GI tract in a few studies, since non-milk based materials are less desirable or not allowed to be added in dairy products. Heidebach et al. formed cold set hydrogel from skimmed milk by first using rennet to cause the casein micelle aggregation, modifying it into microcapsules through emulsification, and then triggering the gelation by increasing the temperature. This method can improve the viability of *B. lactis* from 0.01% to around 10% in the low pH solution [77]. Similarly, Burgain et al. used casein and whey protein to encapsulate LGG and studied the influence of casein to whey protein ratio on the survival of LGG during digestion and successfully determined the optimal formula for improved survival rate of the LGG bacteria [78].

Recently, the trend to incorporate plant-based proteins such as soybean protein, lentil protein and pea protein into food system has become prominent due to the increasing popularity, sustainability and the healthier nature of plant-based protein [79]. Maltais et al. investigated the cold-set gelation of soy protein and calcium cations system and indicated that this cation-induced gelation shared the same mechanism and functional properties with whey protein, e.g. electrostatic interaction [80].

**Complex Coacervation Delivery System**

Another promising encapsulation technique is complex coacervation which refers to a phase separation phenomenon and gel-like structure formation driven by electrostatic interaction between two oppositely charged biopolymers, which is usually done by lowering the pH of the biopolymer mixture (**Fig. 1-2**), including various proteins and polysaccharides [81]. This process

can be influenced by several factors such as pH, polymer concentration, ionic strength, temperature, molecular weight and ratio between biopolymers [82].

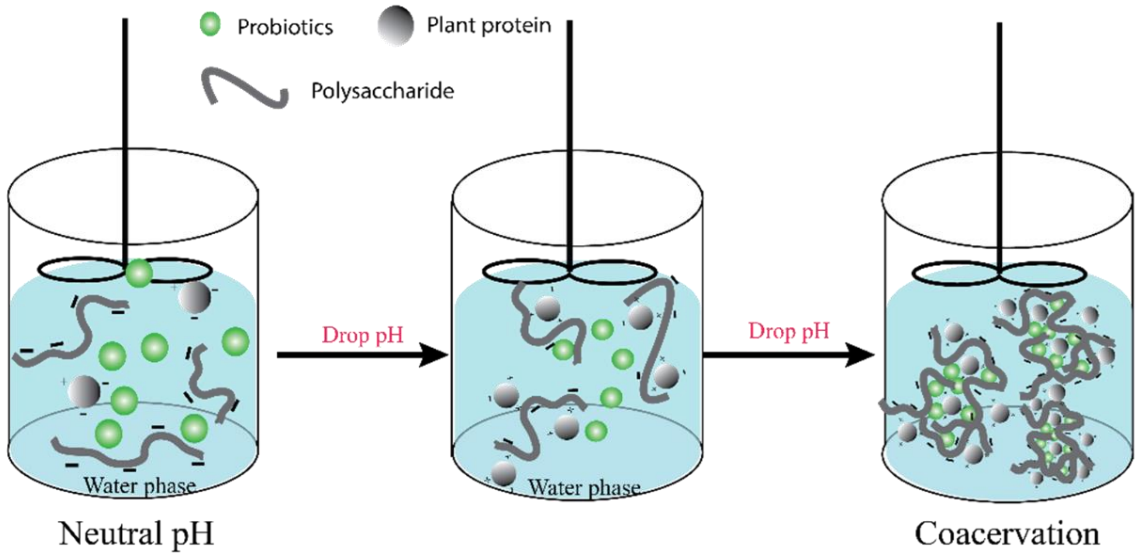


**Fig. 1-2.** Schematic representation of complex coacervation for encapsulation of probiotics.

In the past several decades, protein-polysaccharide complex coacervation has drawn increasing attention since there is no organic solvent or harsh react conditions needed, which fulfills the requirements of application in food industry such as biocompatibility, nontoxicity and biodegradability. Moreover, it possesses properties like good acidity resistance and high encapsulation yield [18]. Particularly, complex coacervation is practical in the encapsulation of probiotic bacteria since the structure collapses in the large intestine due to the neutral pH condition, and then the probiotics are released to exert health benefits [83]. Many researchers have built complex coacervation delivery systems to encapsulate probiotics by triggering the strong electrostatic attraction between protein and polysaccharide in certain condition and applied into food products [22, 84]. The commonly used proteins are gelatin, albumin, beta-lactoglobulin, whey protein, and some plant proteins, and as to polysaccharides, pectin, alginates, gum Arabic,

carrageenan, xanthan gum, and carboxymethyl cellulose are mostly used [82]. For example, Ribeiro et al. indicated that complex coacervation composed of whey protein and ionic gelled pectin-$Ca^{2+}$ microcapsules provided better protection to *L. acidophilus* LA-5 than the simple ionic gelation method [76]. Another example is encapsulated *L. acidophilus* in the complex coacervates formed from casein and pectin improved the viability of probiotics during storage and extend the shelf-life in yoghurt, as reported by Shoji et al. [85]. Likewise, Oliveira et al. also used casein and pectin to form coacervates, which were then subject to spray-drying to encapsulate probiotics. This process resulted in a huge increase in the viability of *L. acidophilus* and *B. lactis* at low pH conditions [22]. Errate et al. indicated that the co-encapsulation of tuna oil and *L. casei* in a whey protein and gum Arabic coacervate matrix significantly improved the viability of probiotics, as well as the oxidative stability of tuna oil [86].

As mentioned in last section, using plant source proteins as wall material is an emerging trend in food industry for certain concerns, also to fulfill the demand of vegetarians and to avoid the safety risk that may be caused by prion in beef gelatins. For instance, Mao et al. studied the effects of the soy protein isolate (SPI) and ι-carrageenan (IC) complex coacervates formation and composition on the viability of *B. longum* in terms of different pH conditions and protein to polysaccharides ratio [20]. They indicated that complex coacervates with a SPI: IC ratio of 10:1 at pH 3 were more capable of protecting the probiotics against the adverse environments during storage, pasteurization and *in vitro* digestion. However, very little information on application of complex coacervation through plant-based protein on probiotics can be found in literature reviews.

**Emulsion Based Delivery System**

Emulsion based deliver system is another well-studied method to encapsulate microorganisms or other bioactive compounds for that it is easy to prepare in research laboratories, and usually obtain a high initial encapsulation yield. However, the application of emulsion in food industry is limited by the difficulties to prepare and the high tendency to breakdown during storage [87]. Emulsion is a fluid system which consists of at least two immiscible liquids (mostly oil and water) among which one is dispersed as small spherical droplets in the other at the presence of emulsifiers. Basic emulsions composed of two liquid phases can be classified to oil-in-water (O/W) emulsion in which oil is distributed in continuous water phase, and on the contrary, water-in-oil (W/O) emulsion, based on the spatial distribution of the oil and water phases [87]. In terms of probiotic application, bacteria are dispersed and encapsulated in the core material at the presence of emulsifiers depending on the composition of the system [88]. Papagianni and Anastasiadou indicated that food grade O/W emulsion system stabilized by xanthan gum as stabilizer ensured the delivery of large populations of live *Pediococcus acidilactici* cells to the targeted area after the simulated GI digestion [89]. In many cases, some protective agents, usually polysaccharides, are added to the emulsion to further protect the probiotics. For instance, Rao et al. formed an emulsion from white light palm oil and cellulose acetate phthalate which improved the survival numbers of *B. pseudolongum* after the simulated gastric environment [90]. Favaro-Trindade and Grosso[91] formed an O/W emulsion with the addition of cellulose acetate phthalate and spray-dried it to microencapsulate the *L. acidophilus* and *B. lactis* (Bb-12) and the encapsulated probiotics showed good tolerance to acid and bile solutions.

Beyond the basic emulsions, water-in-oil-in-water (W/O/W) emulsion has been studied to further improve the stability of the microcapsules and the viability of the encapsulated bacteria. The W/O/W emulsion is a double emulsion delivery system: an inner aqueous phase is firstly dispersed in an oil phase by homogenization to form W/O emulsion, and the W/O emulsion formed is then dispersed in an aqueous phase solution to form W/O/W emulsion, and the probiotics are mostly encapsulated in the inner aqueous phase. Usually this method is followed by a drying process for the ease of the sequential usage. Shima et al. designed several W/O/W emulsion systems to compare the relative viability of *L. acidophilus* in simulated gastric digestion and they indicated that larger droplets size and the higher inner-phase volume ratio led to the relative higher viability of the *L. acidophilus* [92]. Afterwards, Shima et al. studied the protection of the W/O/W emulsion system on the viability of *L. acidophilus* in a simulated intestinal juice and a significantly improved cell viability was also obtained [93].

**Emerging Encapsulation Technology**

As probiotics and functional foods have drawn more and more attention in last few decades, researchers are adapting creative emerging encapsulation technologies to aid the survival of probiotics. Overall, it can be divided into two directions, one is the combination of different traditional methods instead of focusing on single method. For example, Frakolaki et al. combined a W/O/W double emulsion and extrusion methods to encapsulate *B. lactis* (BB-12), and results indicated that this method was able to maintain the numbers of viable BB-12 cells on a high level after storage at 4 °C and -18 °C for 4 weeks and after simulated digestion as well [94] . The second direction is to discover new encapsulation technologies or employ cross-disciplinary technologies such as electrospinning [95, 96] and electrospraying [97, 98]. Though some of these novel

technologies still need optimization and verification for further application in food industry, they have shed light on the future directions for other researchers.

**Finishing Technology**

To produce convenient and applicable probiotic products for food, pharmaceutical and feed industries, encapsulated probiotics matrixes are generally dried through different technologies, such as freeze-drying and spray-drying. However, most of the drying methods expose the extreme environmental stresses to the probiotics and cause adverse effects on the viability and activity of probiotics. In general, the damages to the probiotics caused by drying process are dependent on a number of factors like strain variety, operating parameters and the presence of protectants or not. For instance, Fonseca et al. indicated that probiotics with higher surface area of the cell were more prone to the membrane damage caused by the formation of extra-cellular ice crystal during freezing [99].

Freeze-drying has been used as a finishing technology in most of the encapsulation systems such as hydrogel, emulsion and coacervates because of its low operating temperature and convenient operating conditions. However, freeze-drying processing has been found to cause viability loss of probiotics. For example, Xu et al. freeze-dried the encapsulated probiotics in pea protein isolate (PPI)-ALG hydrogel matrix and observed a 1.42 log CFU reduction of viable cells after 48h post freeze-drying [100]. Similarly, Quintana et al. conducted a 48h post freeze-drying to the probiotics encapsulated in layer-by-layer biopolymer wall materials, and probiotics could not survive after the freeze-drying process [101]. From these studies it is evident that even under the low drying temperature, not all strains can survive the freeze-drying process. Some of them undergo a severe viability loss since large quantity of intracellular loss alters the cell structure and lead to death [28]. Additionally, some research suggested that protectants such as bulking agent

or sugar could greatly protect the viability of probiotics during freeze-drying. For instance, Sohail et al. observed an improved survivability of probiotics after freeze-drying by applying maltodextrin in ALG hydrogel matrix, but in a strain dependent manner [102]. Hence, various protectants have been studied and applied along with freeze-drying process. Zayed and Roos reported that *L. salivarius* freeze-dried in media composed of trehalose, sucrose and skim milk remained the highest viability (83-85%) after freeze-drying, and showed enhanced stability during storage compared to control samples [103].

Despite of the involved high temperature as a potential drawback, spray-drying is considered as a continuous, low cost, and high yield desiccation method compared to freeze-drying [104]. Numerous research studies have shown that spray-drying is a promising way to protect the probiotic bacteria against the harsh conditions that they would face during processing, storage and digestion [105, 106]. Sohail et al. incorporated the ALG hydrogel in a maltodextrin solid matrix to encapsulate two lactobacilli strains by spray- and freeze-drying. Their work indicated that spray-dried probiotics possessed improved subsequent probiotic survivability than those that were freeze-dried[102]. In addition, the survival rate of probiotics during spray-drying, strongly dependent on the inlet air temperature, outlet air temperature and drying medium[107]. Different inlet air temperatures used in spray-drying were investigated and turned out highly correlated to the viability of encapsulated *L. acidophilus* La-05 [108]. Outlet air temperature also plays a major role on affecting the survival of probiotics during spray-drying. Decrease of viable cells and encapsulation efficiency with increasing outlet air temperature was reported by a number of studies on different probiotics strains [109, 110]. Consequently, enhanced viability can be fulfilled by reducing the inlet and/or outlet temperature during spray-drying while ensuring the powder quality (e.g., the moisture content of ~3.5% is ideal for shelf-stable requirement) [103].

Besides the previously mentioned commonly used drying methods, a novel technique called spray-freeze-drying (SFD) method has been developed in recent years to obtain the uniform particle size and a reduced drying time at relatively less stressful conditions for probiotics. SFD includes three steps: (1) atomize the liquid or solution into droplets, (2) solidify the droplets by contacting with a cold fluid, and (3) sublime the solidified droplets at low temperature and pressure [111]. Researchers indicated that probiotic microcapsule powder dried by SFD showed good encapsulation efficiency, physicochemical properties and stability during storage [112, 113]. Apart from the methods mentioned above, some other techniques such as fluidized bed drying [114], vacuum drying [115] are also employed in drying the probiotics containing cultures and products as well, even though they are not used as much as freeze-drying and spray-drying.

**Technologies for Evaluating the Physicochemical Properties of Encapsulated Bacteria**

**Particle Size**

In the encapsulation system, some basic physical properties, such as particle size and shape, can not only provide a direct impression of probiotic microcapsules but also elucidate their functionalities to some extent. In terms of characterization of particle size of probiotic products, various methods have been developed to evaluate their particle size. Zaeim et al. took pictures of the hydrogel particles formed from an electrospraying process by a low-magnification stereomicroscope and binarized the pictures with ImageJ software to evaluate the particle size of the microcapsules. The particle size in their study had a range of diameter from 200 to 600 μm [116]. Similarly, Atia analyzed the size of hydrogel particles with a camera assisted with ImageJ software while the samples had a much larger diameter which was around 3 mm [117]. This method is useful for particles in a spherical shape since it provides the uniformity and the diameter of the

samples at the same time. As to determine the particle size of dried powder, the laser diffraction technique has been widely applied in many studies [24, 118]. It can measure the intensity of the light scattered by the dispersed sample and give the particle size and particle distribution processed by the built-in software. This kind of equipment is versatile and especially useful for the non-uniform samples since it usually has a wide range of detectable particle size range.

**Morphology and Microstructures**

The morphological properties and microstructure of the probiotic encapsulated samples have been extensively observed by using some microscopy techniques, such as scanning electron microscopy (SEM), transmission electron microscopy (TEM), atomic force microscopy (AFM), and confocal laser scanning microscopy (CLSM). SEM is a method to provide images by scanning the surface of the sample, and it requires the samples in a dry state and fixed [119]. To obtain the inner structure of the samples rather than the surface morphology, sometimes a destructive process is required [120]. For some high moisture products, cryo-SEM is applied to characterize the morphological properties of samples to avoid the distortions caused by fixation and drying process. The biggest difference between cryo-SEM and SEM is that the hydrated sample is fixed in a cryogenic chamber, which is usually achieved by liquid nitrogen. Then the cryogenically fixed sample is fractured and sputter-coated to acquire the images same as SEM. This particular trait makes it a great method to truly restore the microstructure of highly hydrated samples, such as most kinds of the hydrogels [121-123]. Similar to SEM, TEM also applies a beam of electrons to the samples and the difference is that TEM creates images based on the transmitted electrons which are passing through the sample and consequently provides valuable information on the inner structure. Allan-Wojtas et al. observed the microstructure of probiotic containing ALG hydrogel particles under SEM, cryo-SEM and TEM, respectively [124]. They indicated that

cryo-SEM and TEM provides more accurate and detailed microstructure of the sample compared to the conventional SEM.

Another kind of scanning microscopy technology, which is also a kind of fluorescence microscopy, CLSM is also widely used for imaging biological samples that containing fluorescence molecules. Different from a conventional microscope under which the light travels and penetrates the sample as far as it can, CLSM only focuses on a smaller beam of light at a narrow depth level at one time by conjugating with a plane in front of the detector to eliminate the distraction from the out-of-focus signal. Therefore, CLSM is capable of constructing a 3D image from a thicker specimen by processing the serial images taken from continuous sections [125]. Also, CLSM can detect several compounds at one time by using different fluorescence labels and filters, therefore, it is broadly applied to observe the distribution of the biopolymers used in encapsulation [10, 101, 117] and the identification from live to dead bacterial cells in the sample [62, 126]. Furthermore, AFM is a type of probe scanning method. Basically, it receives the force signal from the contact between the probe and the sample and provides the information of the mechanical properties such as stiffness of the sample and image of a sample surface. By analyzing the AFM results, Yao et al. suggested that the addition of magnesium oxide nanoparticles protected the probiotics containing ALG hydrogel from cracking during freeze-drying [127].

**Rheological Properties**

The rheological or textural properties of the probiotics delivery system, such as the hardness, rupture force of the hydrogel, the viscoelasticity of the coacervates and the kinetics of gelation, are usually tested as indicators of the structure and mechanical stability of the samples. The commonly used technique to characterize the textural properties of probiotics containing

particles is the texture analyzer which can apply compressing force to the sample to a certain deformation through a probe and the force applied is recorded. For example, the hardness and rupture force represent the mechanical strength of the hydrogel particles and are related to the viability of the encapsulated probiotics on some level. Hence, they have been used as indicators to optimize the hydrogel formulation [128, 129]. In terms of rheological properties of probiotics delivery system, the storage modulus (G') and loss modulus (G") which respectively represent the elastic and viscous property of a viscoelastic material are normally measured. In a measurement, material is subjected to a sinusoidal stress or strain and the changes are recorded and reported as a function of time, temperature, strain or stress amplitude and frequency. The obtained results can provide structural property information such as concentration, crosslinking density of polymers or shape, interface properties of multiphase fluids [130]. Therefore, this method is widely used to identify the optimal pH range for the formation of hydrogel [131], to determine the least gel point [128], and to compare the crosslinking strength between hydrogels and coacervates [129, 132].

**Other Properties**

Since most of the encapsulation systems involve more than one material or polymer, the Fourier-transform infrared spectroscopy (FTIR) is popularly employed to detect the presence of the functional groups and the changes on the molecular structure level of the sample. It uses infrared light to scan test samples and measures the light the sample absorbs at each wavelength and then processes the raw data to the desired results. Since FTIR can conduct the scan over a wide range, it can detect a wide range of functional groups rapidly without destruction to the samples. The shift of peaks at certain wavelength, the appearance and disappearance of some

peaks in the FTIR spectra are recognized as a proof of the interaction between different materials in a system [117, 133-135].

Furthermore, differential scanning calorimetry (DSC) is widely used to analyze the thermal characteristics like melting temperature, enthalpy values, glass transition temperature, and crystallization temperature which may provide important information about the thermal stability, progress of chemical reactions, and mechanical behavior. It is a controlled temperature program, and the thermal behavior of the sample is recorded while exposing to the heat. Ashwar et al. indicated that the probiotic containing microcapsules formed from rice resistant starch presented better thermal properties than those from native starch by analyzing the DSC results [136]. For products that need to undergo heat treatment during processing or storage, this technique is useful to evaluate the possible changes caused by heat and helpful to predict the influence of the heat on the viability of the encapsulated probiotics.

## Methodologies for Testing the Viability of Encapsulated Bacteria under Harsh Conditions

### Methods to Evaluate Viable Bacterial Cells

The ultimate goal of developing a delivery system for encapsulating probiotics is to ensure enough numbers of viable cells are ingested and released in the target area. As such, it is necessary to determine the viability of encapsulated probiotics to represent whether an encapsulation system is efficient during every stage of processing, storage and under harsh conditions, such as heat, low pH condition and particularly the GI digestion [120, 137, 138]. The most commonly used and conventional method to evaluate the viability of probiotics in a laboratory is the plate count method. This method involves culturing the bacteria on a nutrient medium at the desirable environment and then counting the total colonies formed on a plate when the colonies become visible to the naked eye. The bacterial containing samples usually need serial dilution to

obtain the average counts between 30 and 300, which is considered as effective results [139]. After counting, the total numbers of the targeted bacteria per gram or milliliter are calculated by the level of serial dilution and volume of the sample used.

However, it is a time-consuming method and also employs a large amount of media as well as laboratory spaces. Therefore, some alternative methods, such as mechanical spreading the sample on the preformed agar plates [140], application of coated membranes to directly immobilize the bacteria followed by standard plate culture [141] have been developed. In recent years, some real-time viable cell counting methods like using "vital" stains to stain and count "live" cells under fluorescing microscope, detecting ATP of live cells that trapped in special membranes [142] have also been developed and used in the food industry for quality control. Nakajima et al. established a rapid enumeration method that can count the total and active bacteria in less than an hour through a fluorescent staining method by using two stains: 6-carboxyfluorescein diacetate and 4,6-diamidino-2-phenylindole [143].

**Methodologies for Measuring the Viability of Probiotics during Digestion**

**in vitro *approach***

Subject to the large sample quantity required and the long-term trial needed for the *in vivo* assay, the initial evaluation the performance of microencapsulated probiotics is mostly *in vitro*. In order to develop an *in vitro* digestion model to predict the *in vivo* survival rate of microencapsulated probiotics, various simulated dissolution media had been developed since 1998, which mostly containing salts, acids and digestive enzymes [144, 145]. Based on the United States Pharmacopeia recipe, solutions composed of HCl and salts with pH 1.0–2.0 are most commonly used conditions to simulate gastric fluids (SGF) [146, 147]. An acidified growth medium is also a choice of some other studies [148]. Meanwhile, a variety of simulated intestinal fluids

(SIF) have been established by several researchers in these years [149, 150]. As indicated by Bhagat, human intestinal fluid generally contains bile salts, monoglycerides, phospholipids, free fatty acids and cholesterol [151]. To better mimic *in vivo* digestion, some authors have collected digested samples from simulated gastric phase and transferred them to simulated intestinal conditions [152, 153]. On the other hand, some studies conducted the two digestion parts separately [90, 154]. At chosen time points, digesta were collected and recovered by centrifugation or screening and the viable cells are counted by serial dilution and plate count method in most of the studies[153, 155, 156]. Overall, it is difficult to compare the results from different studies since no single model has been standardized for the evaluation of bacterial viability during *in vitro* digestion.

**in vivo *approach***

To strengthen the findings from *in vitro* experiments and provide more accurate information, some researchers conducted *in vivo* test as well. Though rodents are by far the mostly commonly used laboratory animals, some studies also investigated the effects of probiotics on larger mammals. According to Kararli's research, there is no animal model that can provide ideal characteristics to mimic the human GI physiology. However, he suggested that 'dogs and humans have similar stomach morphology and emptying characteristics' whilst 'pig and human colon morphology appears similar' [157]. To obtain the counts of the encapsulated probiotics from *in vivo* trials, euthanizing animals in different stages of the digestion process give precise results of the distribution and release profile of the probiotics. Alternatively, using molecular biology techniques, such as polymerized chain reaction (PCR) and fluorescence in-situ hybridization (FISH), to detect specific probiotic strains in the test animals without killing the animals is also feasible [158, 159].

## Future Trend of Probiotics

Incorporation of probiotics into a wide range of foods is still challengeable due to the stressful processing conditions such as high temperature (UHT), high shear (extrusion) causing an unacceptable viability loss of the encapsulated probiotics. Usually a dry powder product is preferred because of the low cost on handling, transportation, and less storage space required. This asks for even higher demands on the efficacy of the microcapsules on not only maintaining a high viability also a good cultivability after rehydration.

First, screening of new probiotic strains or mutants with improved biological properties and probiotic features is a direct approach to overcome the long-existing limitations of the application of probiotics. Guglielmotti et al. studied the probiotic potential of the phage resistant mutants of *L. delbrueckii* and demonstrated that these mutants possessed adequate technological and biological properties and probiotic characteristics for potential industrial applications [160].

It is necessary to discover or develop new GRAS (generally recognized as safe) status materials with improved functionalities to encapsulate the probiotics. Mokhtari et al. indicated that an extra layer extracted from *S. cerevisiae* cell wall compounds apparently improved the viability of *L. acidophilus* after the simulated GI digestion on a strain dependent basis [161]. Furthermore, by using the emerging technologies, the functional properties of the existing materials can be altered and improved [162-164]. Studies showed that ultrasound pretreatment significantly improved solubility of the soy protein isolates compared to the untreated one [165]. This is a potential resolution to overcome the limitation of plant-based proteins on encapsulating probiotics. Moreover, efforts to optimize the conventional standard process conditions have been put to reduce the adverse effects on the viability of probiotics caused by processing. Calligaris et al. suggested that the energy needed to form nanoemulsions was significantally reduced by

combining the high pressure homogenization and high power ultrasound and the formed nanoemulsion possessed lower mean particle size and higher viability of probiotics [166]. These treatments showed the opportunities to develop new probiotic encapsulation methods on industry scale.

# CHAPTER 2. VIABILITY OF LACTOBACILLUS RHAMNOSUS GG MICROENCAPSULATED IN ALGINATE/CHITOSAN HYDROGEL PARTICLES DURING STORAGE AND SIMULATED GASTROINTESTINAL DIGESTION: ROLE OF CHITOSAN MOLECULAR WEIGHT


## Abstract

Sodium alginate (ALG) hydrogel particles coated with cationic biopolymers has shown to be one of the promising means for probiotics encapsulation and protection. In this study, the objective was to systematically explore the effect of molecular weight of chitosan coating on the functional properties of ALG hydrogel particles and improving viability of encapsulated *Lactobacillus rhamnosus* GG (LGG). Firstly, three different molecular weights of chitosan, i.e., chitosan oligosaccharide (COS), low molecular weight chitosan (LMW–chitosan) and medium molecular weight chitosan (MMW–chitosan) were electrostatically deposited on ALG hydrogel particles. Both SEM and FTIR results indicated that chitosan was successfully deposited to the surface of the hydrogel particles. Then the effects of chitosan MW on the viability of LGG encapsulated in the hydrogels during long-term storage and under simulated gastrointestinal digestion were evaluated. Among them, the hydrogel particles coated with COS prevented the viability loss of LGG during long-term storage under different temperature (4, 25 and 37 °C). However, no spectacular improvement on the viability of encapsulated LGG by all three chitosan coatings was found in simulated digestion.


## Introduction

In recent years, a number of studies have proved that probiotics such as *Lactobacillus rhamnosus* GG (LGG) have positive effects on alleviating inflammatory conditions, infectious and immunity system problems in human beings [167, 168]. These findings have triggered the

consumers' desire for relevant products and promoted the application of probiotics in the food industry. To exert the health effects, it is recommended to ingest food containing at least $10^6$-$10^7$ colony forming units (CFU)/g viable probiotics [169]. However, most of the probiotics are highly susceptible to all kinds of environmental stresses during food processing and storage, as well as passing through human gastrointestinal (GI) tract, thus causing the loss of their viability and potential health benefits [170]. For example, it was observed that two strains of probiotics, *L. acidophilus* and *B. bifidum* showed a constant loss of viability during refrigerated storage in five commercial yogurts [59]. The considerable loss of viability of probiotics was also observed during food manufacturing procedures and improper storage conditions in other probiotics-containing products, such as cheeses [60], fruit juices [171], and chocolate [172]. In terms of human digestion, the loss of the majority or even the entire probiotic viability was frequently reported in the literature [78, 173]. This is presumably caused by the low gastric pH in conjunction with the presence of bile salt and enzymes in the GI tract [174].

Recently, microencapsulation of probiotic bacteria in food biopolymer matrix using different technologies such as emulsion, coacervation, and extrusion have been applied and achieved varying degrees of success on improving the cell viability [88, 175, 176]. Among these, cross-linked ALG hydrogels have received the most interest because of its good gelling property with nutritional minerals such as $Ca^{2+}$ [177], low cost, non-toxicity, considered GRAS (generally recognized as safe) and simplicity of operation [55, 178]. Nevertheless, previous study also showed that the semi-permeable ALG hydrogels were degraded or even collapsed in the presence of excess monovalent, $Ca^{2+}$ chelators, and at acidic pH (e.g., pH 3) [179]. In order to overcome the semi-permeability of a single hydrogel system, some attempts have been made to create a multilayer coating of biopolymers on the outside of the ALG hydrogel particles by blending

alginate with other food biopolymers, such as starch, whey protein, and chitosan through electrostatic deposition at designated pH [180, 181, 182].

Chitosan is a linear cationic polysaccharide consisting of randomly distributed β-(1→4)-linked D-glucosamine and N-acetyl-D-glucosamine residues. Under acidic conditions, the positively charged amine groups (pKa~6.5) in chitosan enables the electrostatic interaction between chitosan and other anionic biopolymers including sodium alginate [183]. Based on the molecular weight (MW), chitosan is divided into four types: chitosan oligosaccharide (COS), low–molecular–weight (LMW) chitosan, medium–molecular–weight (MMW) chitosan, and high–molecular–weight (HMW) chitosan. As different types of chitosan contain variable amount of surface charge, one would expect the physicochemical properties of chitosan coatings on ALG hydrogel particles could be influenced by their different molecular weight. In addition, different types of chitosan exhibit unique mechanical properties, e.g., low molecular weight of chitosan has higher textural strength compared to higher molecular weight of chitosan [184]. Thus, the molecular weight of chitosan may also influence the fate of the encapsulated probiotics, such as cell release during storage and/or in GI tract. Hence, the objective of this research was to investigate how chitosan with different molecular weight behaves differently on modulating survivability of LGG (a widely studied and used probiotic) encapsulated in chitosan coated ALG hydrogels during storage at different temperature as well as in simulated GI digestion. In addition, the physiochemical properties of chitosan coated ALG hydrogels including size, surface charge, texture profile, and microstructural morphology were also investigated to determine the possible mechanisms by which physical properties of hydrogels impact the viability of encapsulated probiotics.

## Materials and Methods

### Materials

Sodium alginate, low molecular weight chitosan (50–190 kDa, degree of deacetylation: 75~85%), medium molecular weight chitosan (190–310 kDa, degree of deacetylation: 75~85%), sodium citrate, pepsin, bile extract and pancreatin were purchased from Sigma-Aldrich Chemical Co., Ltd, (St. Louis, MO, USA). Chitosan oligosaccharide (COS, 5 kDa) was purchased from Tokyo Chemical Industry Co., Ltd, (Tokyo, Japan). Ultrapure water was obtained from a Barnstead GenPure Pro water purification system (18.2 MΩ·cm, Thermo Fisher Scientific Inc., USA).

### Strains and Culture Conditions

*Lactobacillus rhamnosus* GG (LGG) ATCC 53103 was purchased from the American Type Culture Collection (ATCC) (Manassas, VA, USA). The LGG was cultured in MRS broth (Sigma-Aldrich Chemical Co., Ltd, St. Louis, MO, USA) or MRS agar (Beckton Dickinson and Company, Sparks, MD, USA) at 37 °C under anaerobic condition for 24 h. The bacterial cells in broth were harvested by centrifugation (Sorvall$^{TM}$ biofuge primo centrifuge, Thermo Scientific Inc., MA, USA) at 8,000 rpm (≈6440 ×g) for 15min at 4 °C and washed twice by ultrapure water. The pellet was resuspended in 0.1% (w/v) peptone solution to obtain a suspension containing approximately 11 log (CFU/ml) cells. For each experiment, cell suspensions were prepared freshly, which was then dissolved in 1% (w/v) sodium citrate solution and numerated by plating appropriate ten-fold dilutions onto MRS agar after 48 h of incubation at 37 °C.

### Encapsulation of LGG Sodium Alginate Hydrogel Particle

LGG was encapsulated in ALG hydrogel particles through an extrusion method described by Trabelsi et al [9] with slight modifications. Briefly, bacterial cell suspension was mixed with 2

% (w/v) ALG solution to achieve an approximate concentration of 10 log (CFU/mL). The mixture was then extruded from a syringe with a 22 gauge needle equipped with a syringe pump (LEGATO® 100 syringe pmp, KD Scientific Inc., MA, USA) at the rate of 4 mL/ min into 100mL 0.15 M $CaCl_2$ solution with stirring. The hydrogel particles were immediately formed by contacting with the $CaCl_2$ solution and left in the solution to harden for 30 min with continuous stirring. The hydrogel particles were then harvested using a sieve. Approximately loading number of bacterial cells reached $9.4 \times 10^9$ per gram particles.

**Preparation of Chitosan Coated Hydrogel Particles**

Bulk chitosan solutions (COS, LMW–chitosan and MMW–chitosan) at a fixed concentration of 0.1% (w/v) were prepared by dissolving 1g of chitosan in 1 L acetic buffer (10 mM), and then pH was adjusted to 6 using 1M NaOH. The ζ–potential of each solution was measured by Malvern Zetasizer Nano ZS (Malvern Panalytical Ltd., Worcestershire, UK).

Harvested alginate hydrogel particles were washed with ultrapure water twice. The chitosan coated alginate hydrogel particles were prepared by adding 10g of ALG particles into 90 mL of freshly prepared chitosan solutions (0.1%, w/v). Alginate hydrogel particles in the absence of chitosan were used as a control. All samples were stirred at 300 rpm for 45 min, and the particles were harvested and washed with ultrapure water prior to use.

**Diameter of Hydrogel Particles**

The images of 30 randomly selected particles of each treatment were captured by an Olympus SHE dissecting light microscope (Olympus Optical Co., Ltd., Japan) with moticam 5 digital camera (Motic Instruments Inc., Richmond, BC, Canada) and the average diameter was analyzed by the Motic Images Plus 3.0 software.

**Textural Properties of the Hydrogel Particles**

Method used to measure the textural properties of hydrogel particles was adapted from Bourne [185] by a Stable Micro Systems Texturometer model TA–XT2i (Texture Technologies Corp., White Plains, NY, USA) equipped with a 5 kg load cell. A 35 mm diameter cylindrical steel probe was applied on 30 g of harvested particles for each treatment in a compression mode at a constant crosshead velocity of 2 mm/s. The rupture force measurements were carried out on the entire particles of each treatment at the velocity of 5 mm/s in a distance mode. The peak force was measured in Newtons. The automatic detection of the contact between the probe with the particles was carried out with a contact force of 0.005 N. Textural properties of the hydrogel particles including hardness, springiness, cohesiveness, and resilience were obtained from the Texture Expert Software for Windows Version 3.2 installed in the equipment [153].

**Structural Properties of Hydrogel Particles**

Scanning electron microscopy (SEM) (JEOL Mod. JSM-6490LV, Jeol, Peabody, MA, USA) was applied to evaluate the surface morphology and the microstructure of the hydrogel particles. Briefly, the hydrogel particles were frozen in liquid nitrogen to prevent the particle shrink during freeze-drying process and to maintain the original structure of the particles, followed by freeze-drying for 24 h (Lyophilizer, SP scientific, Gardiner, New York). The dried particles were cut in half and attached to adhesive carbon tab on cylindrical aluminum mount, and then the sample was coated with gold (Cressington 108auto, Ted Pella Inc., CA, USA) and examined at different magnifications with an accelerating voltage of 15 kV.

**Fourier Transform Infrared Spectroscopy (FTIR)**

FTIR spectra of all dried hydrogel particles and control powders (ALG, chitosan) were obtained by a Varian FTIR spectrophotometer (California, USA) according to previously published paper without any modification [186].

**Survival of the Encapsulated Cells in Simulated GI Condition**

One gram of freshly prepared hydrogel particles was added in a tube with 9 mL of simulated gastric fluid (SGF) (0.08 M HCl containing 0.2 % w/w NaCl, pH 2) with 0.3 % (w/v) pepsin and incubated in a shaking water bath (VWR shaking water bath, VWR International, LLC, PA, USA) at 37 °C, 150 rpm for 30, 60, 90, 120 min. After incubation, the particles were filtered and rinsed by ultrapure water twice and then added into 1 % (w/v) sodium citrate solution to release the bacterial cells from the hydrogel particle. The viable cells after SGF were counted by plating the serial dilutions onto the MRS agar and incubating under 37 °C for 48 h.

To investigate the survival of LGG in simulated intestinal fluid (SIF), 1g of hydrogel particles was added into a tube with 9mL SIF (0.05M $KH_2PO_4$, pH 7.4) containing 1% (w/v) bile salt and 1% (w/v) pancreatin [90, 100]. The tubes were incubated at 37 °C, 150 rpm for 150 min. After incubation in SIF, the viable cells were counted by above-mentioned method.

**Storage Property Measurement**

For storage stability test, freshly prepared hydrogel particles were stored in sterilized 0.1 % peptone at three different temperatures, i.e, 4 °C, 25 °C and 37 °C. The viability of encapsulated LGG during storage was measured by the same method described above.

**Statistical Analysis**

The characterization of physical properties of freeze-dried hydrogel particles were performed at least twice. The viability of cell measurement was performed at least four time

using freshly prepared samples and values were expressed as means ± SD. Significant differences between means ($p < 0.05$) were conducted by one-way analysis of variance (ANOVA) (Version 9.3, SAS Institute Inc., NC, USA).

## Results and Discussions

### Chitosan Solution and Hydrogel Properties

#### *ζ–potential of chitosan solutions*

As mentioned earlier, chitosan is a product of deacetylation and degradation of chitin, and as the degree of deacetylation (DD%) increases, the more amine groups are exposed to the environment. This is important for the electrostatic attraction between chitosan and ALG, since the amine groups will be protonated which confers net positive charge while ALG brings negative charge under acidic conditions. The DD% of COS is usually higher than 90% and sometimes can even reach up to 99.9% according to previous publications [187-189]. Due to the varied DD%, it was expected that three kinds of chitosan used in the current study should have different electrostatic binding potentials to the surface of ALG hydrogel particles, which can be partially presented by the ζ–potential of the chitosan solution.

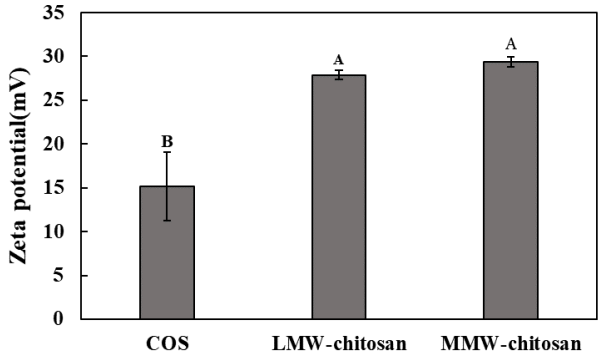


**Fig. 2-1.** Zeta potential of 0.1% (w/v) chitosan oligosaccharides (COS), low-molecular-weight chitosan (LMW-chitosan) and medium-molecular-weight chitosan (MMW-chitosan) at pH=6. Different superscripts indicate that the means differ significantly ($p < 0.05$).

As shown in **Fig. 2-1**, COS showed an apparently lower ζ–potential compared to LMW–chitosan and MMW–chitosan ($p < 0.05$), while there was no statistically significant difference between the other two at pH 6.0. These results were consistent with other research [190, 191]. The relatively lower ζ–potential of COS could be explained by the destruction of the amine groups caused by the harsh conditions, such as acid, base, oxidative reductive agents and/or high-energy impact treatments used to achieve the higher DD% and smaller molecular weight of COS during the producing process [192]. However, the ζ–potential of chitosan solution is not the only and ample indicator of the interaction between chitosan and ALG hydrogel particles. The particle size of chitosan also plays a vital role in chitosan coated hydrogel. The bigger the particle size of chitosan is, the more steric hindrance there will be in the system. Therefore, the SEM images of the hydrogel particles in the presence and absence of chitosan coatings were taken to elucidate how the particle size of chitosan molecule influenced their electrostatic interaction with ALG and the corresponding morphology of hydrogels in the following part.

***Hydrogel particles size and morphology***

It has been reported that the diameter of the hydrogel particle was strongly influenced by extrusion operation parameters such as wall material, needle gauge, needle to calcium chloride solution distance and ion strength of gelling solution. Among all the factors, needle gauge of syringe used during extrusion predominantly determines the diameter of hydrogel particles [193]. Muthukumarasamy et al. [123] reported that ALG hydrogel particles formed from extrusion method with a diameter in 2–4 mm range showed the better protective effect on the probiotic encapsulated in it.

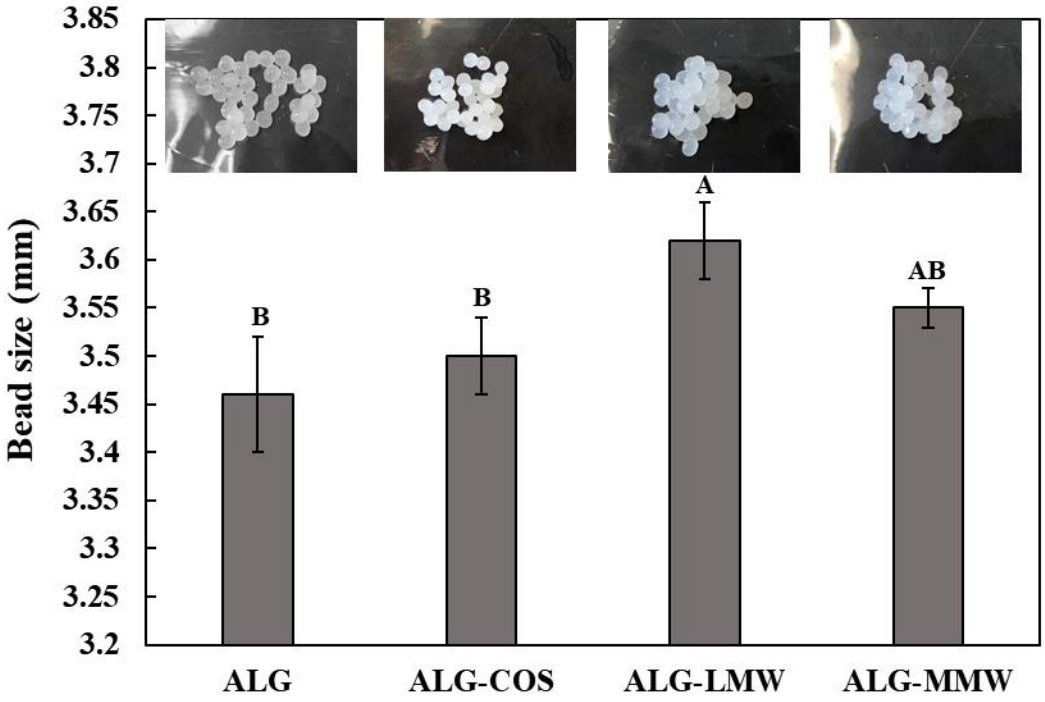


**Fig. 2-2.** Diameter of hydrogel particles in the presence and absence of chitosan coating. Picture above the column shows the corresponding morphology of the hydrogel particles. Different superscripts indicate that the means differ significantly ($p < 0.05$).

With regarding to the impact of chitosan coating on the size of hydrogel particles, some research found that the addition of chitosan coating had no influence on the size of ALG hydrogel particles [194]. According to the current results (**Fig. 2-2**), coating increased the diameter of hydrogel particles, which was 3.45 mm in the absence of chitosan coating and it was comparable with other reports [195]. And LMW–chitosan and MMW–chitosan exerted greater increment on particle size, which were in good agreement with earlier studies [11]. These results were supported by the cross-section SEM images (**Fig. 2-3 B-2, C-2, & D-2**) of hydrogel particles in which the external porous surface of ALG hydrogel particles was at least partially covered by chitosan, thus prevent the hydrogel particles from shrinking. Among all the chitosan coated ALG hydrogel particles, ALG–COS had the smallest particle size that is in comparable

with control (ALG) which was supported by SEM image where a thinnest layer with the smoothest surface was observed in ALG–COS particles (**Fig. 2-3 B-3**). Interestingly, ALG–LMW had significant larger ($p < 0.05$) particle size. Presumably, the smaller MW of LMW would form less steric hindrance, thus larger amount of LMW could be electrostatic deposited on the surface of ALG particle than that of MMW–chitosan. As demonstrated in **Fig. 2-3 D-3**, part of the MMW-chitosan coating was more irregular and partially exfoliated from the hydrogel particle.

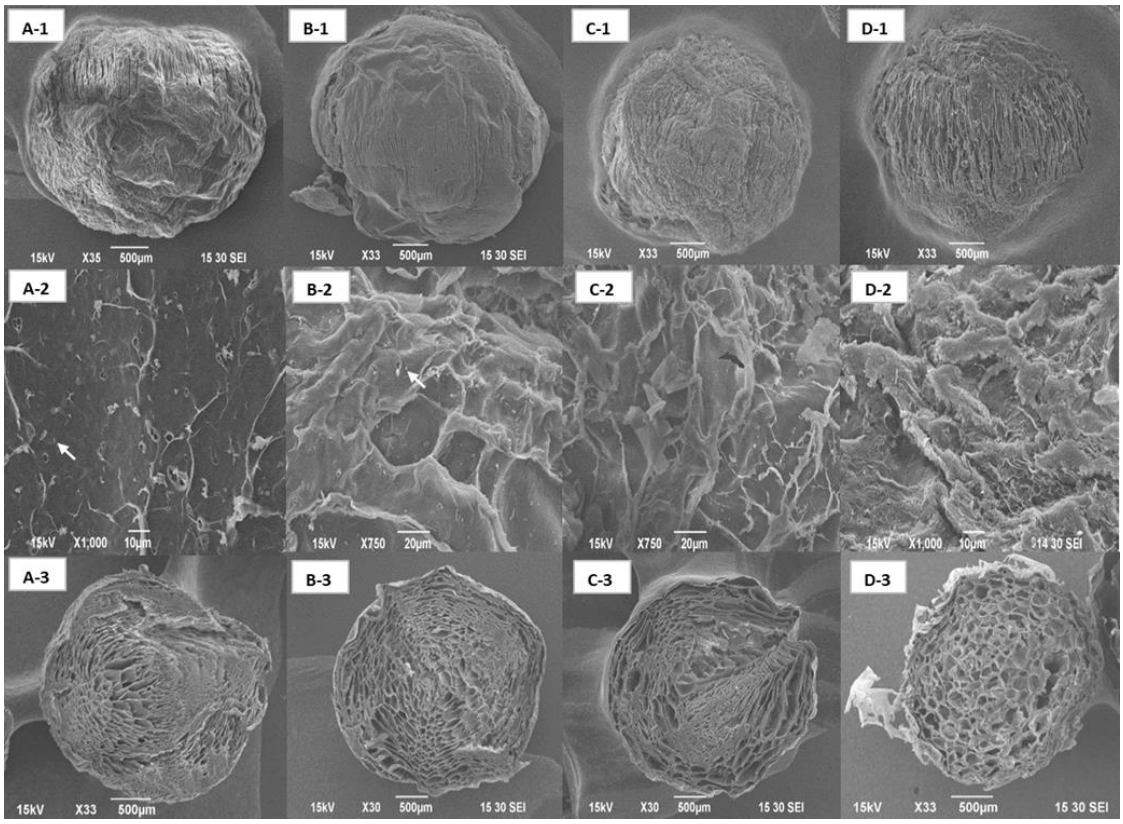


**Fig. 2-3.** Exterior surface and cross section morphology of freeze-dried hydrogel particles in the presence and absence of chitosan coating obtained by SEM. A-1, A-2 and A-3: sodium alginate hydrogel particles (ALG); B-1, B-2 and B-3: sodium alginate hydrogel particles coated with chitosan oligosaccharides (ALG-COS); C-1, C-2 and C-3: sodium alginate hydrogel particles coated with LMW-chitosan (ALG-LMW); D-1, D-2 and D-3: sodium alginate hydrogel particles coated with MMW-chitosan (ALG-MMW). LGG cells under microscopy are pointed by the arrows in A-2 and B-2. Arrow in D-3 shows the protruded chitosan layer.

From the exterior and interior morphology of particles, it was also observed that the freeze-dried ALG hydrogel particles produced by extrusion method maintained a spherical or relatively spherical shape, independent of chitosan coating. However, the surface morphology of samples coated with different MW of chitosan was strongly altered as compared to the control. Analyzing the results from a closer perspective as in **Fig. 2-3 A-2, B-2, C-2 & D-2**, ALG particle presented a relative smooth surface, whereas chitosan coating contributed to a more irregular and jagged surface. The images clearly indicated that the chitosan has been successfully deposited onto the external surfaces of the ALG hydrogel particles. Similar appearance of chitosan coated ALG hydrogel particles was also recorded in microencapsulated *Bifidobacterium longum* [11]. Among all chitosan coated particles, the secondary layer formed by COS presented the smoothest surface, followed by LMW–chitosan. The MMW–chitosan formed the roughest surface on the hydrogel particle. This was in consistent with ζ–potential of the chitosan solutions with different MW. As the molecular weight of chitosan increasing, stronger electrostatic interaction was anticipated between ALG and chitosan, giving rise to the higher portion of the secondary layer to be protruded to the outside of the hydrogel particles. As a result, the surface of the hydrogel particles became more tangle. Similar results were also reported that the smaller molecular weight of chitosan used, the more uniform coating on particle surface were formed due to its low viscosity [196].

The interior structure of the hydrogel particles (**Fig. 2-3 A-3, B-3, C-3 & D-3)** was porous, which was a result of the ionic bridges formed between the G blocks on the backbone of ALG and $Ca^{2+}$ [197]. This "egg–box" model that illustrated the ionotropic gelation between ALG and $CaCl_2$ has been well demonstrated [198]. Overall, the hydrogel particles coated with chitosan tended to have larger and more open cells inside than that of the control. Previous study also

demonstrated that more chitosan molecules attached to the ALG hydrogel particles could break the "egg–box" model, resulting in a higher porosity of alginate core [199]. Interestingly, results represented in **Fig. 2-3 A-3**, the hydrogel particle maintained the porous property with visible rod-shaped LGG on the surface (the arrows in **Fig. 3 A-2**). These characters were maintained to some levels in LMW–ALG particle in **Fig. 2-3 B-3** and became invisible in **Fig. 2-3 C-3 & D-3**. It could be possible that the extruded part of the chitosan on the surface of ALG–LMW and ALG–MMW particles blocked the sights from visualizing the pores. Therefore, no visible bacteria were observed on surface. Still, further information is required to confirm this assumption.

**FTIR Spectra of Freeze-dried Hydrogel Particles**

In order to better understand whether and how MW of chitosan could influence the functional group interaction between chitosan solution and ALG hydrogel particles, the IR spectra of the four samples (ALG, ALG–COS, ALG–LMW, ALG–MMW) and control (COS, LMW–chitosan and MMW–chitosan) were recorded in the range of 4000–750 $cm^{-1}$ (**Fig. 2-4**).

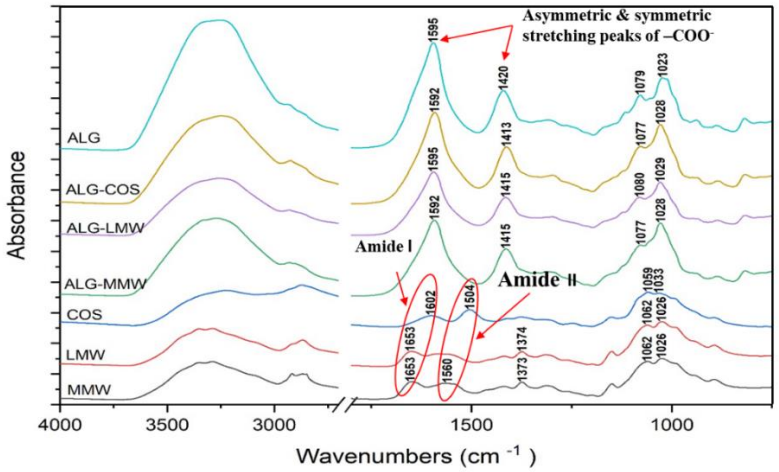


**Fig. 2-4.** FTIR spectra of hydrogel particles in the presence and absence of chitosan coating (ALG, ALG-COS, ALG-LMW and ALG-MMW) and three kind of chitosan chemicals (COS, LMW and MMW).

The three spectra presented on the bottom in **Fig. 2-4** belonged to three types of chitosan. The overall spectra of chitosan showed strong similarity except for slightly differences in the signal strength. The band in the region 3290–3350 $cm^{-1}$ is attributed to the N–H and O–H stretching, in conjunction with the intramolecular hydrogen bonds. The absorptions at 2875 and 2920 $cm^{-1}$ corresponded to asymmetric and symmetric C–H stretching bands, respectively, which were widely reported in the spectra of other common polysaccharides, such as xylan [200] and carrageenan [201]. A similar absorption pattern around this region was observed in the spectrum of ALG hydrogel particles, as shown on the top of **Fig. 2-4**. The existence of residual N-acetyl groups in chitosan was confirmed by the bands at around 1653 $cm^{-1}$ in the spectra of LMW and MMW chitosan and around 1602 $cm^{-1}$ in the spectrum of COS (C=O stretching of amide I group), as well as the absorptions at 1560 $cm^{-1}$ in the spectrum of MMW chitosan and 1504 $cm^{-1}$ in the spectrum of COS (N–H bending of amide II group), respectively. The band at 1374 $cm^{-1}$ is attributed to the $–CH_3$ symmetrical deformations. The bands at 1062 and 1026 $cm^{-1}$ corresponded to C–O stretching, which were also present in the spectrum of ALG. These characteristics were consistent with the findings of others [202, 203]. With respect to the spectrum of ALG, except for the general bands mentioned above, the strong absorptions at 1595 and 1420 $cm^{-1}$ were registered to the asymmetric and symmetric stretching peaks of $–COO^–$, respectively [204].

The three spectra in the middle of **Fig. 2-4** corresponded to the three types of chitosan coated ALG hydrogel particles. It was clear that the all chitosan coated hydrogel particles showed slight shift in peaks of amide II, and III towards to lower wavenumbers compared to ALG presumably due to the electrostatic interaction between the amino groups of chitosan ($NH_4^+$) and carboxylic groups of ALG ($–COO^–$). A similar wavenumber shift was also reported in chitosan coated calcium-ALG nanocapsules [182]. Furthermore, wavenumber shifts occurred in

the two peaks in "fingerprint region" (approximately 1020–1080 $cm^{-1}$) of chitosan coated particles. In short, the FTIR results demonstrated that chitosan with different molecular weight had similar IR spectrum and all of them were attached to the surface of ALG hydrogel particles through electrostatic interaction.

**Textural Properties of the Hydrogel Particles**

Several studies suggested that the textural properties and functional performance (e.g., viability of probiotics, control and release) of probiotics encapsulated by hydrogel particles were largely determined by the coating and/or wall materials composition and concentration [153, 205]. For example, it was reported that there was a positive correlation between storage stability of probiotics encapsulated in hydrogel particles and hardness of hydrogel particles [181]. Consequently, the textural properties of hydrogel particles were measured and presented in **Table 2-1**.

**Table 2-1.** Textural properties of hydrogel particles with and without chitosan coating.

| | **Hardness (N)** | **Rupture force (N)** | **Springiness** | **Cohesiveness** | **Resilience** |
|---|---|---|---|---|---|
| **ALG** | 3.53 ± 0.18 B | 1.24 ± 0.09 B | 1.86 ± 0.01 B | 8.25 ± 1.52 A | 0.42 ± 0.00 A |
| **ALG-COS** | 4.19 ± 0.10 A | 1.48 ± 0.05 A | 2.01 ± 0.00 A | 8.19 ± 0.23 A | 0.44 ± 0.02 A |
| **ALG-LMW** | 3.00 ± 0.17 C | 1.26 ± 0.06 AB | 1.88 ± 0.04 B | 6.91 ± 0.35 A | 0.45 ± 0.01 A |
| **ALG-MMW** | 2.61 ± 0.02 D | 1.24 ± 0.12 B | 1.91 ± 0.04 B | 6.57 ± 0.40 A | 0.46 ± 0.01 A |

Different superscripts indicate that the means differ significantly ($p$ <0.05).

Among all the samples, ALG–COS showed a significantly higher hardness and springiness. It also required more force to be ruptured compared to the others but had comparable cohesiveness and resilience ($p$ > 0.05). This was expected since smaller MW of COS can form a homogeneous, intact and rigid layer outside of the ALG hydrogel particles as corroborated by the morphological study (**Fig. 2-3F**). Besides, the hardness of particles

decreased with increased MW of chitosan. For instance, MMW chitosan coated ALG particles had the lowest hardness value among all the tested hydrogel particles ($p < 0.05$), which can be explained by the relatively looser interaction between ALG and chitosan on the surface of particles and MMW chitosan promoted the decrease in the internal $Ca^{2+}$ cross–linking between ALG and $Ca^{2+,}$ as indicated by cross-section morphology of particles (**Fig. 2-3H**).

**Viability of Microencapsulated LGG during Long-term Storage**

One of the major challenges slowing down the application of probiotics in the food industry is the viability loss during product storage period. Commercial probiotics products may experience a variety of different temperatures such as stored under refrigerated or ambient conditions. The impact of chitosan on the viability of encapsulated LGG in hydrogel particles at different storage temperature (i.e., 37, 25 and 4 °C) were shown in **Fig. 2-5**.

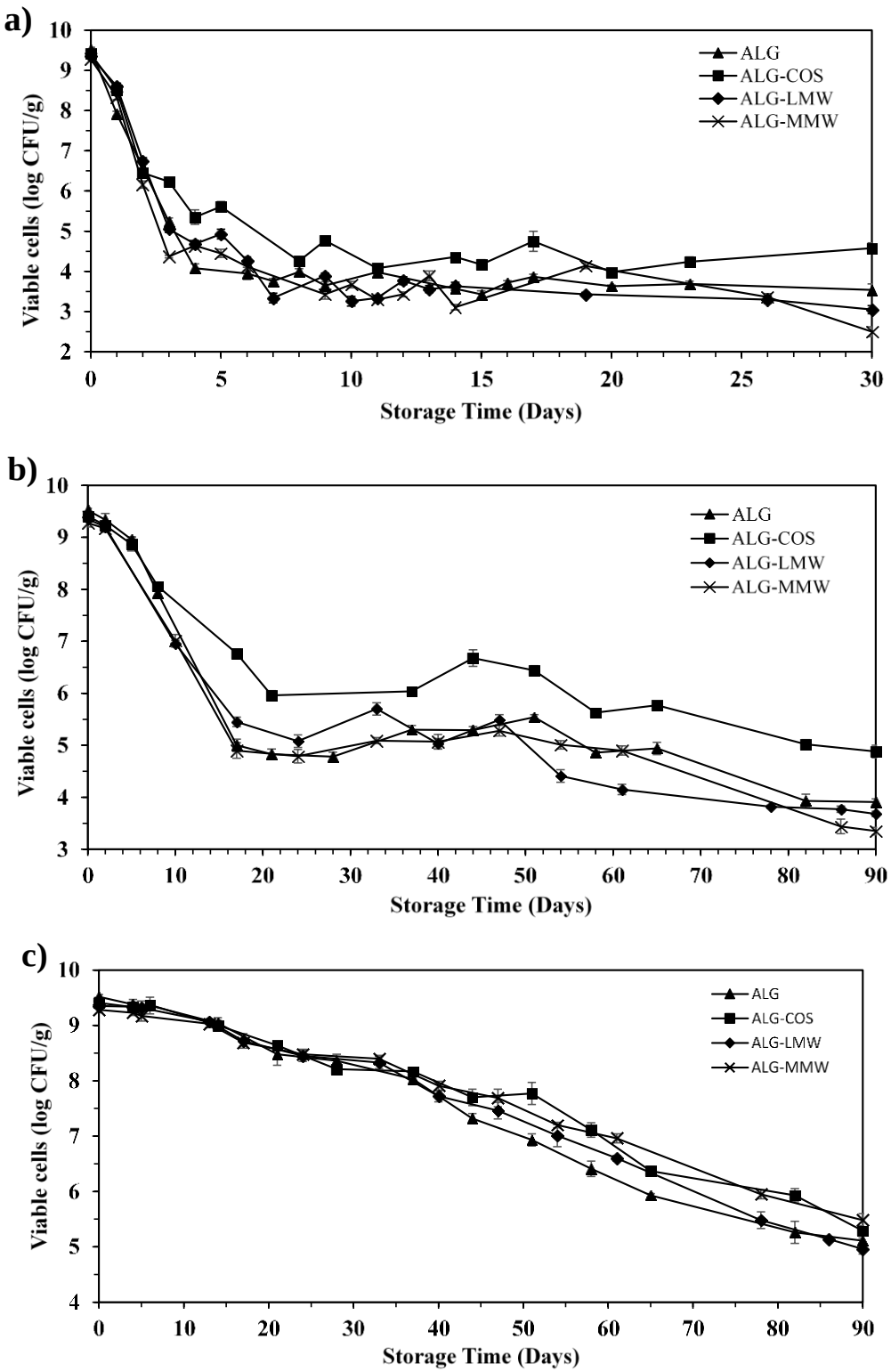


**Fig. 2-5.** Viable cells of LGG encapsulated in hydrogel particles in the presence and absence of chitosan coating during storage at (a) 37°C; (b) 25 °C and (c) 4°C.

Under 37 °C storage, a significant loss of viability (≈6 log CFU/g) was observed after 7 days of storage in all samples except for ALG–COS, in which the viability loss was around 5 log CFU (**Fig. 2-5a**). After 7 days, the inactivation rate of the cells slowed down and stayed relatively stable till 30 days of storage. Among all the hydrogel particles, ALG–COS showed a better protection on the viability of encapsulated LGG over the entire course of storage time. **Fig. 2-5b** showed the viability of encapsulated LGG in hydrogel particles during 90 days of storage at 25 °C. A pattern showed up in this figure that the decreasing rate of viable cells was high at the beginning (approximately 13 days), which were then entered into a relatively stable phase (13–50 days), and followed by a gradual decrease afterwards. An apparently higher viable cell count was observed in ALG–COS during storage and it was determined as 4.88 log CFU/g after 90 days of storage. Concerning the other three samples, the counts of viable cells were roughly close during the whole storage period, which indicated that LMW–chitosan and MMW–chitosan showed little improvement on the viability of encapsulated LGG. In light of the reduction of viable cells over storage time, it can be deduced that the majority of loss was appeared in the first several days.

Being different from the higher storage temperature on the pattern of LGG viability, the viability loss of LGG encapsulated in all hydrogel particles was gradually decreased when stored at 4 °C, as shown in **Fig. 2-5c**. After 90 days of storage, the viable cell count was maintained around 5 log CFU/g in all samples. This is not a surprise since 4 °C is a recommended storage condition for bacteria. These results demonstrated storage temperature played an important role on the viability of probiotics in hydrogel particles. As expected, the lower storage temperature rendered the higher shelf life of LGG. An increased storage stability in hydrogel particles was also found after they were coated with chitosan [181]. Additionally, it was found that ALG coated

with COS greatly improved the viability of encapsulated LGG during higher storage temperature (both 37 °C and 25 °C). One possible reason is the penetration of molecular oxygen were largely retarded by homogeneously distributed COS layer outside of ALG hydrogel particles, which was proved by the textural analyzing and SEM results. A number of studies have shown that the oxygen content are the most important factors determining the viability of probiotics during the storage period [206]. Moreover, the prebiotic property of COS, as some previous studies reported [188, 189, 207], may also account for its ability to stimulate the growth of LGG, and hence reducing the viability loss during storage.

**Survival of Encapsulated LGG in Simulated GI Digestion**

As stated earlier, probiotics have to survive in human GI tract in large quantities to carry out positive health effects. Many previous studies have revealed that free LGG cells suffer a severe, even completely viability loss in SGF in a short *in vitro* digestion period [78, 208, 209]. Thus, the possible protective effects of secondary layer of chitosan with different MW on the viability of encapsulated LGG in simulated GI conditions were investigated. The hydrogel particles coated in the presence and absence of different chitosan were incubated in SGF for 30, 60, 90 and 120 min and in SIF for 150 min. The viable counts of LGG at different time points were presented in **Fig. 2-6.**

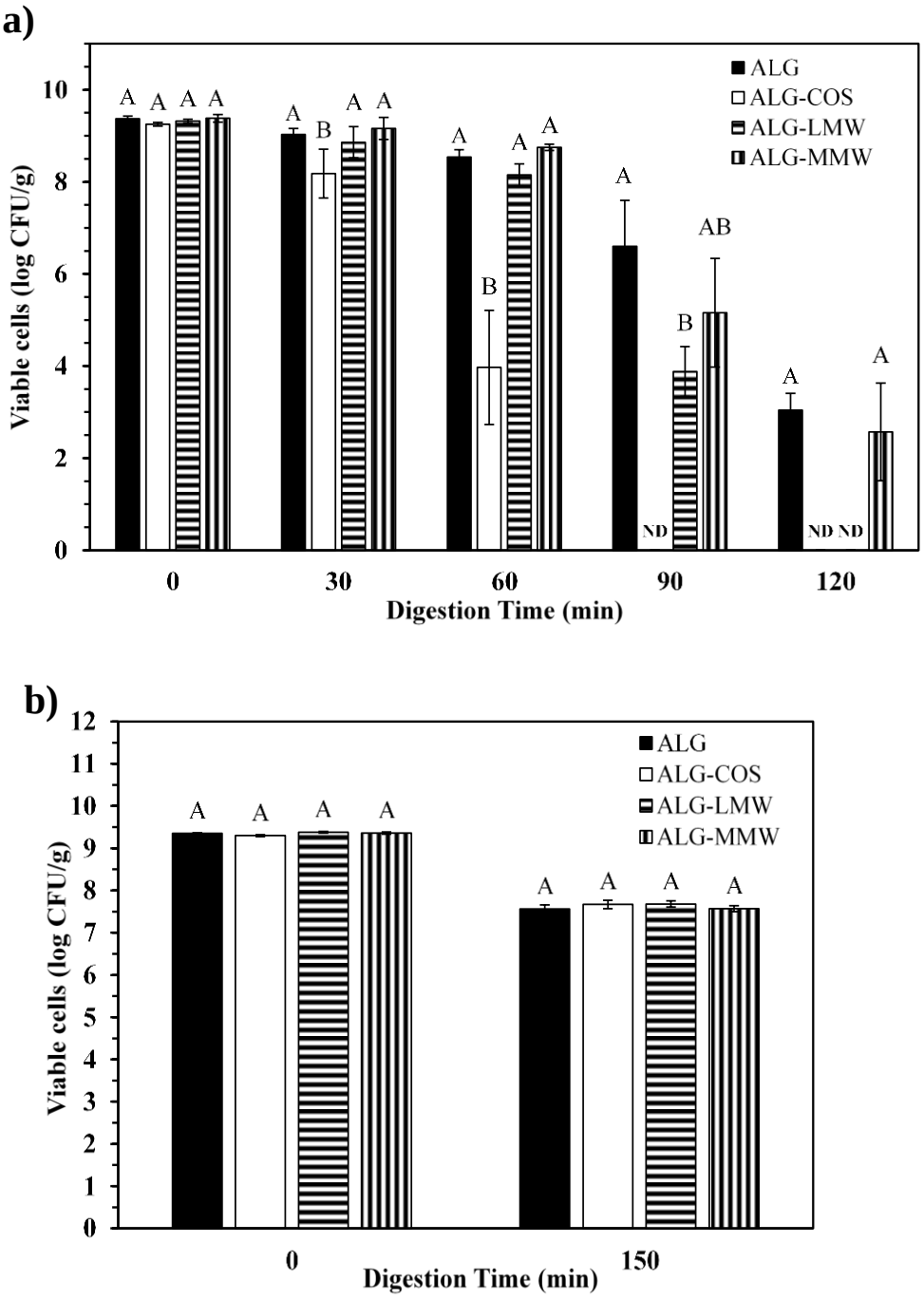


**Fig. 2-6**. Viable cells count of LGG encapsulated in hydrogel particles in the presence and absence of chitosan coating after (a) incubated in simulated gastric fluid (SGF) at 0, 30, 60, 90, 120 min, (b) incubated in simulated intestinal fluid (SIF) at 0 and 150 min. Different letters at same time point means differ significantly ($p < 0.05$). ND: not detectable.

**Fig. 2-6a** showed the viability of encapsulated LGG in SGF. In general, the viable cell counts of 9.4 log CFU/g in fresh hydrogel particles were achieved, and no significant difference was found between the four samples. At the end of SGF stage (120 min), cell viability underwent at least a 6-log reduction. The possible explanation for this result was that the hydrogel particles produced in this method had relatively large pore size which facilitated the diffusion of small molecules, such as organic acids, oxygen and digestive enzymes into the hydrogel, hence deactivating the encapsulated LGG [87]. In terms of the three different chitosan, the number of viable cells in ALG–COS showed a drastic reduction (5.28 log CFU/g) with increasing incubation time and no viable cells could even be detected after 90 min incubation. Conversely, only a slight reduction (~ 1 log CFU/g) was observed in the other three treatments after 60 min digestion but the viable cells in in ALG–LMW became undetectable after 120 min digestion in SGF. Among the three treatments that coated with chitosan, ALG–MMW showed an apparently better protection on the survival of encapsulated LGG. One possible reason could be due to the highest swelling capacity of ALG upon coated by COS, as indicated by springiness value from texture analyzer. Such capacity could potentially decrease the cross-linking density of the ALG, which allowed a larger amount of gastric fluid to penetrate into the hydrogel. In addition, COS is highly soluble at acidic pH, which also favored gastric fluid reflux. This result was in line with previously report [196], where the survival rate of *L. bulgaricus* KFRI 673 was enhanced by high molecular weight chitosan coated ALG particles than that of low molecular weight of chitosan. Similar survival rate of probiotics encapsulated in multilayer chitosan coated ALG particles under SGF solution were also documented [210]. Interestingly, viable cells of LGG encapsulated in ALG and ALG–MMW remained on a comparable level which was 3.04 and 2.57 log CFU/g, respectively, after 120 min digestion in SGF. Apparently, there was no survival rate

improvement in encapsulation of LGG in chitosan-coated ALG compared with cells in ALG particles. In fact, mixed results on the probiotics survival rate were reported when they were encapsulated in ALG and chitosan hydrogel particles. For instance, some studies found the similar results as ours and postulated that modified surface charge of ALG hydrogel by MMW chitosan did not improve viability of the selected bifidobacterial cells in during simulated digestion [11]. Many others found that the survival of probiotics, such as encapsulated lactobacilli in ALG coated with chitosan was greater than in ALG in SGF condition [155]. Such discrepancy may be attributed to the different probiotics applied, concentrations of ALG and chitosan, and formation of hydrogel conditions. For instance, the survival rate of encapsulated probiotics in SGF was strongly dependent on the concentration of the ALG and chitosan as well as other external factors like the concentration of the gelling solution [193, 211].

**Fig. 2-6b** displayed the viable cells count in hydrogel particles in the presence/absence of chitosan coating before and after incubation in SIF for 150 min. The viability losses of encapsulated LGG in all hydrogel particles during SIF digestion were in the range from 1.63 to 1.79 log CFU/g; however, there was also no statistically significant difference among them ($p > 0.05$), indicating the four treatments were identical in probiotic protection under SIF condition. The different performances of hydrogel particles on protecting the encapsulated LGG under SGF and SIF conditions manifested that the main challenge in exerting the protective effect is to prevent the diffusion of $H^+$ in SGF into the hydrogel particles.

## Conclusions

There is a challenge on the survival rate of probiotics during long-term storage and when traveling through the human GI tract. Microencapsulation based delivery systems such as chitosan coated ALG hydrogel particles have been applied for improving the viability of

probiotics. However, the role of chitosan molecular weight in the encapsulation and protection of probiotics is yet to be systematically studied. In this work, the effects of the secondary layer of three types of chitosan on the physicochemical properties of the ALG hydrogels and the viability of the encapsulated LGG during the storage period and in the simulated GI tract were studied.

Successful deposition of three types of chitosan (COS, LMW-chitosan, MMW-chitosan) on ALG hydrogel particles was proved by the FTIR spectrum and SEM images. In terms of the impact of chitosan MW on the storage stability of probiotics, probiotics encapsulated in COS coated sodium hydrogel particles exhibited the highest survival rate during storage at all three temperatures (4, 25, and 37). This is because of the uniform and denser surface and the greater hardness and rupture force delivered by the COS coating deposited on the hydrogel particles that prevent molecular oxygen from diffusion into the hydrogel particles. Although all three secondary layers of chitosan had no significant effect on improving the viability of encapsulated LGG in the stomach fluid compared to ALG hydrogel particles, it provided insights into searching materials that can help probiotics tolerate the harsh H+ environment in the stomach.

# CHAPTER 3. ALGINATE-BASED DOUBLE-NETWORK HYDROGEL IMPROVES THE VIABILITY OF ENCAPSULATED PROBIOTICS DURING SIMULATED SEQUENTIAL GASTROINTESTINAL DIGESTION


## Abstract

The impact of secondary polysaccharide, i.e., low methoxyl pectin (LMP) or κ-carrageenan (KC), and its concentration (0.2, 0.4, and 0.6%) on particle size, shape, morphological, textural properties and swelling behavior of sodium alginate (ALG)- based double-network hydrogel particles, as well as the viability of encapsulated probiotics *Lactobacillus rhamnosus* GG (LGG) in simulated sequential gastrointestinal (GI) digestion was investigated. It was found that the addition of LMP impaired the sphericity of double-network hydrogel particles, while the incorporation of KC increased the particle size. The FT-IR results indicated the miscibility and cross-linking capacity of the two polysaccharides in forming double-network hydrogel particles. With respect to the swelling behavior in simulated GI digestion, all hydrogel particles shrank in simulated gastric fluid (SGF) but swelled in simulated intestinal fluid (SIF). Among the two types of double-networking, ALG–KC hydrogel particles showed noticeable shrinkage in SGF in conjunction with the reduced swelling in SIF, which was unfavorable for protection and the controlled release of probiotics. In the case of death rate of encapsulated LGG, the presence of LMP at a lower level (0.2 or 0.4%) exhibited protective effect against LGG death during the sequential GI digestion, while addition of KC demonstrated an opposite role.


## Introduction

Gastrointestinal (GI) microbiota plays essential roles in maintaining human health, regulating certain GI diseases and cancer [212, 213]. Among many dietary strategies, the

consumption of health benefit conferring probiotics offers an effective means in establishing and maintaining an optimal balance of GI microbiota [1]. As a consequence, functional foods with probiotics have been largely developed and consumed [214]. In order to achieve the healthy benefits, the commonly suggested number of probiotics is no less than $10^8$ viable cells per day/dose for therapeutic use, or $10^6$ as supplements with considerable functional activity [54, 215]. However, it is difficult to deliver such numbers of live microorganisms to the target function site by free probiotics cells. This is because the harsh conditions of human GI tract such as low pH condition and high bile salts concentration can severely jeopardize the viability of probiotics [7, 62]. Encapsulation of probiotics has been recently demonstrated as a reliable technique to prevent probiotics against harsh conditions in GI tract before reaching the designated site [177].

Among all kinds of encapsulation techniques, ionically cross-linked ALG hydrogel particles formed by extrusion have been widely applied due to a number of advantages such as the less damage it causes, generally recognized as safe (GRAS) status, the physical protection and the desirable release profile it provides [216, 217]. Nevertheless, ALG hydrogel particles are very liable to disintegrate under extreme conditions, such as excess of $H^+$, harsh chemical condition, and the presence of $Ca^{2+}$ chelators [153]. In order to overcome these limitations, researchers have attempted to coat ALG particles with polycations (e.g., chitosan) via electrostatic deposition to improve its stability. Previous study suggested that the long term storage stability of probiotics was markedly improved when encapsulated in ALG particles with the electrostatic deposition of chitosan coating; such design, however, was unable to improve the viability of the encapsulated *Lactobacillus rhamnosus* GG (LGG) in simulated gastrointestinal digestion, which was speculated to be due to the dissociation of low acidic tolerance chitosan (high solubility at an

acidic pH) [218]. Thus, the coatings with a good acidic tolerance might be necessary to sustain the viability of probiotics.

In addition to cationic chitosan, a number of other individual anionic polysaccharide or double-network polysaccharide blends have been used to fabricate hydrogel particles for probiotics encapsulation. In such systems, the viabilities of encapsulated probiotics during storage, processing, and in the GI tract are highly dependent on the physicochemical properties of each individual polysaccharide [146]. Carrageenans (CGs) are a group of sulfated polysaccharides which can be divided into six types according to the number and location of sulfate ester groups [219]. Among them, κ-carrageenan (KC) with a single sulfate ester group on galactose has been widely utilized for gelling formation, as stabilizers in many emulsions and suspensions, and to increase viscosity in foods. The proposed gelling mechanism is implemented in the presence of cations (e.g., $K^+$ and $Ca^{2+}$) which assist the backbone structure of KC to form double helices between adjacent molecules and get aggregated [15]. The strength of KC gel is determinant on several factors, such as KC concentration, the type of cross-linking agent, and the presence of other polysaccharides. Usually, the $K^+$ is considered as the most effective ion for the formation of KC gel, researchers also indicated that $Ca^{2+}$ can also perform a good gelling capacity since it encouraged more molecules into aggregation [17]. The combination of KC with another polysaccharide can further enhance the performance. For instance, probiotics encapsulated in KC–carboxymethyl cellulose (CMC) hydrogel particles also displayed a greater acid tolerance compared to CMC alone [16]. Low-methoxyl pectin (LMP) is another acidic tolerance polysaccharide and can form a strong gel by a salt bridge at the presence of $Ca^{2+}$. For these reasons, LMP has also been employed in encapsulation of bioactive compounds and probiotics, facilitating their survival upon digestion in the upper part of GI tract and the release

to colon [12, 13, 220-222]. In addition, biopolymer mixtures of LMP and ALG have been applied to encapsulate bioactive compounds such as vitamin E, folic acid, and caffeine in order to improve the controlled delivery [14].

Whereas KC and LMP have demonstrated a potential role on protecting bioactive compounds, very limited information is available on the encapsulation of probiotics using the mixture of KC or LMP with ALG via $Ca^{2+}$ cross-linked hydrogel particles. Additionally, it is worth noting that most of the conclusions on the enhancement of encapsulated probiotics viability in literature were drawn on the basis of the following conditions: i) by comparing viability of free and encapsulated probiotics [223]; ii) by evaluating the viability of probiotics in separated simulated gastric digestion and intestinal tract digestion rather than a sequential gastrointestinal digestion [104, 224-226]. In order to better mimic the human digestion and truly represent the viability of encapsulated probiotic, the viability of probiotics experiment conducted in a simulated sequential GI digestion is highly encouraged.

In this study, ALG was used as the primary polysaccharide to build the main structure of hydrogel particles. A secondary polysaccharide (KC or LMP) was chosen to blend with the ALG-based gelling system at different ratios for encapsulating a widely studied strain of probiotics, *Lactobacillus rhamnosus* GG (LGG). The hypothesis was that the physical characteristics of double-network hydrogel particles such as shape, size, and texture could be greatly influenced by the polysaccharide type and concentration; thus viability of probiotics being encapsulated might be varied. The objectives of this study are to: i) analyze the physicochemical properties of hydrogel particles formed by different formulas of double-network polysaccharides; ii) determine how LMP and KC influence the inner structure of sodium

alginate-based gelling system; and iii) fabricate a double-network encapsulation system to improve the viability of LGG during a simulated sequential GI digestion.

## Material and Methods

### Materials

Sodium alginate (ALG), κ-carrageenan (KC), and MRS broth were purchased from MilliporeSigma (St. Louis, MO, USA). MRS agar was purchased from Beckton Dickinson Company (Sparks, MD, USA). Low-methoxyl pectin (LMP) (GENU® pectin type LM–12 CG, Lot # GR74485, 76 kDa of Mw) was kindly provided by CP Kelco (Atlanta, Georgia, USA) and used without further purification. Calcium chloride, sodium citrate dihydrate, potassium phosphate monobasic, sodium chloride, and other chemicals used in this study were of analytical grade and purchased from VWR Inc. (Chicago, Illinois, USA). *Lactobacillus rhamnosus* GG (LGG) ATCC 53103 was purchased from the American Type Culture Collection (ATCC) (Manassas, VA, USA). Ultrapure water was obtained from a Barnstead GenPure Pro water purification system (18.2 MΩ·cm, Thermo Fisher Scientific Inc., USA). All concentrations were expressed in weight percentage (wt %).

### Bacterial Cell Preparation

LGG bacteria were cultured in MRS broth and MRS agar at 37 °C under anaerobic condition created by the BD GasPak system (BD BBL GasPak jars and anaerobic indicators) (NJ, USA). After second revivals of this strain in MRS broth, the bacterial pellet was obtained by centrifugation (SorvallTM biofuge primo centrifuge, Thermo Scientific Inc., MA, USA) at 3,500 rpm (≈1233 ×g) for 10 min at 4 °C and washed twice by ultrapure water. The pellet was resuspended in 0.1% peptone solution to obtain a suspension containing approximately 10 ~11 log (CFU/mL) cells.

**Encapsulation of Bacterial Cells**

LGG encapsulated hydrogel particles were prepared by an extrusion method described by Qi et al [218] with a minor modification. Briefly, bacterial cell suspension was mixed with a polysaccharide solution to achieve a 2.0 % final polysaccharide concentration. The mixture was then transferred into a syringe (Fortuna brand glass Syringe-Metal luer lock tip, Air-Tite Products Co., Inc, VA, USA) with a 22–gauge blunt needle (Hamilton Company, Boston, MA, USA). A syringe pump (LEGATO® 100 syringe pump, KD Scientific Inc., MA, USA) was applied to extrude the mixed solution from the syringe to 100 mL 0.15 M $CaCl_2$ solution at an extrusion rate of 4 mL/min. The hydrogel particles were immediately formed when polysaccharide solution submersed into a continuously stirred $CaCl_2$ solution. The particles were kept in the solution for 30 min to complete the hardening. Afterwards, the hydrogel particles were harvested using a sieve and washed twice with ultrapure water. The final loading number of LGG reached approximate 9.2 log CFU/g particles. The total mass of polysaccharides (ALG-LMP or ALG–KC) was fixed at 2.0 % while proportion of individual polysaccharide was varied. Double-network hydrogel particles containing 0.2, 0.4, or 0.6 % LMP were named AP1, AP2, and AP3, respectively; while formulated with 0.2, 0.4, or 0.6 % KC were labelled as AC1, AC2, and AC3, respectively.

**Rheological Properties of Polysaccharide Solutions**

The apparent viscosity of each individual polysaccharide solution and the mixtures was measured using a Discovery Hybrid Rheometer–2 rheometer (TA Instruments Ltd., New Castle, DE, USA) as reported by Lan et al [19].

**Characterization of Particle Size and Shape**

ImageJ software (National Institutes of Health, Bethesda, MD, USA) was employed to characterize the particle size and shape (sphericity) using a method from Atia et al. [117] with some modifications. In brief, the image of particles with LGG being encapsulated was captured and 20 particles were randomly selected for ImageJ analysis. The diameters of a single particle in both horizontal and vertical directions were measured. The mean of the longer ($D_L$) and the shorter diameters ($D_S$) of each particle was used for the comparison of the particle size for each composition and the sphericity was characterized by the ratio of $D_L/D_S$.

**Textural Properties of Hydrogel Particles**

The textural properties of hydrogel particles were evaluated according to the previous study [218] with a minor modification. Briefly, samples were loaded on a Stable Micro Systems Texturometer model TA-XT2i (Texture Technologies Corp., White Plains, NY, USA) equipped with a 5 kg load cell. A 25 mm diameter cylindrical probe was applied on 5 g of harvested hydrogel particles for each treatment at a constant test speed velocity of 2 mm/s. The automatic detection of the contact between the probe and the particles was carried out with a contact force of 0.005 N. The rupture force measurements were carried out on the single particle of each treatment at the velocity of 5 mm/s in a compression mode by a probe with 2 mm diameter. The peak force was measured in Newtons and used to indicate the rapture force of a single hydrogel particle.

**Structural Properties of Hydrogel Particles**

Surface and cross-sectional morphology of probiotics encapsulated hydrogel particles were observed under scanning electron microscopy (SEM) (JEOL Mod. JSM-6490LV, Jeol,

Peabody, MA, USA) following the same procedure with the previous study [218]. The images were presented at 35×, 150×, 1000×, and 7500× magnifications.

**Fourier Transform Infrared Spectroscopy (FTIR)**

IR spectra of freeze-died hydrogel particles and polysaccharide powders (LMP, KC) were obtained by a Varian FTIR spectrophotometer (CA, USA) following the protocol developed by Lan et al. [186].

**Swelling and Shrinking Properties of Hydrogel Particles under Simulated GI Conditions**

Swelling (weight gain) or shrinking (weigh loss) properties of hydrogel particles in simulated digestion fluid were evaluated by measuring their weight change over time. To be detailed, 1.0 g of each sample was accurately weighed ($W_0$) and immersed in 9 mL of simulated gastric fluid (SGF, 0.08 M HCl, 0.2 % NaCl, pH 2.5)[90] with 0.3 % pepsin and incubated under 37 ℃ for 2 h at an agitation rate of 300 rpm. After rinsing the collected particles twice with ultrapure water, hydrogel particles were immersed to simulated intestinal fluid (SIF, 0.05M $KH_2PO_4$, 1% bile salt, 1% pancreatin, pH 7.4) for another 2.5 h [100]. During SGF incubation, the particles were collected by a sieve and the fluid on the surface of the hydrogel particles was drained to dryness by placing them in a petri dish filled with a layer of filter paper. For SIF incubation, the extra water on the hydrogel particles was absorbed as much as possible using soft tissue, and then the particles were directly transferred to the weighing tray to avoid any weight loss during operation. Then, the particles were taken to be weighed ($W_t$) again. The percent of shrinking and swelling of the particles at time t was calculated using Equation (1) and (2), respectively:

$$\text{Shrinking \%} = [(W_0 - W_t)/W_0] \times 100\% \quad (1)$$

$$\text{Swelling \%} = [(W_t - W_0)/W_0] \times 100\% \quad (2)$$

Where $W_t$ and $W_0$ was the weight of the particles at time t and time zero, respectively.

**Death Rate of the Encapsulated Cells under Simulated GI Conditions**

To determine the death rate of encapsulated LGG over the course of digestion, 1.0 g of freshly made hydrogel particles was added in a tube with 9 mL of SGF and incubated in an orbital shaker (MaxQ ™ 4000 Benchtop Orbital Shakers, Thermo Fisher Scientific Inc., USA) under 37 °C at 300 rpm for 2 h. The viable cells in hydrogel particles were measured at a 30 min interval. At each time point, the particles were filtered and rinsed by ultrapure water twice. Bacterial cells were released by smashing hydrogel particle with a hand blender (M133/128-0, Biospec Products, Inc., ESGC, Switzerland) in the presence of 9 mL sodium citrate solution (5.0 %). The viable cells were enumerated by plating the appropriate dilutions onto the MRS agar and incubating anaerobically under 37 °C for 48 h.

After 2 h of SGF incubation, 1.0 g of hydrogel particles was collected and rinsed twice before adding into a tube with 9 mL SIF. The tubes were again incubated under 37 °C at 300 rpm for 2.5 h. After incubation, the viable cells were released in the SIF by the hand blender and counted by the method mentioned earlier. Death rate of encapsulated LGG at a given digestion time was calculated using Equation (3).

$$\text{Death rate } \% = (1-N_t/N_0) \times 100\% \quad (3)$$

Where $N_t$ and $N_0$ was the viable cells at time t and time zero, respectively.

**Statistical Analysis**

The physicochemical properties of freeze-dried hydrogel particles were performed at least twice to achieve a consistent result. The viability of bacterial cells test and other measurements were repeated at least three times using freshly prepared samples and values were expressed as means ± SD. Significant differences between means ($p < 0.05$) were statistically

analyzed by one-way analysis of variance (ANOVA) (Version 9.3, SAS Institute Inc., NC, USA).

## Results and Discussions

### Rheological Properties of Biopolymer Solutions

It has been reported that the microstructure, shape, size and mechanical properties of hydrogel particles are influenced by the viscosity of polysaccharide solutions [227, 228]. Therefore, the viscosity of individual and the mixture of polysaccharide solutions was measured (**Fig. 3-1)**. In general, the apparent viscosity of all individual and the mixed polysaccharide solutions was decreased as shear rate increased from 0 to 80 $s^{-1}$, suggesting a shear thinning behavior. In terms of polysaccharide type, 2.0% KC solution exhibited the highest apparent viscosity, followed by ALG and LMP. As such, the mixture of KC with ALG had a higher apparent viscosity than it did with LMP at a same mass ratio. Previous studies indicated that the ideal viscosity range of polysaccharide solution to prepare hydrogel particles with good mechanical properties and desirable spherical shapes was between 0.06 and 0.5 Pa.s [227]. The viscosity of most of the polysaccharide solutions in this research fell into this range except for AP2, AP3, and LMP. Although hydrogel particles can still be formed by AP2 or AP3, the spherical morphology was impaired (as shown in **Fig. 3-2b**). On the other hand, if the viscosity of polysaccharide solutions is too high, it is very hard to extrude the solution as well as maintain the shape of the particles, which will then be deformed [229].

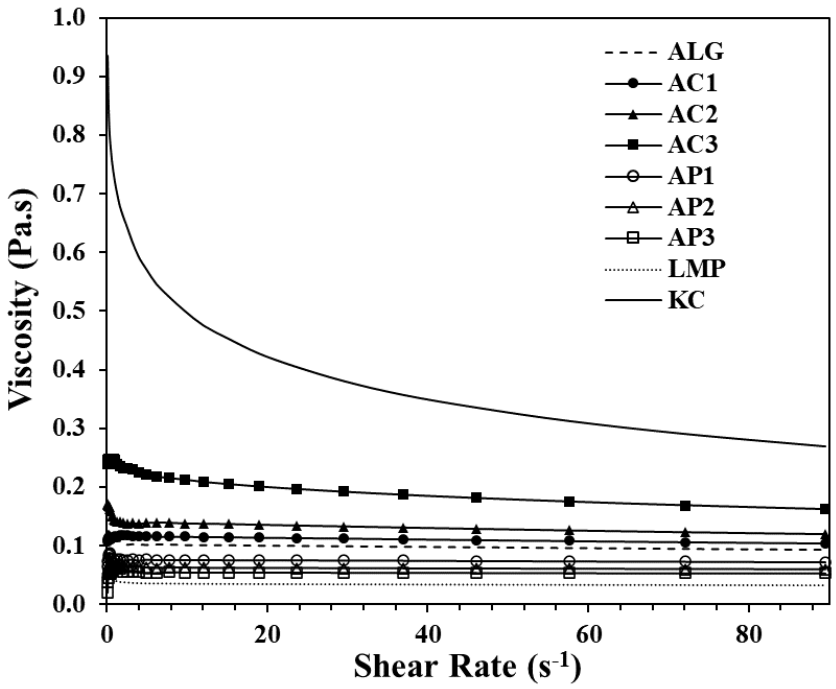


**Fig. 3-1.** Apparent viscosity of polysaccharide solutions (ALG: sodium alginate; AP: sodium alginate and low methoxyl pectin; AC: sodium alginate and κ-carrageenan; 1, 2, and 3 indicates the mass ratio at 1.8%: 0.2%, 1.6%:0.4%, and 1.4%:0.6%, respectively).

**Particle Size and Shape of Hydrogel Particles**

The diameters of each particle on two perpendicular directions were measured, the average of which was used to represent the mean diameter of hydrogel particles. The ratio between them ($D_L/D_S$) can estimate the sphericity of the hydrogel particles made from different compositions of polysaccharide (**Fig. 3-2**).

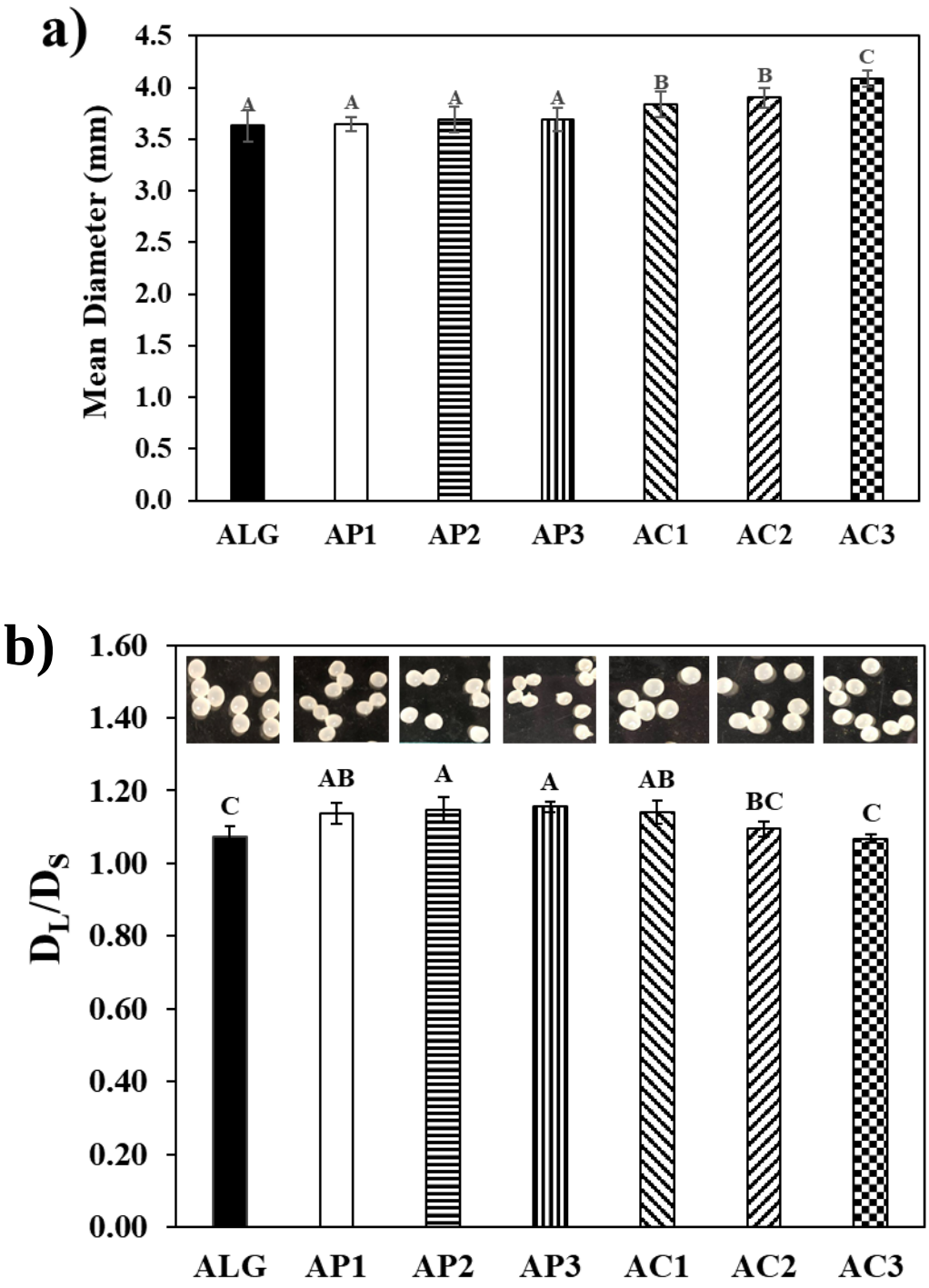


**Fig. 3-2.** (a) Mean diameter and (b) DL/DS ratio of hydrogel particles. (ALG: sodium alginate; AP: sodium alginate and low methoxyl pectin; AC: sodium alginate and κ-carrageenan; 1, 2, and 3 indicates the mass ratio at 1.8%: 0.2%, 1.6%:0.4%, and 1.4%:0.6%, respectively; the inserted images show the photographic image of hydrogel particles.) Different letters indicate that the means differ significantly ($p < 0.05$).

From **Fig. 3-2a**, the diameters of all hydrogel particles varied with different polysaccharide combinations ranging from 3.6 to 4.1mm. It is widely accepted that the size of hydrogel article is influenced by polysaccharide compositions and operation conditions such as diameter of nozzle, extrusion speed, etc. Therefore, a wide range of hydrogel particle size were reported. Zhao et al. reported a similar particle size range as in this study for the hydrogel particles made with ALG and skim milk [195]. In terms of polysaccharide composition, the samples made by ALG–LMP showed no significant difference ($p > 0.05$) on the diameter of hydrogel particles which was independent of their composition. It was observed that the diameter increased in ALG–KC hydrogel particles as the composition of KC increased, among which AC3 presented the biggest diameter. The boost in size as the ratio of KC increased in the mixture of ALG and KC was also observed in other research [230]. A positive correlation between the viscosity of polysaccharide solution and the size of hydrogel particle was reported previously [231]. In other words, biopolymer solution with a higher viscosity produces the larger size of hydrogel particles, which was corroborated by the apparent viscosity results where AC3 had the highest viscosity among all mixtures (**Fig. 3-1**). Such correlation may derive from the greater water holding capacity of KC that has a capability to incorporate more water into the hydrogel particle, hence increasing the size of hydrogel particles.

Regarding the shape of hydrogel particles, the ones fabricated by a single layer ALG or a double-network (AC2 or AC3) were of the most spherical shape in this study as their $D_L/D_S$ ratio was close to 1.00. The remaining four samples showed a ruptured or irregular shape, especially AP2 and AP3 hydrogel particles (inserted image in **Fig. 3-2b**). This result indicated that the substitution of LMP to ALG jeopardized the sphericity of ALG-based hydrogel particles which was in consistent with previous studies [224, 232, 233]. The possible assumption was that the weaker

mechanical strength of pectin-$Ca^{2+}$ network compared to that of alginate-$Ca^{2+}$. When it came to KC, such impact only occurred at a lower KC concentration (0.2%), indicating higher viscosity of KC compensated for the weaker mechanical strength and maintained the spherical shape of the particles. Davarcı et.al. claimed that the higher viscosity helped maintain the spherical shape of hydrogel particles [227]. Although there was a slight difference in particle shape among different polysaccharide solutions, hydrogel particles could still be successfully formed for all tested polysaccharide mixtures, as can be seen in the photographic images in **Fig. 3-2b**.

**Textural Properties of Hydrogel Particles**

It has been reported that the textural properties of hydrogel particles are largely dependent on biopolymer composition and concentration, and the cross-linking agent type and concentration [153, 205, 234]. In this study, the textural profile (hardness, cohesiveness, resilience, and springiness) of batch of bulk hydrogel particles and the rupture force of a single hydrogel particle were characterized (**Table 3-1)**.

**Table 3-1.** Textural profile of the fresh hydrogel particles with different compositions.

| | **Hardness** | **Rupture Force** | **Cohesiveness** | **Resilience** | **Springiness** |
|---|---|---|---|---|---|
| | **(N)** | **(N)** | | | |
| **ALG** | 11.86 ± 0.68 A* | 2.021 ± 0.17 A | 5.04 ± 0.26 C | 0.423 ± 0.01 A | 1.641 ± 0.26 A |
| **AP1** | 10.42 ± 0.96 ABC | 1.799 ± 0.08 B | 5.47 ± 0.44 BC | 0.442 ± 0.02 A | 1.778 ± 0.18 A |
| **AP2** | 10.44 ± 0.06 ABC | 1.614 ± 0.05 C | 6.42 ± 0.20 AB | 0.435 ± 0.01 A | 1.771 ± 0.03 A |
| **AP3** | 9.40 ± 0.33 C | 1.485 ± 0.07 CD | 6.91 ± 0.32 A | 0.436 ± 0.06 A | 1.758 ± 0.01 A |
| **AC1** | 11.26 ± 0.80 A | 1.375 ± 0.05 D | 4.96 ± 0.52 C | 0.434 ± 0.04 A | 1.776 ± 0.07 A |
| **AC2** | 10.13 ± 0.28 BC | 1.033 ± 0.06 E | 3.44 ± 0.45 D | 0.396 ± 0.04 A | 1.760 ± 0.01 A |
| **AC3** | 10.78 ± 0.85 ABC | 0.790 ± 0.01 F | 2.98 ± 0.20 D | 0.364 ± 0.01 A | 1.810 ± 0.08 A |

* Different letters indicate that the intraspecific means differ significantly ($p$ <0.05).

Among all the parameters presented in **Table 3-1**, statistically significant differences ($p$ < 0.05) were observed among samples for hardness, cohesiveness and rupture force. For example, the hardness of samples containing LMP showed a declining trend with the increment of LMP

concentration. The lowest hardness was obtained in AP3 which was significantly lower than that of ALG. As similar pattern was recorded for samples containing KC in which the addition of KC reduced the hardness of hydrogel particles compared with control (ALG). These results indicated that the addition of the secondary polysaccharide in ALG tended to impair the mechanical properties of ALG hydrogel, which agrees with previous research [235]. A lower level of LMP or KC can actually uphold a comparable hardness. This phenomenon again could be explained by the weaker network between secondary polysaccharide and gelling agent $Ca^{2+}$ than between alginate and $Ca^{2+}$. This can be supported by the decrease in rupture force, the force that is needed to break a single particle, in the presence of LMP or KC [236]. Interestingly, incompatible hardness results for ALG–LMP and ALG–KC hydrogel particles was also found in literature [205]. Indeed, the textural properties of hydrogel particles can be influenced by many extrinsic factors such as $Ca^{2+}$ concentration and gel strength. In general, hardness is much higher as $Ca^{2+}$ concentration increased [237]. The cohesiveness describes the force needed to deform the hydrogel particles in the downward movement of the probe. It is a common indicator to evaluate the applicability and biocompatibility of hydrogel for pharmaceutical and cosmetic application [238, 239]. In thus experiment, addition of KC or LMP shifted the tendency of the cohesiveness to two opposite directions. The cohesiveness of the hydrogel particles was enhanced as more LMP was presented; on the other hand, an increase in KC content decreased the cohesiveness. This result indicated that double-network hydrogel particles prepared exclusively by ALG–LMP had the tendency to hold together rather than crumble/break/rupture [240].

**Surface and Cross-sectional Morphology of Hydrogel Particles**

In order to better understand how the secondary polysaccharide (LMP or KC) impacts the microstructure of ALG-based double-network hydrogel particles, the morphological changes of hydrogel particles were evaluated using SEM (**Fig. 3-3**).

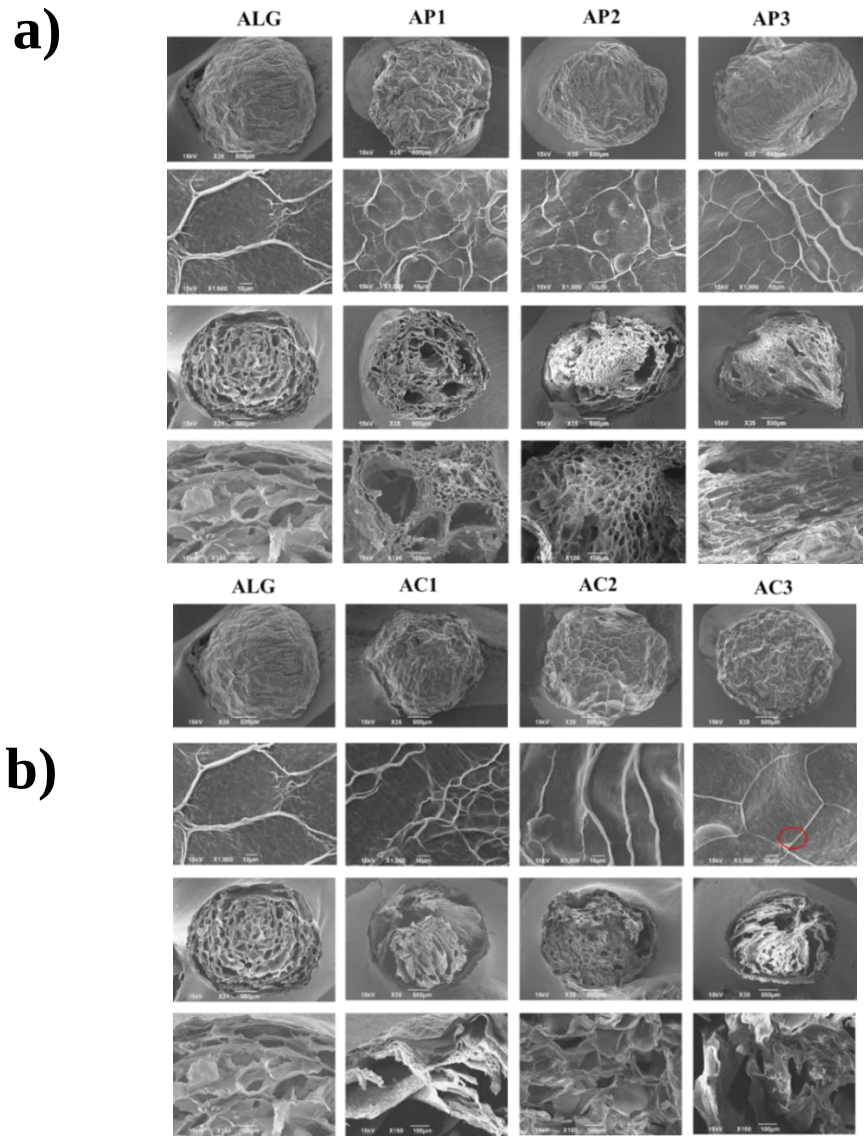


**Fig. 3-3.** Surface and cross-sectional images of *Lactobacillus rhamnosus* GG (LGG) encapsulated in freeze-dried hydrogel particles containing (a) LMP and ALG; (b) KC and ALG under SEM at different magnifications (x35, x1,000 and x7,500 respectively) (ALG: sodium alginate; AP: sodium alginate and low methoxyl pectin; AC: sodium alginate and κ-carrageenan; 1, 2, and 3 indicates the mass ratio at 1.8%: 0.2%, 1.6%:0.4%, and 1.4%:0.6%, respectively).

For easier illustration, the double-network hydrogel particles containing secondary polysaccharide (LMP or KC) were compared to the single ALG hydrogel particles separately. The first two rows represented the surface of the hydrogel particles under different magnifications and the last two rows represented the cross-section of the same samples. A number of studies have reported that pre-treatment with liquid nitrogen prior to freeze-drying process can quickly sublimate the frozen water in hydrogel particles, thus minimizing the shrink of particles and maintain the microstructures closer to their original situation [241]. According to the SEM observation, the wrinkle surface and porous interior structure inevitably appeared even following the same sample preparation method, presumably because of the inherent high water content facilitating the fast formation of bigger crystals rather than sublimation [199]. From both the surface and cross-section images, it was clear that all the AGL–LMP samples (AP1, AP2, and AP3) underwent deformation to some extent (**Fig. 3-3a**); while ALG, AC2, and AC3 particles (**Fig. 3-3b**) maintained a highly spherical shape. This was coincided with the particle shape results of fresh hydrogel samples (**Fig. 3-1b**). Besides, a typical vein-like structure stemming from ionically cross-linked $Ca^{2+}$–polysaccharide hydrogel was spotted on the surface of all samples under 1,000× magnification [11, 76, 234, 242]. However, this structure became weaker in AC3 (circled out in **Fig. 3-3b**) which may allow the encapsulated cell escaping from the particle and exposing to exterior environment. Such alterations on morphology might be a result of the antagonistic effect of the weakened mechanical strength and higher water content of the hydrogel particles in the presence of KC and it is highly possible that such effect was also exhibited in AC1 and AC2 albeit to a lesser extent to be observed in SEM. The surface images under higher magnification (7,500×) confirmed this assumption. Moreover, the surface of ALG–KC particles, especially AC2 and AC3 tended to be rougher and bumpy instead of wrinkled and folded

surface. As such, the probiotics were embedded on these surface shallowly without the presence of folded structure.

Additionally, the cross-sectional images also provided information on the interior structures of the freeze-dried hydrogel particles. Despite of the porous and partially collapsed structure caused by freeze-drying, it was observed from **Fig. 3-3a** that AP1 had more amount of larger cavities compared to ALG which may be more prone for the encapsulated cells to loss their viability in the harsh condition; for example, it is easier for $H^+$ in stomach fluid to diffuse into such particle and deactivate the encapsulated LGG [87]. The pores in AP2 and AP3 were relatively evenly distributed and appeared to be more compact with increased concentration of LMP to 0.4 or 0.6%. Nevertheless, the structure of AP3 was elongated which might be caused by the deformation during extrusion. Taking the regularity and uniformity into consideration, AP2 showed a better morphology in the ALG–LMP group. By replacing LMP with KC in double-network hydrogels, the interior structures of AC1 and AC3 were highly open with the appearance of multiple large cavities or interrupted junctions; while AC2 showed a more regular and comparable structure with ALG. Intriguingly, the microstructure of ALG–KC hydrogel particles did not follow a similar trend as ALG–LMP did upon raising the concentration of KC. When a low concentration of KC (0.2 %) was applied, the decreased ionic bonding between the carboxyl group of KC and $Ca^{2+}$ in the whole network rendered the collapse of the structure. Conversely, the big cavities in AC3 were mainly attributed to the excess water in the particles as a result of the escalated water holding capacity of KC rather than to the collapse of $Ca^{2+}$–ALG cross linking. At an intermediate KC concentration (0.4%), the hydrogen bonds formed by the sulfate ester groups may hold the extra water in the hydrogel particles by the medium dose of KC, giving rise to a balanced force to hold the entity of AC2. Overall, the results indicated that

both the type of secondary polysaccharide and the alginate/secondary polysaccharide ratio determine morphology and porosity of hydrogel particles.

**FTIR Spectrum of the Freeze-dried Hydrogel Particles**

FTIR spectra of the freeze-dried hydrogel particles were recorded in the wavenumber range of 4000–750 $cm^{-1}$ to gain insight into the impact of polysaccharide type and concentrations on the structure of hydrogel particles. **Fig. 3-4a** presented the spectra of hydrogel particles carrying ALG and LMP, and controls (LMP and ALG powder). In the case of ALG, some common bands of polysaccharides were exhibited, such as the broad O–H stretching band around 3600–3000 $cm^{-1}$ corresponding to the inner- and intra-molecular hydrogen bonds [243, 244], the stretching band of carbonyl group (C=O) at 1741 $cm^{-1}$ [245, 246], and the C–O–C stretching vibration at 1023 $cm^{-1}$ and 1079 $cm^{-1}$, respectively [247, 248]. Besides, the characteristic absorption bands of ALG at 1595 $cm^{-1}$ and 1420 $cm^{-1}$ (asymmetric and symmetric –COOH stretching bands) were also registered [193, 249]. In addition to a broad O–H stretching band and C–O–C stretching vibration, the spectrum of LMP displayed a peak at 1731 $cm^{-1}$ corresponding to the carbonyl group of the esterified carboxylic acid [134]. The addition of LMP to ALG showed no significant difference on the spectra but slightly shifted the peak of C=O (as circled in **Fig. 3-4a)** in AP1, AP2, and AP3 towards the lower wavenumbers.

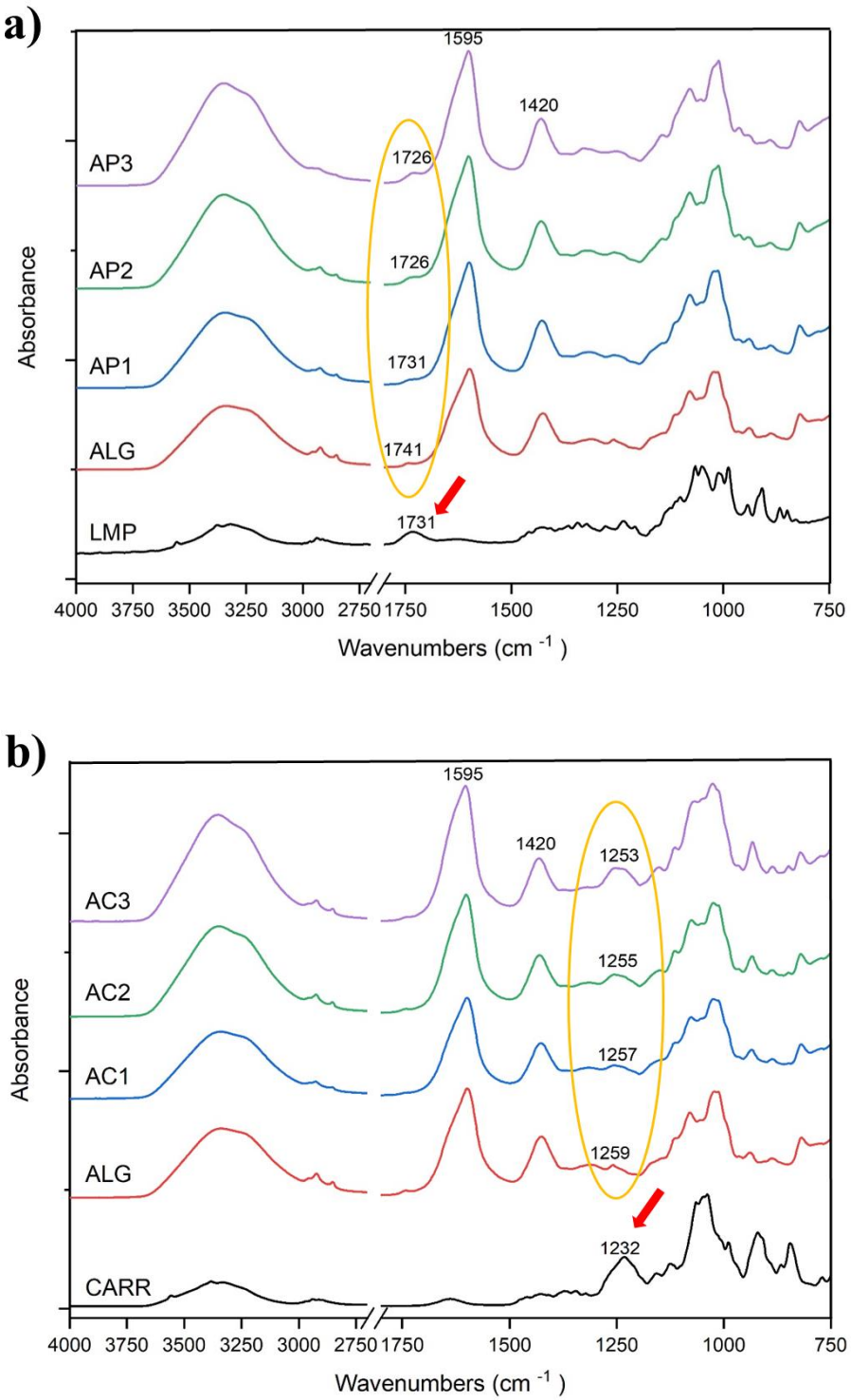


**Fig. 3-4.** FTIR spectra of hydrogel particles formed by (a) LMP and ALG; (b) KC and ALG (ALG: sodium alginate; AP: sodium alginate and low methoxyl pectin; AC: sodium alginate and κ-carrageenan; 1, 2, and 3 indicates the mass ratio at 1.8%: 0.2%, 1.6%:0.4%, and 1.4%:0.6%, respectively).

With respect to the spectrum of KC (**Fig. 3-4b**), it exhibited a broad O–H stretching band between 3600–3000 $cm^{-1}$ along with two peaks appeared at 922 $cm^{-1}$ and 1065 $cm^{-1}$ corresponding to the 3,6-anhydro-d-galactose, and glycosidic linkage, respectively [230]. The peak at 1640 $cm^{-1}$ could be assigned to the O–H bending from the absorbed water [250, 251]. The characteristic peak at 1232 $cm^{-1}$ was attributed to the stretching vibration of S=O from the sulfate ester groups. In terms of ALG–KC mixtures, the characteristic band of KC altered the spectra of AC1, AC2, and AC3 into a broad and shoulder-like shape at around 1250–1230 $cm^{-1}$ (circled in **Fig. 3-4b**). In short, slight changes in the spectra of double-network hydrogel particles induced by the characteristic peaks of LMP or KC demonstrated the miscibility of polysaccharides and the generation of cross-linking in mixed polysaccharides.

**Shrinking and Swelling Behaviors of Hydrogel Particles during Simulated GI Digestion**

The influence of polysaccharide type and concentrations on the shrinking and swelling properties of ALG-based double-network hydrogel particles during simulated sequential GI tract digestion was determined (**Fig. 3-5**). In general, all hydrogel particles shrank to a certain degree over the course of 2 h SGF. Particularly, the shrinking percentage of single layer ALG reached 16.9% after 1 h of digestion and a slight increase (18.9%) was observed after the whole SGF digestion. Similar shrinking behaviors were found in double-network hydrogel particles with a lower LMP or KC concentration (0.2%). The shrinking was substantially suppressed as more secondary polysaccharide was involved which was independent of incubation time (**Fig. 3-5a**). The pH-dependent swelling behavior of hydrogel particles has been well documented. This is because the hydrogels contain pH-dependent functional groups such as carboxyl groups (guluronic acid and mannuronic acid) in ALG. When the environmental pH is above pKa of the functional groups, the repulsion between deprotonated functional groups accounts for the

swelling behavior. On the contrary, the attractive forces (H-bond) between functional groups in polysaccharides dominates the system as the pH is below their pKa as was the case in SGF (pH 2.5), resulting in a shrunken hydrogel with denser textures (**Fig. 3-5c**). A partial replacement of ALG by LMP or KC could counteract such attractive force, thus restraining hydrogel particles from shrinking in SGF. In terms of polysaccharide type, LMP seemed to provide better protection for the particles against severe shrinkage compared to KC. This is reasonable as the pH of SGF was higher than the pKa of LMP (2.0) while it was lower than both ALG (3.5) and KC (4.9) [252-254]. Hence, $Ca^{2+}$–alginate–pectin gels bearing more electrostatic repulsive force had lower shrinking percentage than that of $Ca^{2+}$–alginate–κ-carrageenan hydrogels.

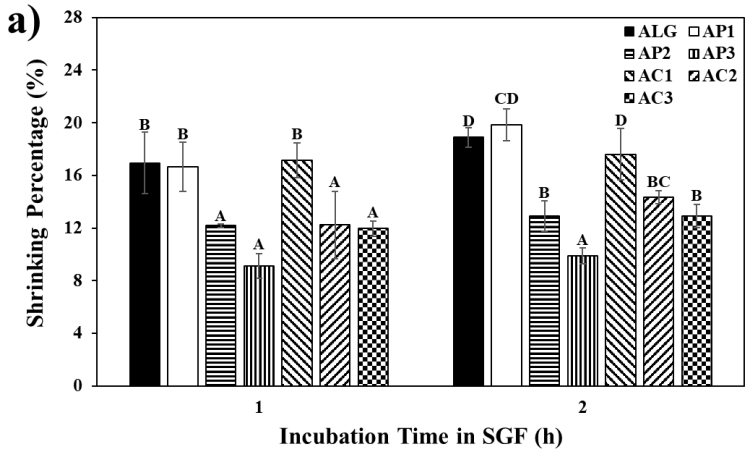


**Fig. 3-5.** Shrinking and swelling properties of hydrogel particles incubated in simulated sequential gastrointestinal (GI) tract (a) in the simulated gastric fluid (SGF) at 1 and 2h; and (b) in the simulated intestinal fluid (SIF) at 1, 2 and 2.5 h, and (c) photographic image of hydrogel particles at corresponding time points. (ALG: sodium alginate; AP: sodium alginate and low methoxyl pectin; AC: sodium alginate and κ-carrageenan; 1, 2, and 3 indicates the mass ratio at 1.8%: 0.2%, 1.6%:0.4%, and 1.4%:0.6%, respectively. Different letters at the same time point indicate that the means differ significantly ($p < 0.05$).

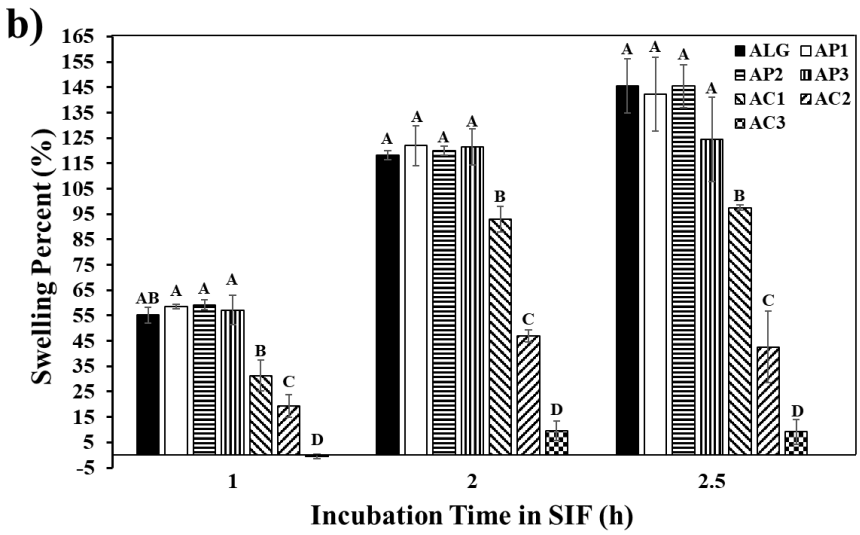


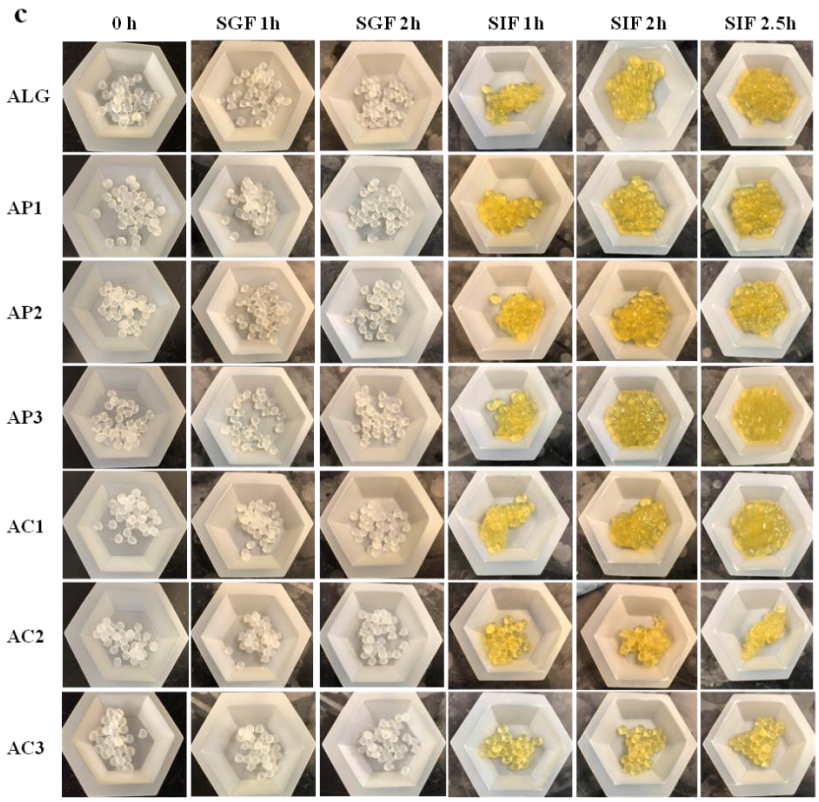


c)

**Fig. 3-5.** Shrinking and swelling properties of hydrogel particles incubated in simulated sequential gastrointestinal (GI) tract (continued). (a) in the simulated gastric fluid (SGF) at 1 and 2h; and (b) in the simulated intestinal fluid (SIF) at 1, 2 and 2.5 h, and (c) photographic image of hydrogel particles at corresponding time points. (ALG: sodium alginate; AP: sodium alginate and low methoxyl pectin; AC: sodium alginate and κ-carrageenan; 1, 2, and 3 indicates the mass ratio at 1.8%: 0.2%, 1.6%:0.4%, and 1.4%:0.6%, respectively. Different letters at the same time point indicate that the means differ significantly ($p < 0.05$).

In order to better reflect the real digestion, a sequential digestion measurement was designed by transferring the SGF digested hydrogel particles directly into SIF after rinsing (**Fig. 3-5b**). Hydrogel particles with pectin showed similar swelling behavior as ALG throughout the SIF digestion except AP3 in which a reduction of swelling percentage took place after 2 h of digestion. By contrast, the presence of KC actually nullified the swelling behavior of ALG even after 1 h of digestion; and this effect became more obvious as the percent of KC increased. These particles were also brittle with ease to shatter instead of dissolving in the SIF, which can barely maintain an intact shape at the end of simulated digestion. A reduction of swelling percentage in ALG–KC hydrogel particles was reported previously which was interpreted by the reinforced gel network by the hydrogen bond between the two polysaccharides and/or a cross-linking effect of calcium ions [234]. The reduced swelling behavior is unfavorable to the fast release of bioactive compound in small intestine. In term of digestion time, swelling behavior reached the equilibrium after 2 h. Combining both shrinking and swelling properties, the double-network hydrogel particles prepared by AP1 are particularly desirable among all seven formulas as they had lowest shrinking percentages at SGF to protect the encapsulated compounds while having the greatest swelling at SIF to release them.

**Viability of the Encapsulated LGG in Simulated GI Digestion**

Lastly, the probiotics protection of hydrogel particles prepared by different polysaccharide mixtures in the simulated sequential digestion system were evaluated (**Fig. 3-6)**. The death rate, which is calculated as the percentage of dead cell at each time point divided by the initially live cell count, was used as an indicator to compare how LGG survived during digestion when encapsulated in different hydrogel particles. This part of the experiment had been repeated for at least five times in order to achieve a relatively consistent result.

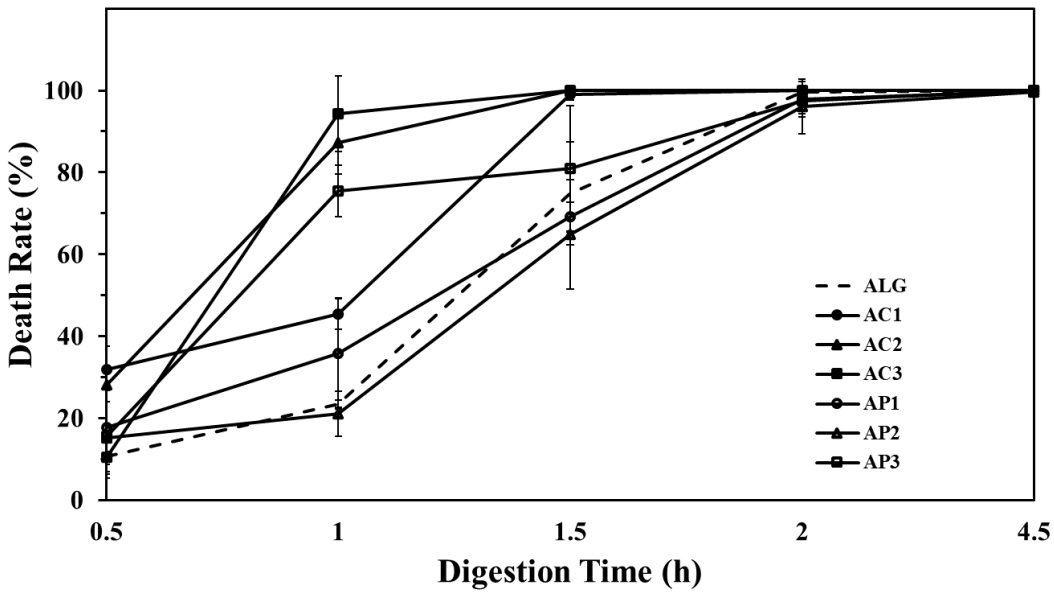


**Fig. 3-6.** Death rate of encapsulated LGG in hydrogel particles formed by different polysaccharide solutions at different time points during simulated sequential GI digestion (ALG: sodium alginate; AP: sodium alginate and low methoxyl pectin; AC: sodium alginate and κ-carrageenan; 1, 2, and 3 indicates the mass ratio at 1.8%: 0.2%, 1.6%:0.4%, and 1.4%:0.6%, respectively).

After 30 minof digestion in SGF, LGG in AC1 and AC2 showed significantly higher ($p$ < 0.05) death rate; while it remained a comparable death rate in the rest of hydrogels (11%–18%). After 1 h of digestion in SGF, the death rate of LGG in AP3, AC2, and AC3 increased drastically to 75%, 87%, and 94%, respectively. The death rate of LGG in other hydrogel particles including ALG, AP1, AP2, and AC1 also raised but to a lesser rate, among which AP2 endowed the greatest protection against the death of LGG. As the digestion time exceeded 1.5 h, a death rate of > 90% was observed for LGG in ALG–KC double-network hydrogel particles, which indicated that the substitution of ALG by KC (0.2, 0.4, or 0.6%) accelerated the death of the probiotics. The presence of KC weakening the total mechanical strength of the hydrogel particles as evidenced by texture analyzer results (**Table 3-1**) may account for the poor viability of probiotics the hydrogel particles encapsulated. Besides, the detainment of harsh gastric fluid in

the particles to interact with LGG may be facilitated in the wake of the increased water holding capacity of ALG–KC hydrogel particles. It wasobserved from the SEM images that the cross-linking vein structure disappeared and the surface exhibited distinct wrinkles and folds as the KC concentration increased (**Fig. 3-3b**). Such structure aided the exposure of the undefendable probiotics to the stressful environment conditions such as gastric condition in the case of simulated digestion. After 2 h of digestion, the death rate of LGG in AC1, AC2, and AC3 reached 100%, indicating viable cells were not detectableby the plate count method. Overall, these results ruled out the use of KC in the alginate-based double-network hydrogel to encapsulate probiotics for improved viability.

On the other hand, LGG in ALG–LMP double-network hydrogel particles maintained a comparable death rate as it in ALG after 1.5 h of SGF digestion, with AP2 offering the best protection followed by AP1. The results indicated that the mixing ratio between alginate and pectin influenced not only the microstructure of hydrogel particles, but also the viability of encapsulated probiotics during digestion. The dense network areas with homogeneous distribution of small pore of gelling network in AP2 (0.4% LMP) might have contributed to the improved protection against LGG death. Whereas the death rate of LGG was above 95% at the end of SGF digestion (2 h), it was still the lowest when encapsulated in ALG–LMP, again demonstrating the protective effect of LMP against the death of LGG.

Among all the samples incubated at the end of the simulated intestinal digestion (4.5 h), LGG in AP2 showed a lowest death rate follow by it in AP1 although statistically they were identical. All these results indicated that ALG–LMP double-network protected the encapsulated LGG to a greater level than ALG–KC. Therefore, AP2 provided a better protection to the entrapped LGG during simulated sequential GI digestion. It has been reported that gelling

mechanisms are different among the pure alginate, pure pectin, and alginate–pectin mixture. A "egg box" model has been proposed to describe the cross-linking gel network structure of $Ca^{2+}$–alginate, and the shifted "egg-box" model is used to explain the cross-linking network gel structure of $Ca^{2+}$–pectin [237]. However, in the case of the $Ca^{2+}$–alginate–pectin double-network system, the binding mechanism of polysaccharides with $Ca^{2+}$ becomes more comprehensive due to the potential interactions between alginate and pectin. Further studies will be necessary to understand gelling mechanism so as to completely explain the protective effect provided by pectin in alginate–pectin double-network hydrogel particles.

## Conclusions

In this study, double-network hydrogel particles using two different types of polysaccharide mixtures (ALG–LMP or ALG–KC) at a fixed total concentration (2.0%) but diverse mixing ratios (1.8%:0.2%, 1.6%:0.4%, and 1.4%:0.6%) were fabricated. The physicochemical properties of hydrogel particles including particle size, shape, textural and morphological properties were examined. Furthermore, the swelling properties and death rate of LGG in hydrogel particles were evaluated in simulated sequential GI digestion at different time points. In general, LGG encapsulated hydrogel particles could be successfully fabricated using abovemetioned polysaccharide compositions via ionically cross-linking as evidenced by FTIR and SEM images. The apparent viscosity of polysaccharide solutions had a positive effect on the spherical shape and size of hydrogel particles. ALG–KC group had a larger particle size than that of ALG–LMP group and control sample (ALG) because of its higher apparent viscosity. Texture properties and microstructure of ALG-based hydrogel particles was also altered upon the addition of secondary polysaccharide. Specifically, the hardness and rupture force of particles decreased appreciably with the addition of secondary polysaccharide (LMP or KC).

Interestingly, the cohesiveness of ALG–LMP group increased as the LMP concentration increased compared with control; while an opposite trend was appeared in ALG–KC group as the increase of KC concentration. This phenomenon suggested that ALG–LMP double-network hydrogel particles had the tendency to hold together to reinforce the structure. In terms of microstructure of hydrogel particles, ionically cross-linked vein like surface structure was gradually disappeared with increased KC concentration in ALG–KC group. Additionally, the cross-sectional SEM image of ALG–KC showed more cavities compared to ALG–LMP or control group. As a consequence, probiotics encapsulated in ALG–KC double-network hydrogel particles had the highest death rate among all treatments. The lowest death rate of LGG was found in ALG–LMP (AP2) with mixing ratio of 1.6%:0.4%. This is because AP2 featured uniformed morphological properties, giving rise to less shrinking in SGF and more open space (swelling) in SIF.

# CHAPTER 4. THE VIABILITY OF COMPLEX COACERVATES ENCAPSULATED PROBIOTICS DURING SIMULATED SEQUENTIAL GASTROINTESTINAL DIGESTION AS AFFECTED BY WALL MATERIALS AND DRYING METHODS


## Abstract

The objective of this study was to investigate the impact of protein type (sodium caseinate and pea protein isolate), protein to sugar beet pectin (SBP)ratio (5:1 and 2:1) on complex coacervation formation, as well as the impact of finishing technology (freeze-drying and spray-drying) on improving the viability of encapsulated *Lactobacillus rhamnosus* GG (LGG) in the complex coacervates during simulated sequential gastrointestinal (GI) digestion. The physicochemical properties of LGG encapsulated microcapsules in liquid and powder form were evaluated. The state diagram and ζ-potential results indicated that pH 3.0 was the optimum pH for coacervates formation in the current systems. Confocal laser scanning microscopy (CLSM), viscoelastic analysis, and Fourier transform infrared spectroscopy (FTIR) confirmed that the gel-like network structure of complex coacervates were successfully formed between protein and SBP at pH 3.0 through electrostatic interaction. In terms of physiochemical properties and viability of LGG encapsulated in the microcapsules powder, drying method played a crucial role on particle size, microstructure and death rate of encapsulated LGG during simulated sequential GI digestion compared to protein type and biopolymer mixing ratio. For example, the microstructure of spray-dried microcapsules exhibited smaller spherical particles with some cavities, whereas the larger particle size of freeze-dried samples showed porous sponge network structure with larger particle sizes. As a result, spray-dried LGG microcapsules generally had a lower death rate during simulated sequential gastrointestinal digestion compared to the freeze-dried counterpart. Among all samples, spray-dried PPI–SBP microcapsules

demonstrated superior performance against cell loss and maintained more than 7.5 Log CFU/g viable cells after digestion.

## Introduction

Probiotics are living microorganisms that can confer the host with numerous health benefits, such as anti-pathogenic activity [2, 31], anti-diabetic activity [3], anti-inflammatory activity [32, 255], anti-allergic activity [33, 34], and potential anti-cancer activity [4]. A number of probiotics like *Lactobacillus* and *Bifidobacterium,* as well as some other species including *Escherichia*, *Saccharomyces*, *Bacillus*, *Streptococcus* and *Propionibacterium* have been applied in a wide range of functional foods, beverages, supplements, and pharmaceuticals [256]. However, these potential health benefits offered by the probiotics can only be achieved if sufficient numbers of live cells are maintained after passing through the human gastrointestinal (GI) tract. The common consensus of attaining these benefits is that the number of probiotics should be no less than $10^6$ viable cells per dose/day for supplement at the time of consumption [54]. Nevertheless, majority of the probiotics have remarkable loss of their viability after they pass through the GI tract because of their poor tolerance of low pH at stomach and high bile salt concentration in small intestine. As such, various encapsulation techniques have been explored for improving the viability of the probiotics during GI tract [170].

Among most of the techniques, complex coacervation is one of the most promising encapsulation techniques due to its relatively high encapsulation yield and biocompatibility, as well as good protection effect under acidic pH [18]. In general, complex coacervation is an associative phase separation phenomenon originated from electrostatic attraction between two oppositely charged biopolymers [81]. Depending on the strength of electrostatic attraction, the biopolymer mixture can be separated into solvent-rich phase and biopolymer-rich phase. The

biopolymer rich phase is a gel-like structure that can be applied as wall materials for encapsulating probiotics. Previous studies have proved that complex coacervates have a favorable impact on improving the viability of the encapsulated probiotics [22, 76, 84]. The typical procedure of forming probiotics encapsulated in complex coacervation starts with mixing of probiotics with protein–polysaccharide solution at a proper mass ratio, followed by the adjustment of pH of this ternary mixture to a certain pH to induce phase separations between the biopolymers and solution. At last, the liquid probiotics encapsulated by means of complex coacervates can be turned into powder form through drying processing. The physical properties of complex coacervates are dependent of several factors, such as wall material compositions, the mass ratio between protein–polysaccharide, and optimum complex coacervates formation pH [19]. These factors also determine the functional performance of complex coacervates as a microencapsulation wall material for protecting the viability of probiotics under harsh conditions.

Regarding the complex coacervates formula, the inherent physiochemical properties (e.g. charge density and protein structure) of proteins from different sources greatly influence the formation of complex coacervates [257]. One would expect that the type of protein is critical for complex coacervate systems to successfully enhance the viability of the microencapsulated probiotics. Animal proteins, such as gelatin [21, 258], sodium caseinate (SC) [22], and whey protein [23] have been widely applied in the formation of complex coacervates to encapsulate probiotics over the last few years, owing to their flexibility for encapsulating any types of probiotics [259]. Among them, SC seemed to have advantages of protecting probiotics during thermal processing and GI tract because of its more hydrophobic and higher thermal stability properties [24]. On the other hand, the trend to fabricate of pea protein-based complex coacervates as microencapsulation

vehicles is on a quick rise due to the emerging usages of plant-based ingredients in food systems [25, 26]. However, the protective effects of plant protein-based complex coacervates as capsule materials on the encapsulated probiotics has yet to be explored.

Upon formation of complex coacervates encapsulated probiotics, drying is the last step to develop commercially available probiotics functional foods. In general, spray-drying and freeze-drying are the two most common methods for drying microcapsules of probiotics, with which different microstructure is formed [27]. Freeze-drying is a mild technology for protecting viability of probiotics during drying processing; it, however, cannot efficiently reduce the particle size of microcapsules as compared to spray-drying. To date, there are few studies which focus on the drying methods on viability and functionality of probiotics [28]. Consequently, it is necessary to take into account drying processing in combination of complex coacervates formula on the viability of probiotics.

This study was aimed to gain more insights into how protein type and drying processing influence the physicochemical properties of complex coacervates and the protective effects on probiotics. Two different proteins (SC and pea protein isolate) were selected to form complex coacervates with sugar beet pectin (SBP) to improve the viability of a well-studied probiotic strain, *Lactobacillus rhamnosus* GG (LGG) during simulated sequential GI digestion. Besides, considering the application of complex coacervates in the food systems, two different drying methods (i.e. spray-drying and freeze-drying) were employed to transform gel-like complex coacervates to powder form and to compare their impact on the viability of probiotics. Therefore, this investigation was undertaken to i) optimize the complex coacervates formation pH between protein–SBP at different mixing ratios, ii) characterize the physicochemical properties of LGG encapsulated microcapsules by means of complex coacervates, and iii) compare different

proteins and drying methods on the improvement of the viability of encapsulated LGG during GI tract.

## Materials and Methods

### Materials

Freeze-dried pea protein isolate (PPI) was extracted from yellow pea flour by alkali extraction-isoelectric precipitated method, as described by [19] without any modification. The final PPI powder contains 79.50% protein (wet basis, %N × 6.25) according to the results obtained from LECO combustion analyzer (St. Joseph, MI). Sugar beet pectin (SBP) (Betapec RU301, Lot # 11710767, 45 kDa Mw, 55% of degree of esterification (DE), 65% of galacturonic acid, as reported by the manufacturer) was kindly donated by Herbstreith & Fox KG (Neuenbürg, Germany) and used without any purification. Sodium caseinate (SC) from bovine milk (C8654, Lot # SLBS5159), potassium phosphate monobasic, and potassium phosphate monobasic were purchased from Sigma-Aldrich (St. Louis, MO, USA). CRITERION™ Lactobacilli MRS broth was purchased from Hardy Diagnostics (Santa Maria, CA, USA). MRS agar and the multi-use sachets with indicator for creating anaerobic atmosphere were obtained from BD (Franklin Lakes, NJ, USA). Other chemicals and reagents used in this study were of analytical grade and purchased from VWR (Chicago, Illinois, USA). All solutions were prepared using ultrapure distilled de-ionized water (DDW, 18.2 MΩ cm) by the Barnstead Nanopure ultrapure water system (Thermo Scientific, Waltham, MA, USA).

### Optimization of pH Condition for Complex Coacervates Formation

#### *Preparation of biopolymer stock solutions*

Both PPI (2.0 wt%) and SBP stock solutions (2.0 wt%) were prepared according to the previous published procedure without any modification [26]. SC stock solution (2.0 wt%) was

prepared by dispersing SC into 10 mM phosphate buffer (pH 7.0) and stirred at 500 rpm for 12 h at 25 °C, and then adjusted to pH 7.0 using 0.1 M NaOH.

***Preparation of biopolymer mixtures***

The protein concentration was fixed at 1.0 wt% and the SBP concentration was varied to achieve the initial protein–SBP ratio at 5:1 and 2:1. The pH of biopolymer mixture was then adjusted from 5.0 to 2.5 with 0.5 decrement by the addition of HCl with various concentrations (0.1, 0.3, 0.6, 0.9, 2.0 M) to minimize dilution effects as well as conductivity changes in mixture [260].

***Optimizing the pH Condition for complex coacervation between protein and SBP***

*Construction of state diagram*

The biopolymer mixtures prepared in section 2.2.2 were left to stand static for 24h at 4°C to allow phase separation, the state diagram of protein–SBP mixtures was constructed based on visual observation as stated by Lan et al. [19]. Three different symbols were applied to describe different phase behaviors of the observed phase separations in the test tubes; they were □, ▲, and ■ which represented turbid solution, precipitation & cloudy solution, and precipitation & clear solution, respectively.

*Surface charge analysis*

Surface charges of single biopolymer solutions (1.0 wt% SC, PPI, and SBP) and protein–SBP mixtures were measured using a Zetasizer Nano-ZS 90 (Malvern Instruments, Worcestershire, UK), and reported as zeta-potential (ζ, mV).

**Encapsulation of Probiotics in Protein-SBP Complex Coacervates**

LGG bacterial cells were cultured in MRS broth at 37 °C under anaerobic condition. After second revival of this strain in MRS broth, the bacterial pellet was obtained by

centrifugation at 3,500 rpm (≈1233 ×g) for 10 min at 4 °C and washed twice by ultrapure water. The pellet was weighed and added to biopolymer mixture at a total biopolymer solid: bacteria ratio of 2:1 (by weight). The final uniform probiotics biopolymer suspension contained approximately 8.5–9.2 Log CFU/mL cells. According to the optimized conditions (section 2.2.3), the pH of the probiotics biopolymer suspension was adjusted to 3.0 using 0.1–2.0 M NaOH to promote complex coacervation between protein and SBP, and left for 1h at 4°C. The viscoelastic and microstructure properties of wet microcapsules were then characterized (section 2.4).

**Viscoelastic and Microstructure Properties of Wet Microcapsules**

Wet microcapsules were first centrifuged at 2,000 rpm (≈402 ×g) for 10 min using Sorvall™ biofuge primo benchtop centrifuge (Thermo Scientific Inc., MA, USA), and precipitates were collected. The dynamic viscoelastic properties of precipitates were evaluated using a Discovery Hybrid Rheometer-2 rheometer (TA Instruments Ltd., New Castle, DE, USA) described by Lan et al [26] with no modification.

LSM 700 confocal laser scanning microscope (CLSM) (Carl Zeiss Microscopy Ltd., Jena, Germany) was applied to investigate the microstructure of the wet microcapsules by following a previously reported method (Chen, Li, Ding, & Suo, 2012) with some modifications. In brief, rhodamine B (50 mg/L), the dye to stain proteins, was prepared by dissolving it in water. Subsequently, 2.0 mL of the wet microcapsules were mixed with 20 μL rhodamine B (50 mg/L) in a test tube and vortexed for 2 min. Afterwards, 200 μL of the stained mixture was placed on a μ-plate 96 well (ibidi USA, Inc., WI, USA), and then the shape and size of rhodamine B-labeled protein–SBP complex coacervates were observed under CLSM using excitation wavelength of 555 nm and emission wavelength of 630 nm.

**Preparation of Microcapsule Powders by Different Drying Methods**

In total, eight microcapsules encapsulated probiotics powders were produced by either spray-drying or freeze-drying. **Table 4-1** listed the formulations and codes of eight microcapsule powders prepared in this study. Spray-dried samples were obtained by feeding liquid sample into a Büchi mini spray-dryer B-290 (New Castle, DE, USA) with feed rate of 0.15 L/h and aspirator flow of 40 L/h. The inlet and outlet air temperature were maintained at 130℃ and 55℃, respectively. Regarding freeze-drying process, liquid samples were first frozen in -80 ℃ freezer for 2h, then placed in a foil plate and lyophilized using a SP scientific Lyophilizer (Gardiner, NY, USA) for 24h. The freeze-dried microcapsules were ground into uniform powder with mortar and pestle. Eight microcapsule powders were collected and stored in glass bottles at 4℃ for further characterization.

**Table 4-1.** The formulation code of the complex coacervates and the particle size of microcapsules with *Lactobacillus rhamnosus* GG (LGG)

| Code of sample | Protein source | Protein to pectin ratio | Total solid (%) | Drying method | Particle size $D_{(50)}$ (μm) |
|---|---|---|---|---|---|
| **C5-S** | SC | 5:1 | 1.2 | Spray-dry | 51.93 ± 2.69 |
| **C2-S** | SC | 2:1 | 1.5 | Spray-dry | 119.67 ± 2.36 |
| **P5-S** | PPI | 5:1 | 1.2 | Spray-dry | 55.57 ± 3.21 |
| **P2-S** | PPI | 2:1 | 1.5 | Spray-dry | 11.75 ± 0.64 |
| **C5-F** | SC | 5:1 | 1.2 | Freeze-dry | 120.5 ± 2.12 |
| **C2-F** | SC | 2:1 | 1.5 | Freeze-dry | 78.48 ± 3.23 |
| **P5-F** | PPI | 5:1 | 1.2 | Freeze-dry | 87.42 ± 2.52 |
| **P2-F** | PPI | 2:1 | 1.5 | Freeze-dry | 114.31 ± 11.71 |

Abbreviations: PPI, pea protein isolate; SC, sodium caseinate.

**Characterization of Microcapsules Powders**

IR spectra of microcapsule powders and individual biopolymer powders (CS, PPI, and SBP) were acquired by a Varian FTIR spectrophotometer (CA, USA) following the protocol

developed by Lan et al. [186]without any modification. The particle size and size distribution of microcapsule powders were measured using a Mastersizer 3000 equipped with Hydro LV (Malvern Instrument, Worcester, UK) by the method of Lan et al. without any changes [118]. Microstructure of eight microcapsule powders was imaged by scanning electron microscopy (SEM) (JEOL Model JSM-6490LV, MA, USA) and CLSM (Carl Zeiss Microscopy Ltd., Jena, Germany) as reported previously [118]. For the CLSM, an appropriate amount of dry powder was evenly distributed to fully cover the bottom of the μ-plate wells (μ-Plate 96 well, ibidi USA, Inc., Wisconsin), and then 200 μL of rhodamine B (0.5 mg/L) was added to the wells to stain protein. The samples were allowed to be incubated for 1h before observation. Images were taken at room temperature and acquired in 1024 × 1024 pixels using pre-installed image processing software.

**Death Rate of LGG in Microcapsules Powder during Simulated Sequential GI Digestion**

To determine the viability of encapsulated LGG in the microcapsule powders over the period of simulated sequential GI digestion, 0.1 g of microcapsules was mixed with 9.9 mL of simulated gastric fluid (SGF) (0.08 M HCl containing 0.2% w/w NaCl, pH 2.0) with 0.3% (w/v) pepsin in a tube, and incubated in an orbital shaker (MaxQ™ 4000 Benchtop Orbital Shakers, Thermo Fisher Scientific Inc., USA) under 37 °C at 300 rpm for 2 h. The viable cells were measured at a 1h interval. After 2 h of incubation in SGF, the gastric digests were recovered by centrifugation at 8,000 rpm (≈6440 ×g) for 10 min, and then the collected powders (~ 0.1g) were added to 9.9 mL of simulated intestinal fluid (SIF) (0.05M $KH_2PO_4$, pH 7.4) containing 1.0% (w/v) bile salt and 1.0% (w/v) pancreatin [90, 100], followed by 2.5h incubation under 37 °C at 300 rpm. At each time point, the suspension of intestinal digests were taken to count the viable cells as reported previously [261]. Death rate of the encapsulated LGG at a given digestion time was calculated using Equation (1).

$$\text{Death rate} = (1\text{-Log } N_t/\text{ Log } N_0) \times 100\% \quad (1)$$

where $N_t$ and $N_0$ were the viable cells at time t and time zero, respectively.

The viability and integrity of the encapsulated LGG during GI tract was also visualized using CLSM. The LIVE/DEAD BacLight bacterial viability kit (L-7012, Thermo fisher scientific, Inc. Waltham, MA, USA) with two color fluorochromes was applied to discriminate the alive cells from dead cells based on their cell membrane integrity. In general, bacteria with intact cell membranes (alive) emit green fluorescence, whereas bacteria with damaged membranes (dead) emit red fluorescence [117]. According to the manufacture instruction, equal volumes of SYTO-9, a green-fluorescent nucleic acid dye (3.34 mM) and propidium iodide, a red-fluorescent nucleic acid dye (20 mM) in the kit were first mixed thoroughly, and then 3 μL of dye mixture was taken to dye 1.0 mL of the serial diluted digesta at each time point during digestion. For the microcapsule powder (before digestion), 10.0 mg microcapsules were first dissolved in 990.0 μL 10mM phosphate buffer (pH 7.0), and then 3.0 μL of dye mixture was taken to dye 1.0 mL of the serial diluted samples. Subsequently, the mixture stayed in the dark for 15 min, and 200.0 μL of stained mixture was then placed on a μ-plate 96 well. Image was observed under CLSM at excitation/emission wavelength of 480 nm/500nm and 490 nm/635nm for SYTO-9 and propidium iodide, respectively.

**Statistical Analysis**

The physicochemical properties of the complex coacervates were performed at least twice to confirm a consistent result. The viability of bacterial cells test and other measurements were repeated at least three times on freshly prepared samples and the values were expressed as means ± SD. Significant differences between means ($p < 0.05$) were statistically analyzed by one-way analysis of variance (ANOVA) (Version 9.3, SAS Institute Inc., NC, USA).

## Results and Discussions

### Optimizing pH Condition for Complex Coacervation Formation

The formation of complex coacervates and the corresponding physiochemical properties highly rely on environmental pH, protein type, and protein–polysaccharide mixing ratio. Considering the application of complex coacervates in the field of encapsulation, a large number of researchers have suggested to fabricate microcapsules at the critical complex coacervation formation pH named $pH_{opt}$, under which the strongest electrostatic interaction is achieved between protein and polysaccharide. In this way, the maximum yield of complex coacervates is achieved [262]. As such, state diagram in conjunction with ζ-potential measurement were applied to elucidate the phase behavior of complex coacervates as a function of pH and to identify the $pH_{opt}$ of complex coacervates [26]. According to the previous study, complex coacervation of PPI–SBP usually happened in the pH range of 5.0–2.5 [26]. Therefore, the phase behaviors of protein–SBP mixtures with different mixing ratios as a function of pH (5.0–2.5) were evaluated after standing for 24h at 4 °C (**Fig. 4-1a**), and a state diagram was constructed as shown in **Fig. 4-1b**.

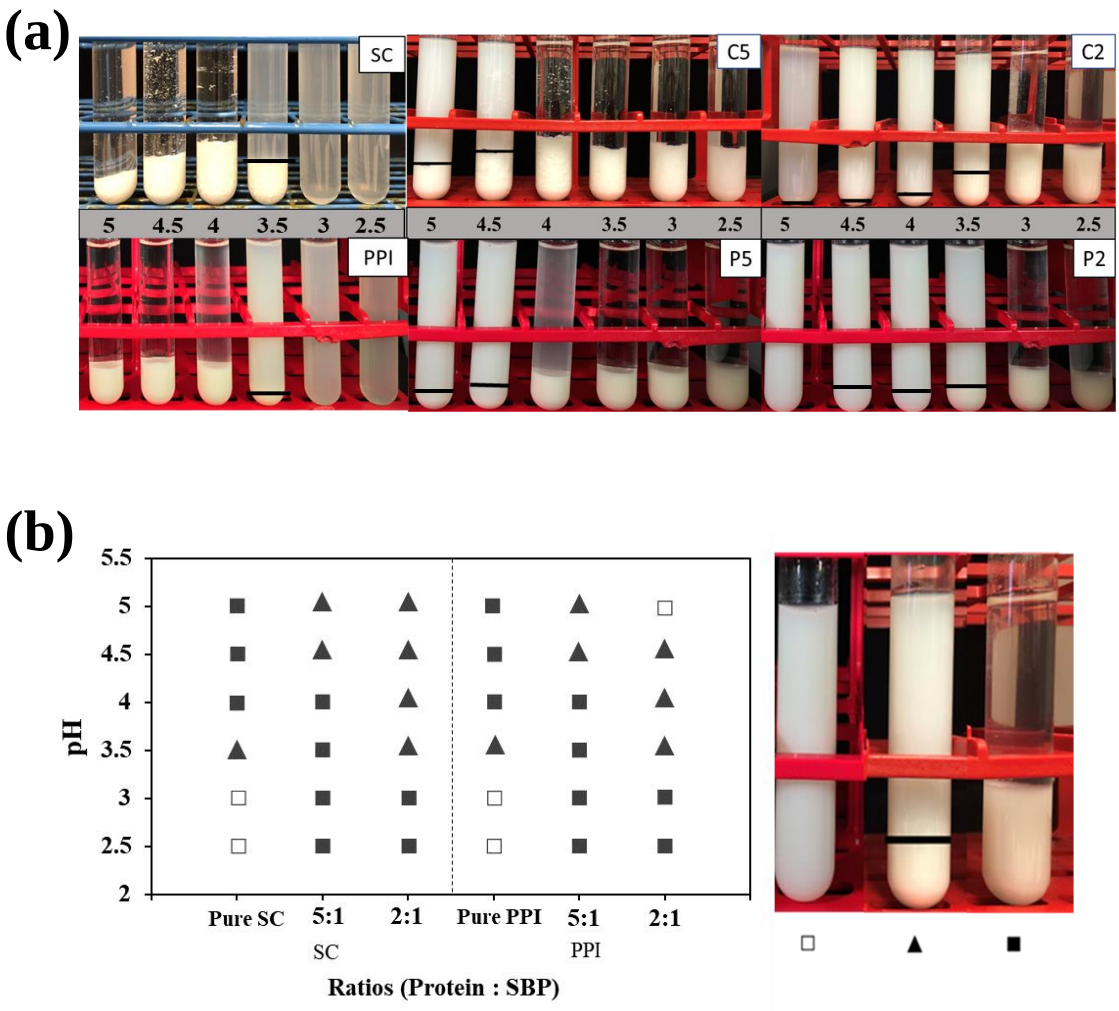


**Fig. 4-1.** (a) The appearance of SC, PPI, SC-SBP and PPI-SBP mixture at different mixing ratios as function of pH. The appearance was observed after 24 h standing. (b) State diagram of SC, PPI, SC-SBP and PPI-SBP mixtures at different mixing ratios during acid titration□ represents turbid solution; ▲ represents precipitation and cloudy solution; ■ represents precipitation and clear solution. (c) The dependence of zeta potential of SC, PPI, SBP, SC-SBP and PPI-SBP mixtures at different mixing ratios on pH values.

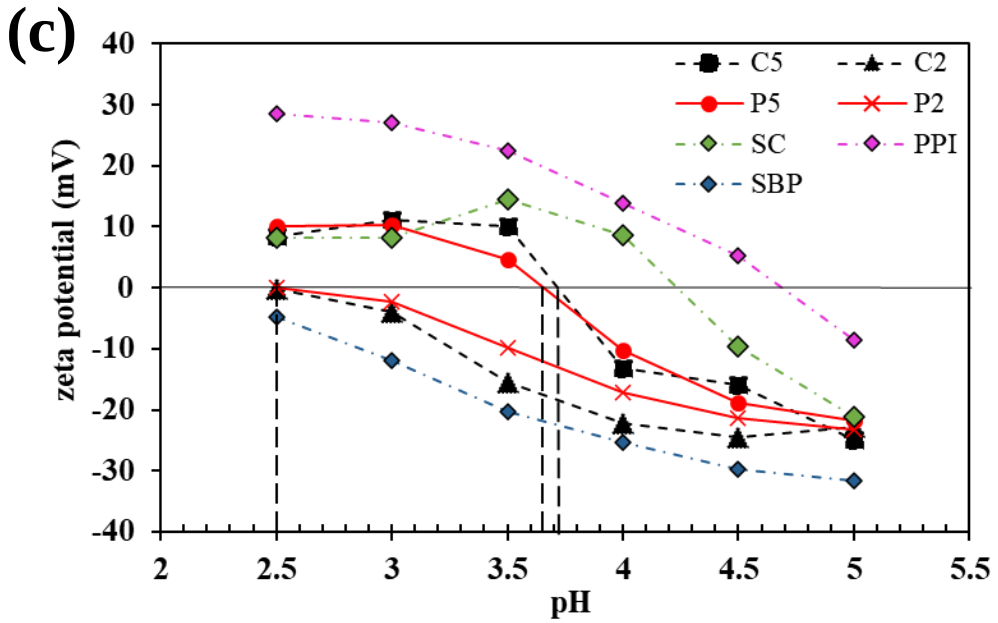


**Fig. 4-1.** (a) The appearance of SC, PPI, SC-SBP and PPI-SBP mixture at different mixing ratios as function of pH. The appearance was observed after 24 h standing. (b) State diagram of SC, PPI, SC-SBP and PPI-SBP mixtures at different mixing ratios during acid titration□ represents turbid solution; ▲ represents precipitation and cloudy solution; ■ represents precipitation and clear solution. (c) The dependence of zeta potential of SC, PPI, SBP, SC-SBP and PPI-SBP mixtures at different mixing ratios on pH values (continued).

At pH 5.0, clear phase separation occurred in the pure protein solutions (SC and PPI) since it is close to their pIs, while precipitation and cloudy solution existed in all the tested samples except PPI: SBP ratio of 2:1 (P2) (**Fig. 4-1a**). This is mainly attributed to the electrostatic attraction between protein and SBP as suggested by the results of ζ-potential (**Fig. 4-1c**). For example, most of protein–SBP mixtures displayed intermediate ζ-potentials that were in between that of protein and SBP solutions. As the pH decreased from 5.0, more insoluble complexes were formed especially in the protein to SBP ratio of 5:1(e.g. C5 & P5), indicating the higher protein concentration combined with lower SBP concentration favorable insoluble complexes formation. This is because SBP is not sufficient enough to cover protein molecular at lower SBP concentration, thus protein aggregation plays the dominate role at pH 5. In this research, three distinguishable phase behaviors/appearances (turbid, precipitation and clear

solution, precipitation and cloudy solution) were constructed and presented in the state diagram (**Fig. 4-1b**). According to the widely accepted definition of complex coacervates [26, 263], both precipitation and cloudy solution (▲) and precipitation and clear solution (■) presented in this study could be considered as complex coacervates bearing distinct structural and functional properties. In terms of application of complex coacervates in microencapsulation, the higher solid mass content of complex coacervates usually is associated with a greater encapsulation yield because of wall (e.g., coacervates) to core (e.g., bioactive compounds) ratio effect. In this study, precipitation and clear solution (■) displayed a higher amount of solid mass than precipitation and cloud solution (▲). This is because stronger electrostatic interactions between protein and SBP were exhibited in precipitation and clear solution (■) phase separation, leading to a larger coacervates yield. Consequently, precipitation & clear solution (■) phase behavior is more suitable to encapsulate probiotics than precipitation & cloud solution (▲) phase in this study. Such conclusion was further confirmed by the ζ-potential results (**Fig. 4-1c**). In general, the precipitation phenomenon between protein and polysaccharide tends to be more obvious under an environment where a greater strength of electrostatic attraction is provided. Concomitantly, the net surface charge of the mixture is close to zero. As marked in Fig. 4-1c, the three dash lines indicated the zero net charge of the two proteins (SC and PPI)–SBP mixtures with two different mixing ratios at various pH ranging from ~3.7 to 2.5. It is noted that all of the four treatments produced precipitation & clear solution (■) phase at pH between 3.0–2.5 (**Fig. 4-1b**).

Regarding the impact of protein–SBP mixing ratio on phase behavior of the mixture, the occurrence of precipitation and clear solution (■) was shifted towards more acidic pH as the

protein–SBP ratio decreased. This phenomenon was also in agreement with other studies [264, 265] . It suggested that phase behavior of complex coacervates can be influenced by altering the charge of one or both biopolymer macroions through changing environmental pH, and/or the mixing ratios of the biopolymers. Combing state diagram and ζ-potential results, as well as the potential impact of pH on the viability of probiotics, pH 3.0 was selected as the optimum pH for preparing protein–SBP complex coacervates in the following experiments.

**Viscoelastic and Microstructure Properties of Wet Microcapsules**

***Viscoelastic properties***

Viscoelastic properties of complex coacervates not only provide insight on intermolecular interactions of biopolymers, but also furnish a useful information about the textual properties of final food products [266]. Herein, the storage modulus (G') and loss modulus (G'') of the complex coacervates prepared at pH 3.0 over the angular frequency range of 0.01–100 rad/s were determined, and the results were shown in **Fig. 4-2**.

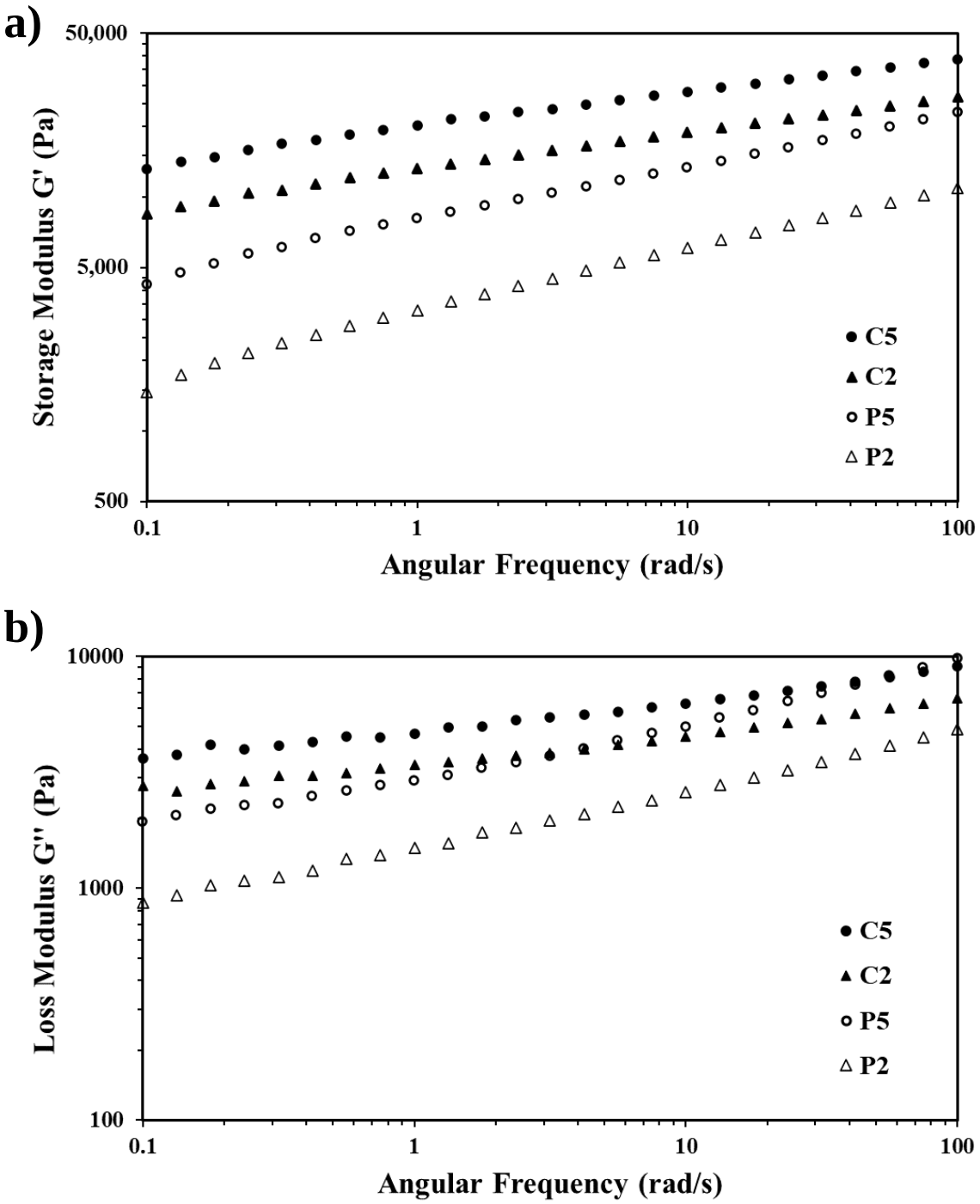


**Fig. 4-2.** The impact of protein to SBP mixing ratios (5:1 and 2:1) on (a) storage modulus G'; and (b) loss modulus G" of the complex coacervates at 1 rad/s frequency under pH 3.0. C5 represents SC–SBP complex coacervates prepared at 5:1 mixing ratio; C2 represents SC–SBP complex coacervates prepared at 2:1 mixing ratio; P5 represents PPI–SBP complex coacervates prepared at 5:1 mixing ratio; P2 represents PPI–SBP complex coacervates prepared at 2:1 mixing ratio.

In this study, the G' of all the samples was higher than G", which usually reflected a gel-like network structure [266-268]. This result suggested that the network structure between protein (SC or PPI) and SBP was successfully formed at pH 3.0 in all tested samples. From **Fig. 4-2a**, the highest to lowest G' in the tested samples were C5, C2, P5, and P2. Since a higher G' typically indicates a stronger interaction between the biopolymers, the results suggest that the overall interaction strength of SC–SBP samples was stronger than that of PPI–SBP samples. This different interaction strength between the two proteins with the same SBP might have attributed to the varied protein gel and complex coacervates structure between SC–SBP and PPI–SBP at acidic pH. In general, acidic pH promotes the formation of protein gel. By adding polysaccharide in acidic protein solution, both protein gelling and complex coacervation of protein and polysaccharide could happen simultaneously. Previous study proposed that SBP generally adsorbed on the surface of SC micelle aggregates to form SC–SBP complexes at acidic pH [269]. By contrast, positive patch of PPI molecules could adsorb on the segments of an anionic SBP molecule and form an intramolecular complex coacervates. Additionally, SC gel had a higher gel strength compared to PPI gel at the same protein concentration. This is because particulate gel of PPI through protein aggregation had limited amount of junction zones compared to SC ones. As a result, the distinguishable viscoelastic properties of complex coacervates from two different proteins were observed. In terms of protein to SBP ratio, both dynamic moduli (G' and G") of the complex coacervates were decreased upon the increase of SBP percentage, which was in line with the previous study [26]. This could be explained by interference of polysaccharide for the aggregation of protein gel structures which prevented the formation of protein strands and clusters [270]. Consequently, both dynamic moduli (G' and G") were decreased with increasing SBP concentration.

***Microstructure***

In order to better understand the impact of protein type and protein to polysaccharide mixing ratio on physical properties of the complex coacervates, the microstructure of the same sample set used in rheological experiment were characterized via CLSM (**Fig. 4-3)**. In general, the microstructure of the complex coacervates was greatly impacted by protein type in the biopolymer mixtures since protein accounted for the majority of the ingredients in the protein–SBP–probiotics ternary system. For example, at a relatively low SBP content in the ternary mixture (protein to SBP ratio of 5:1, **Fig. 4-3a**), the microstructure of SC–SBP was more like acid casein gel, featuring two distinct structures; these were the coherent network with large pores composed of casein micelles, and strands and clusters combined with SBP that absorbed on the surface of casein micelles. As the SBP concentration increased in this system, the microstructure was altered dramatically as reflected by the presence of a large amount of small pores in the gel network, which was in line with previous study [270]. On the other hand, highly cross-linked gel network with condensed globule aggregation were observed in PPI–SBP system (**Fig. 4-3c**). Interestingly, altering the concentration of SBP did not impose drastic impact on the microstructure of PPI–SBP complex coacervates in this study (**Fig. 4-3d**).

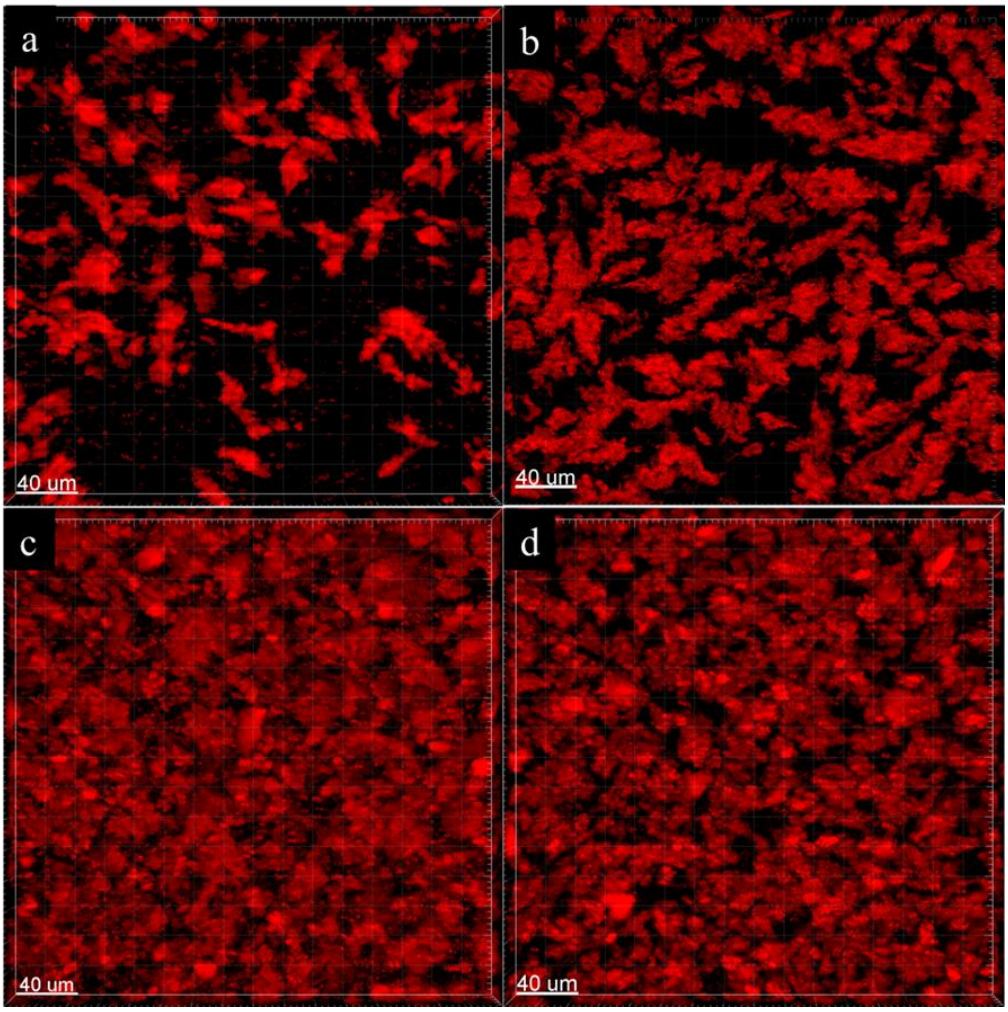


F**ig. 4-3.** The confocal laser scanning microscopy (CLSM) images of liquid SC–SBP and PPI–SBP complex coacervates prepared at pH 3.0 and mixing ratio of 5:1 and 2:1. (a) C5; (b) C2; (c) P5; and (d) P2. Protein was labeled as red color. C5 represents SC–SBP complex coacervates prepared at 5:1 mixing ratio; C2 represents SC–SBP complex coacervates prepared at 2:1 mixing ratio; P5 represents PPI–SBP complex coacervates prepared at 5:1 mixing ratio; P2 represents PPI–SBP complex coacervates prepared at 2:1 mixing ratio.

**Impact of Drying Methods on Physical Properties of Dried Microcapsules**

***FTIR***

FTIR was employed to further understand the interaction of the functional groups between the protein (SC or PPI) and SBP, as well as the impact of drying methods on such interaction.

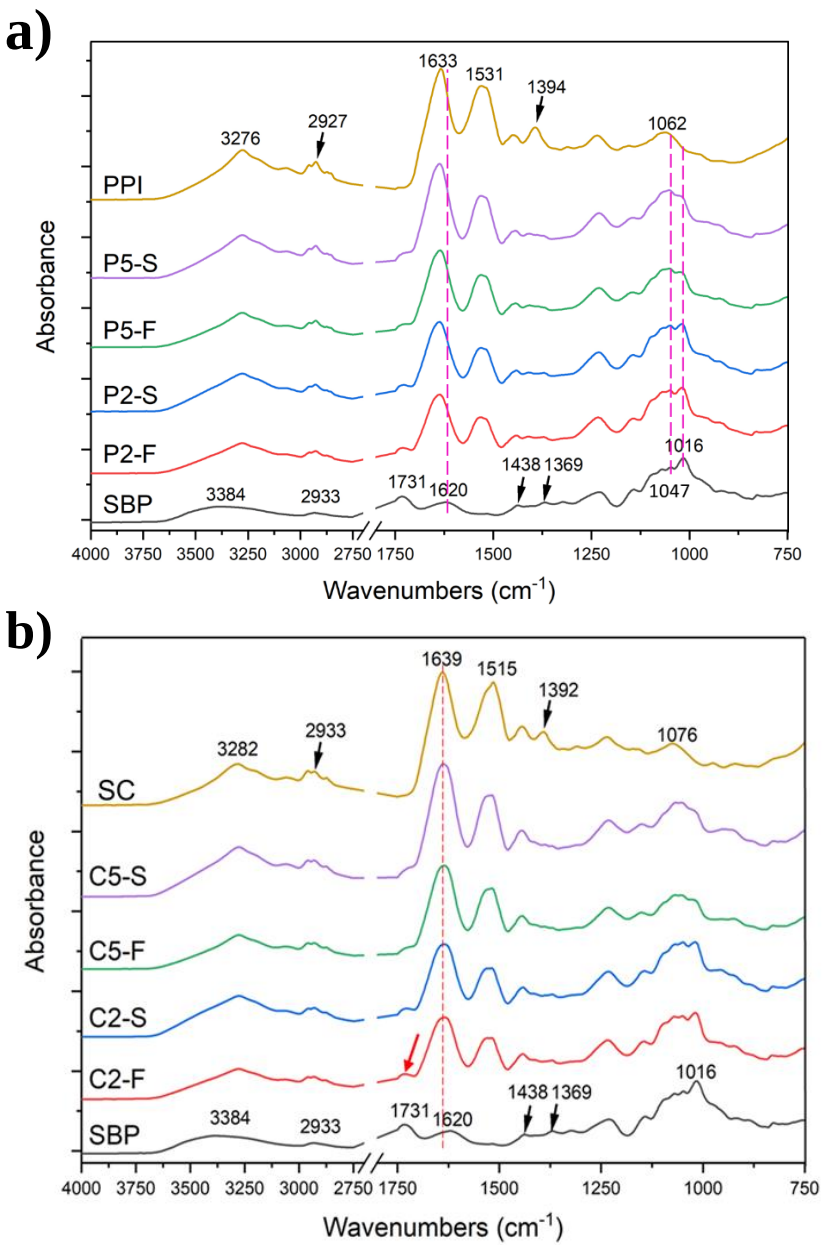


**Fig. 4-4.** FTIR spectra of LGG encapsulated microcapsules by means of protein–SBP complex coacervates with different drying method (spray-drying and freeze-drying). (a) PPI–SBP complex coacervates (b) and SC–SBP complex coacervates. The formulation and code of the samples are listed in **Table 4-1**.

The spectra of the control samples (SC, PPI, and SBP) were consistent with previous reports [26, 186, 271]. Different drying methods did not exert any appreciable impact on the

interactions among functional groups as indicated by these identical spectra. In terms of complex coacervates, their spectra in the higher wavenumber region (1450–4000 $cm^{-1}$) were mainly dominated by the proteins, and the higher the protein ratio, the more similarities they displayed (**Fig. 4-4a&b**). On the other hand, pectin dominated the spectra in the lower wavenumber part (700–1450 $cm^{-1}$) which was corroborated by the serried peaks, such as the peaks at 1016 and 1047 $cm^{-1}$, associated with the functional groups of pectin [272, 273]. In addition, the distinct peak at 1731 $cm^{-1}$ in SBP became a shoulder-like region in all tested complex coacervates around the same wavenumber, and the symmetric $-COO^-$ stretching vibration (1620 $cm^{-1}$) in SBP shifted slightly toward the amide I group (1633 $cm^{-1}$) when forming the complex coacervates (as pointed by the dash line in **Fig. 4-4**). Besides, peaks at 1438 $cm^{-1}$ and 1369 $cm^{-1}$ found in SBP, as well as the amide III group region from the protein were significantly influenced by the protein−SBP complex coacervation. For example, some characteristic peaks in the initial biopolymers such as 1620 $cm^{-1}$ of SBP, 1392 $cm^{-1}$ of SC, and 1394 $cm^{-1}$ of PPI, were vanished in all protein−SBP complex coacervates indicating electrostatic interaction occurred between the amine groups of protein ($-NH_4^+$) and carboxyl groups of SBP ($-COO^-$). Similar results were also reported in various complex coacervation systems, e.g. the fish skin gelatin and gum Arabic complex coacervation [274] and the interaction between egg white protein and xanthan gum [275], where electrostatic interaction was proved to be the major driven force for the formation of complex coacervations.

***Particle size***

The results of particle size distribution of the dried microcapsules as influenced by protein type and drying methods were shown in **Fig. 4-5,** and the particle size $D_{(50)}$ of the samples were also measured as supportive data as shown in **Table 4-1**. The particle size

distribution indicated that the higher SBP content led to the formation of bigger particles in spray-dried samples. This could be explained by the intensive involvement of SBP chains in the complex coacervates, particularly in the higher SBP ratio, thus promoting the formation of a bigger structure. More specifically, it was noticed that the SC−SBP microcapsules (both spray-dried and freeze-dried) showed a monomodal particle size distribution. As to the PPI−SBP microcapsules, they all presented multimodal particle size distributions among the range of 0.05−1,000 μm. The spray dried PPI−SBP microcapsules had wider size ranges than the freeze-dried counterparts. For example, the P2-S displayed three peaks with huge size differences, as smallest as ~0.4 μm and largest as ~600 μm, which was also confirmed by the SEM (**Fig. 4-7**). The presence of non-uniform particle size of spray-dried PPI was also reported in previous study [186], which might be generated by the different fractions (e.g., albumin, vicilin, and legumin) of PPI interacting with SBP to form particles with variable size [276]. Conversely, the freeze-dried PPI−SBP microcapsules (dashed lines in **Fig. 4-5**) were mostly distributed in a bigger but narrower size range (80−100 μm). The longer freeze-drying time (> 48 h) may promote the aggregation of complex coacervates to form big chunk of flakes, which would remain intact with a mild manual milling process after freeze-drying.

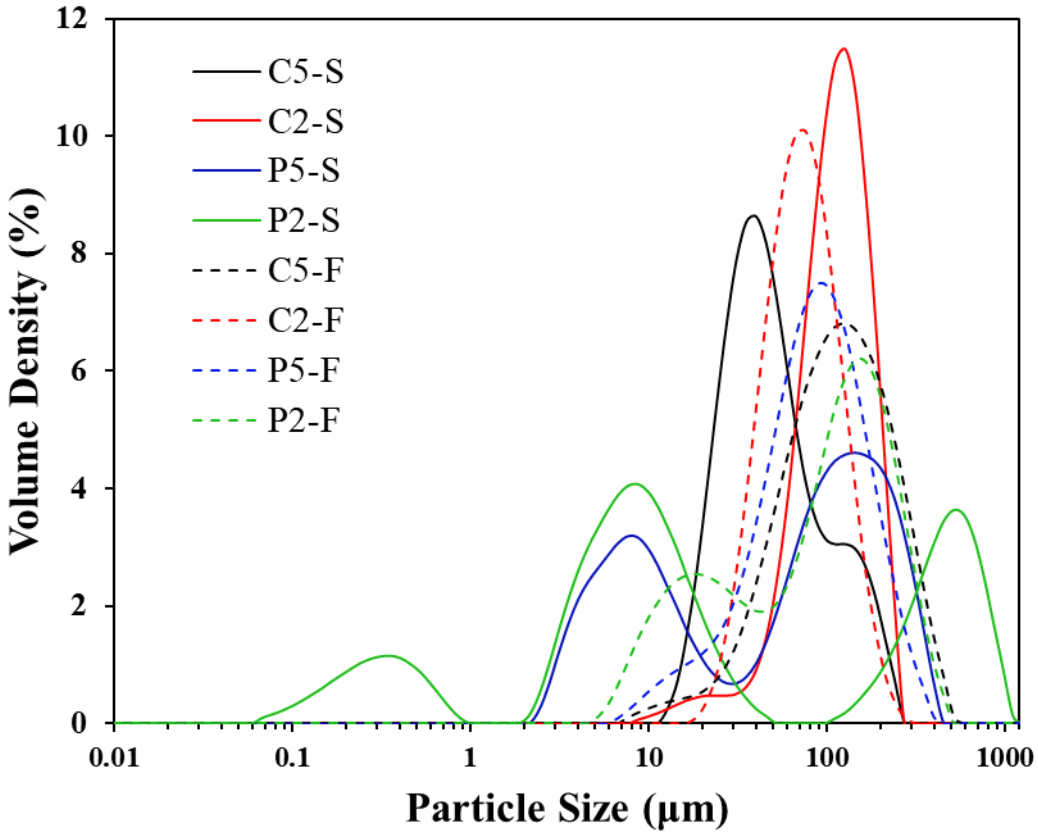


**Fig. 4-5.** Particle size distribution of *Lactobacillus rhamnosus* GG (LGG) encapsulated spray-dried and freeze-dried microcapsules. The formulation and code of the samples are listed in **Table 4-1**.

***Microstructure***

CLSM was applied to visualize the microstructures of the spray-dried and freeze-dried microcapsules by staining protein with rhodamine B (**Fig. 4-6**). Compared with the images in **Fig. 4-3** which displayed the microstructure of the wet complex coacervates, it was clear that drying methods remarkably changed the morphology of the dried microcapsules in multiple ways. For example, all the spray-dried microcapsules exhibited a spherical shape due to the nature of spray-drying process. By contrast, freeze-drying process converted the liquid complex coacervates to a lamellar, scale-like structure, and no significant structural difference was found between samples. Such observation was reasonable since i) both the pre-freeze treatment (frozen

in -80 ℃ freezer for 2h) prior to freeze-drying and the freeze-drying process itself promoted the conjugation of the complex coacervates particles into bigger and flat pieces; ii) the samples were ground to a maximum extent with manual mortar and pestle grinding. Similar phenomenon was also reported in gelatin− gum Arabic and chitosan−carboxymethylcellulose systems [277]. In terms of protein type, all dried microcapsules with PPI showed smaller spherical particles, but contained more un-uniform particle aggregates compared to SC microcapsules, which was in line with the particle size results (**Table 4-1**).

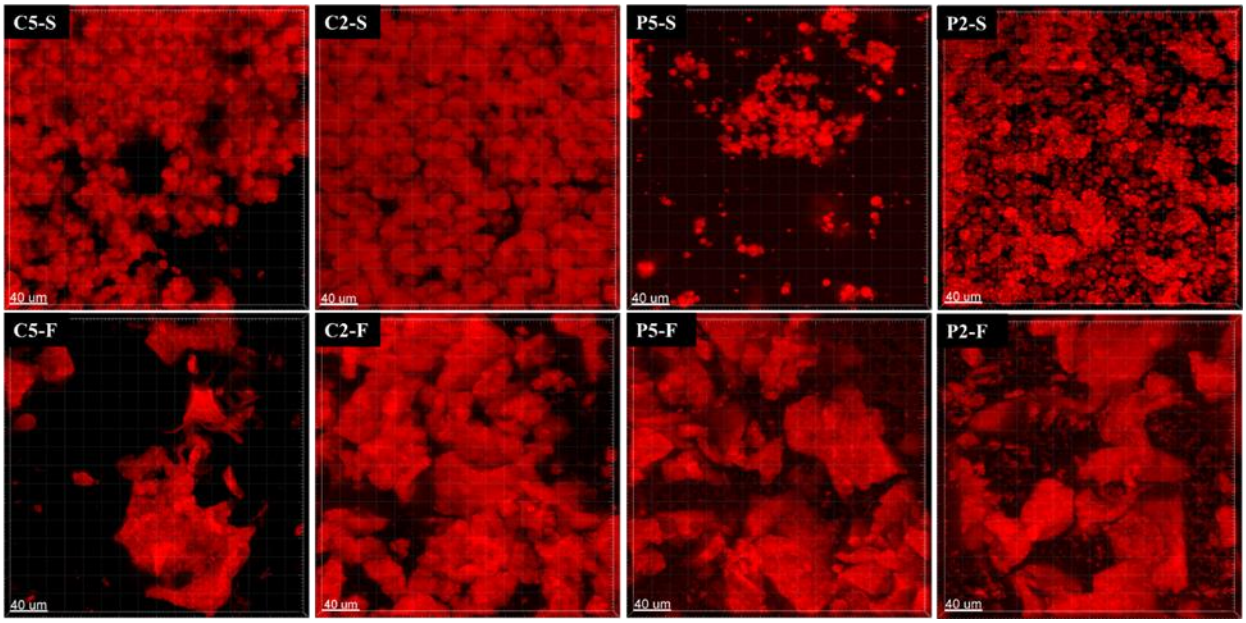


**Fig. 4-6.** The confocal laser scanning microscopy (CLSM) images of LGG encapsulated spray-dried and freeze-dried microcapsules. Bar represents 40 μm. Protein was labeled as red color. The formulation and code of samples are listed in **Table 4-1**.

The microstructure of the dried microcapsules and the distribution of LGG probiotics within the matrix (pointed by the arrows) were further investigated by SEM under different magnifications (**Fig. 4-7a&b**). Similar to the CLSM images in **Fig. 4-6**, the drying process played a crucial role on the microstructure of microcapsules and the location/distribution of LGG. Therefore, all the images were displayed by grouping them based on drying process rather

than the protein type. In general, the spray-dried samples presented mostly spherical shape with cavities and creases caused by the rapid loss of moisture during spray-drying [278, 279], with varied particle sizes among samples (**Fig. 4-7a**). Moreover, the outer topography of the particles indicated that the shell was intact, with the absence of rupture and visible broken shells. In addition to the insights gained in the microstructure of the dried microcapsules, it was also observed that the bacterial cells LGG were successfully encapsulated, but randomly distributed within biopolymer matrixes (as indicated by the arrows in **Fig. 4-7a**). Regarding the protein type in the spray-dried microcapsules, the SC−SBP samples seemed to a greater shrinkage due to the presence of some severely contracted particles and more crumpled surface (as shown in **Fig. 4-7a** with the circles). Previously study also indicated that the presence of different biopolymers as wall matrices led to varied microstructure of spherical particles during spray-drying [280].

For the freeze-dried samples, tiny pieces of the samples without grinding were applied to SEM directly to maintain the original microstructure of the microcapsules (**Fig. 4-7b**). As seen in the first row in **Fig. 4-7b**, the overall structure of the samples was highly bonded with porous sponge network, similar to previously reported results [112, 281]. A clear structure can be visualized in the image with a magnification of ×1,000 (second row in **Fig. 4-7b**). Regardless of protein type, samples with a higher protein ratio (5:1) always exhibited a denser and more compact structure compared to a lower protein ratio (2:1) ones, especially in PPI group. When protein type was taken into consideration, the network in PPI−SBP samples was apparently thinner and more fragile with larger pore sizes when compared to that in SC−SBP samples, which meant the P2-F sample possessed a distinguishly poor structure among the freeze-dried samples. This conclusion was further confirmed by the images under ×7,500 magnification where it appeared

that some of the structures were supported by the bacteria (P2-F). One potential reason might be due to the lower viscoelastic properties of the wall materials (**Fig. 4-2)**.

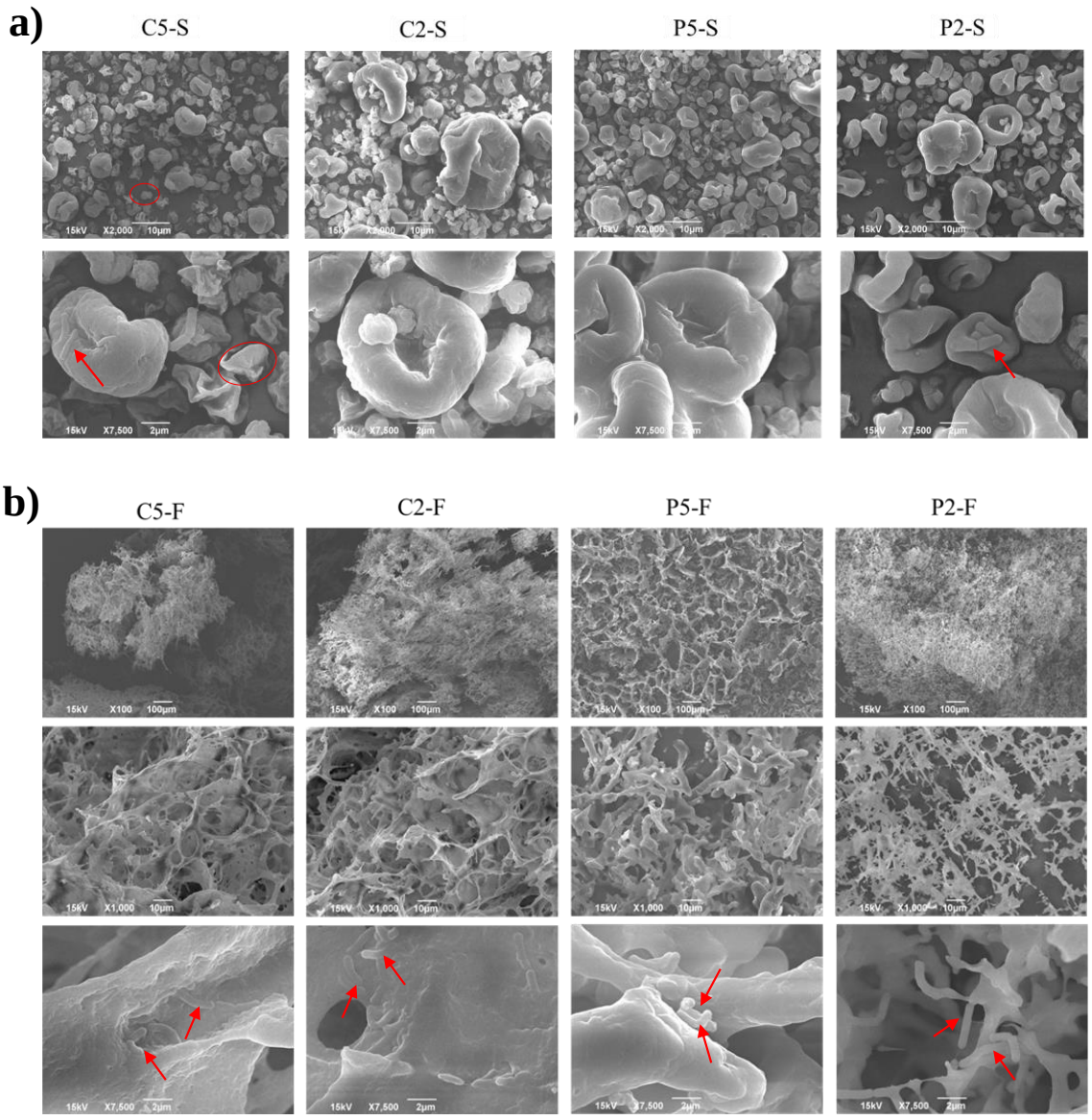


**Fig. 4-7.** SEM images of (a) LGG encapsulated spray-dried microcapsules; and (b) LGG encapsulated freeze-dried microcapsules under different magnifications. Arrow indicated LGG cells, and the severely crumpled surface was marked by circle. The formations and code of the samples are listed in **Table 4-1**.

**The Death Rate of Encapsulated LGG in Microcapsules during Simulated Sequential GI Digestion**

The death rate of LGG in each dried microcapsule at chosen time point during simulated gastrointestinal sequential digestion was compared (**Fig. 4-8)**. The viable cell count of each sample was at 8.5−9 Log CFU/g before digestion and had no significant difference ($p < 0.05$) among the samples (**Table A-1**).

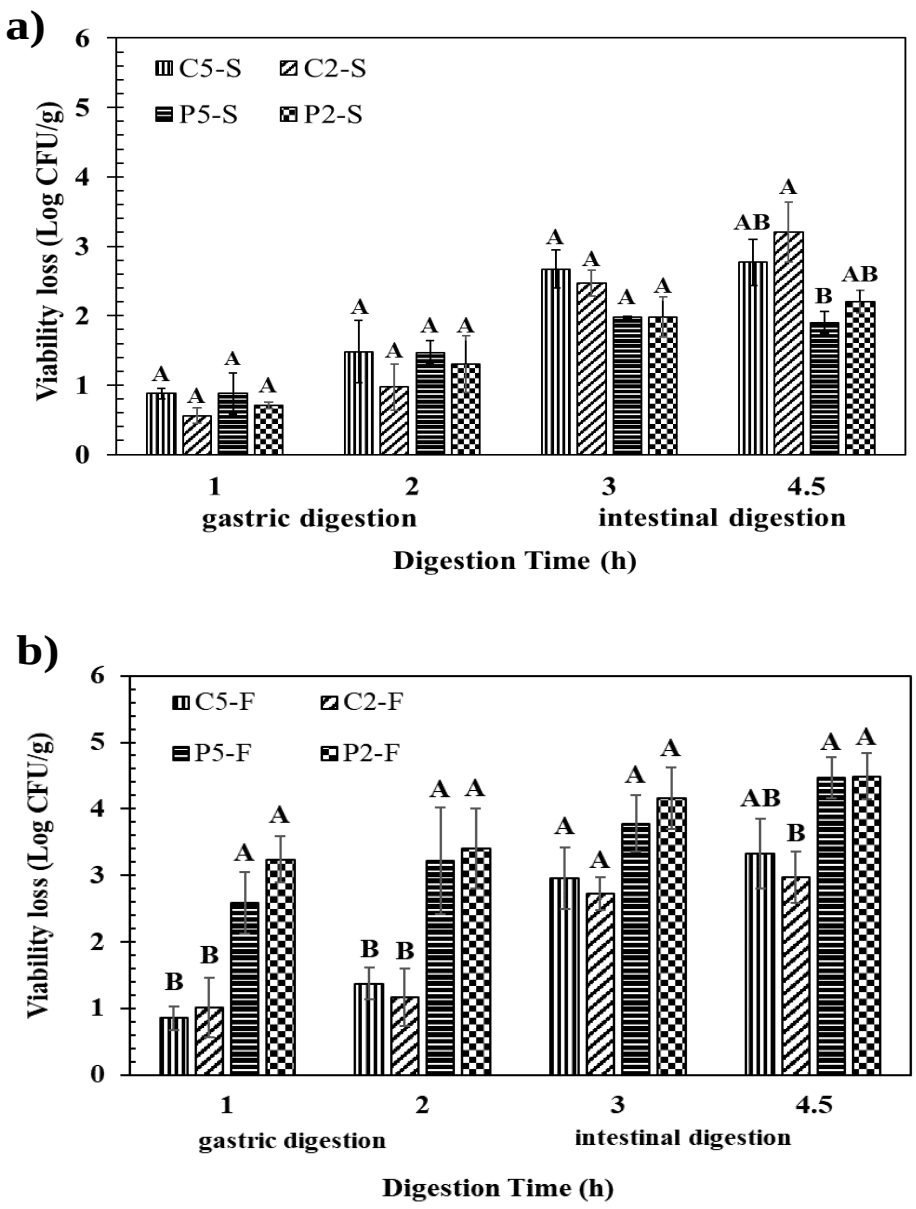


**Fig. 4-8.** Death rate (%) of LGG encapsulated in (a) spray-dried microcapsules; and (b) freeze-dried microcapsules by means of complex coacervation as a function of time during simulated sequential gastrointestinal digestion, and (c) Live and dead cells observation under CLSM before digestion, after gastric digestion and small intestinal digestion. The live cells and dead cells were labeled as green and red color, respectively. The values with different superscript letters within same time point are significantly different ($p < 0.05$).

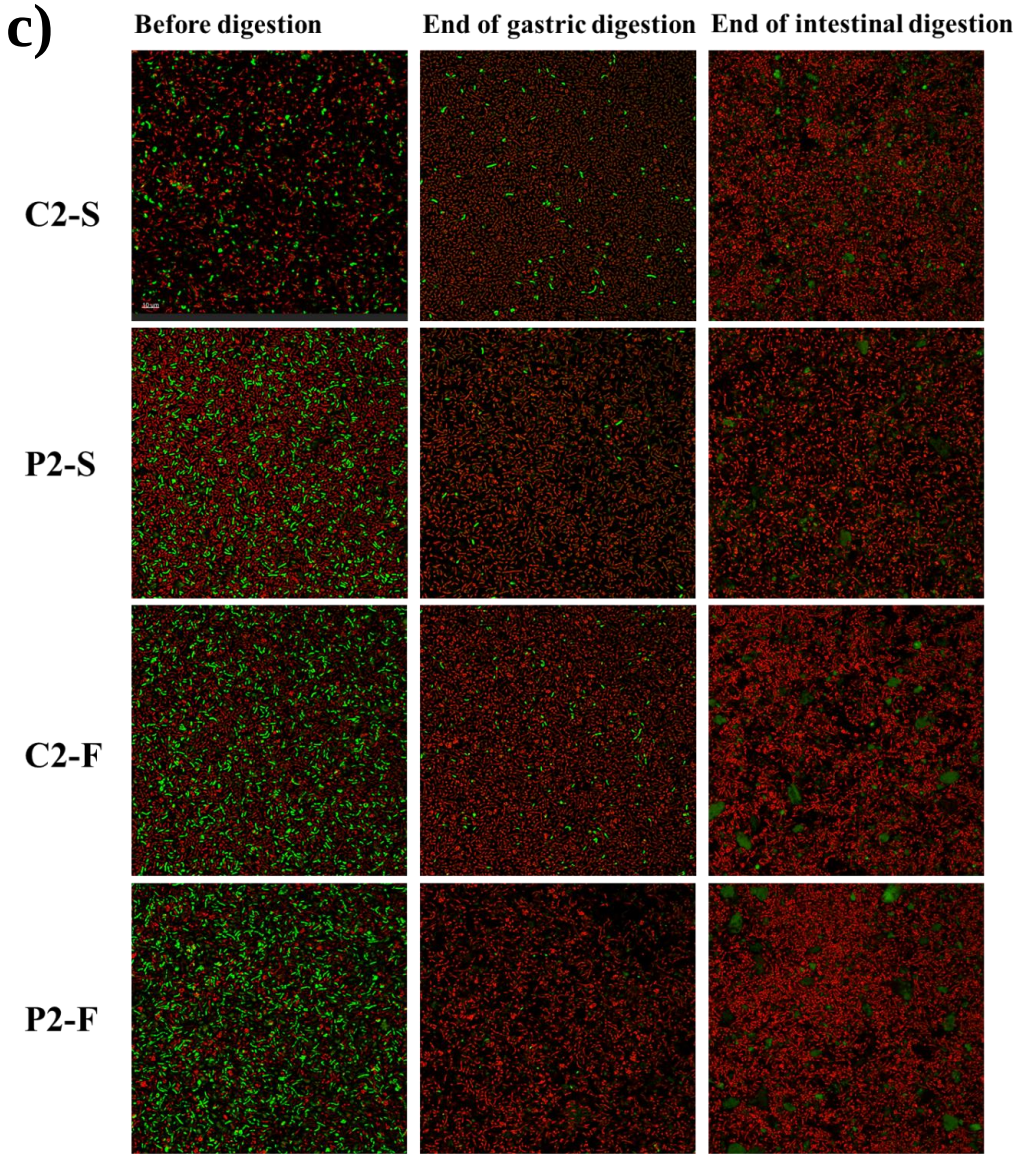


**Fig. 4-8.** Death rate (%) of LGG encapsulated in (a) spray-dried microcapsules; and (b) freeze-dried microcapsules by means of complex coacervation as a function of time during simulated sequential gastrointestinal digestion, and (c) Live and dead cells observation under CLSM before digestion, after gastric digestion and small intestinal digestion (continued). The live cells and dead cells were labeled as green and red color, respectively. The values with different superscript letters within same time point are significantly different ($p < 0.05$).

As shown in **Fig. 4-8a**, in the period of simulated gastric digestion (SGD), the death rate of all spray-dried samples remained at a very low level (< 10%) with no significant difference ($p$ <0.05). This was reasonable since the structure of spray-dried microcapsules maintained very

well at acidic pH. Interestingly, it could be noticed that LGG in the microcapsules with a higher protein content presented a greater death rate during SGD (e.g., C5-S *vs* C2-S). Part of the reason might be derived from their particle size differences. In general, C5-S and P5-S samples had a relatively smaller particle size compared to C2-S and P2-S (**Fig. 4-5**). As such, they would have a relatively larger surface area for pepsin and $H^+$ to access, thus leading to the death of LGG. After transferred to the simulated intestinal digestion (SID) for 1h, it was noticeable that a drastic increase of death rate of all the samples, especially when SC was presented. This was because the gradual disassociation of the complex coacervates structure under the SID condition, and the collapse of the gel-like structure allowed the hydrolytic enzymes and salts to be more accessible to the bacteria. The reason that SC group showed worse protective effect in SID rather than PPI group could be mainly due to their different microstructures. Spray-dried microcapsules with PPI as protein source showed a wider range of particle size distribution in conjunction with smooth surface compared with those containing SC. Previous study concluded that the particle size and smoothness of the microcapsules greatly influenced the viability of the encapsulated cells. The better protection for encapsulated cells was postulated to be largely originated from the relatively smooth surface of microcapsules that had higher integrity of particles and lower permeability of oxygen and simulated GI fluid [282]. In the last 1.5 h of SID, a slight increase in the death rate was observed in spray-dried PPI−SBP microcapsules, in which more than 7.5 Log CFU/g viable cells were maintained (**Table A-1**). As for the spray-dried SC−SBP samples, they were still able to maintain a population of probiotics higher than 6 Log CFU/g, albeit they provided a relatively less protection to the cells. The protein to polysaccharide ratio did not show obvious influence on the death rate of LGG in spray-dried samples; however, widening the current ratios in further study is possibly necessary to confirm this conclusion.

By contract to the spray-dried sample, a consistent tendency was found in the freeze-dried microcapsules over the entire course of the simulated digestion. The death rate rose gradually with increasing digestion time. Overall, the performance of the spray-dried samples was superior to those of the freeze-died counterparts in terms of death rate during GI tract, which indicated that the morphological properties of microcapsules affected the rate of the hydrolysis reaction to a greater extent. Zhao et al. [24] also reported that spray-drying possess improved mechanical strength and barrier property of the complex coacervates. As denoted by the SEM result, spray-dried samples had more contact and integrated structures than freeze-dried samples. In terms of protein sources, the freeze-dried PPI−SBP samples had a poor ability to protect the bacteria when exposed to digestive environment at the beginning, but the death rate of freeze-dried SC−SBP microcapsules during gastric digestion was comparable to that of the spray-dried SC−SBP samples. This also could be explained by the microstructural differences revealed by the SEM images in **Fig. 4-7**. where the P5-F and P2-F samples exhibited more porous and thinner structure compared to C5-F and C2-F, especially for P2-F. When all the microcapsules reached the end of the simulated digestion time, C2-F had the greatest protective effect on the viability of LGG among all the freeze-dried samples.

In addition, the changes of live cells during simulated gastrointestinal sequential digestion were investigated using CLSM images (**Fig. 4-8c**). Herein, only the images of each protein with one protein−polysaccharide ratio (2:1) were demonstrated here because of their much similarities with altered ratio. As one can see, there were numerous live cells (green ones) visible in all dried microcapsules before digestion. After the gastric digestion, only a few cells remained alive while most of them dead (red ones). After further digested in the intestinal condition, the viable cells were fewer as expected. Although these images were not

proportionally correlated to the death rate of each sample shown in **Fig. 4-8a&b**, this was reasonable because only a tiny proportion of the sample could be presented in the images under CLSM observation and usually the death of cells was found exponentially. Interestingly, more live cells appeared in all freeze-dried samples (C2-F and P2-F) rather than in spray-dried samples before digestion. One reason might be attributed to the different solubility of microcapsules powder. To stain the cells in the microcapsules for CLSM, the sample powder has to be dissolved in the buffer system. The higher dissolution rate and solubility of the freeze-dried samples compared to the spray-dried ones was observed during the experiment. This might be part of factors contributing to a higher death rate of probiotics in the freeze-dried microcapsules compared to spray-dried ones during digestion.

## Conclusions

In this work, the effects of pH (2.5–5.0), protein type (SC or PPI), and protein to SBP mixing ratio (5:1 or 2:1) on the formation and microstructure of complex coacervates were systematically investigated. The ζ-potential and FTIR results indicated that complex coacervates were successfully formed primarily through electrostatic interaction in all tested systems at pH 3.0. The formation of a gel-like structure was confirmed by their viscoelastic properties. Both SC−SBP and PPI−SBP complex coacervates formed at pH 3.0 were applied to encapsulate LGG probiotics, and two different drying methods (spray-drying and freeze-drying) were applied to convert liquid complex coacervates into convenient powder form. The particle size, morphological properties of microcapsules, and their protective effect on the viability of encapsulated LGG during simulated sequential GI digestion were assessed. The results indicated that spray-dried microcapsules presented a uniform spherical shape and smooth surface, while the freeze-dried ones were shattered, scale-like and porous. Considering the impact of protein

type, spray-dried PPI−SBP microcapsules had a smaller particle size with smooth surface, whereas the freeze-dried PPI−SBP microcapsules had larger porous size networks with thinner strings. Taken all the varieties into consideration, the spray-dried microcapsules showed an overall better protection on LGG which mainly resulted from the structure differences. In terms of protein type, recognizable differences on the microstructure of microcapsules from the same drying processing could be observed. Spray-dried SC−SBP microcapsules possessed a lager particle size with crumped surface compared to spray-dried PPI−SBP ones. Consequently, LGG in spray-dried PPI−SBP microcapsules had a lower death rate than that in SC−SBP over the course of simulated sequential GI digestion. Among all the samples, P2-S (spray-dried LGG microcapsules at the PPI−SBP ratio of 2:1) and P5-S (spray-dried LGG microcapsules at the PPI−SBP ratio of 5:1) followed by C5-S (spray-dried LGG microcapsules at the SC−SBP ratio of 5:1) favored the survival of LGG by maintaining over 7 Log CFU/g viable cells after digestion. Overall, the selection of protein type as well as the designing of a proper drying processing are necessary to ensure the viability of the encapsulated probiotics by means of complex coacervation.

## OVERALL CONCLUSION

The severe viability loss of probiotics during processing, transportation, storage and especially in the extreme environment in human GI tract makes it a considerable challenge for probiotics to apply in food and pharmaceutical industries. Encapsulation as a widely and extensively used method in protecting bioactive compounds were applied in this project to improve the viability of encapsulated LGG during storage and simulated GI digestion. The overall objective is to establish a food-grade biopolymer system to deliver sufficient numbers of the live probiotic cells (LGG) to the target area, i.e., the large intestine. In this research, two kinds of encapsulation systems were constructed, e.g., modified ALG hydrogel particles and protein-polysaccharide complex coacervate powder. The influences of the polysaccharide type on hydrogel particles, composition of the wall material in complex coacervates and preparing conditions such as the drying methods on the physicochemical properties of the microcapsules and the viability of encapsulated LGG during simulated GI were evaluated.

Firstly, the hydrogel particles results indicated that chitosan with different molecular weight were successfully deposited on the surface of the basic ALG hydrogel particles through the electrostatic interaction. Due to the varied molecular weight of the chitosan, the formed hydrogel particles exhibited different physical properties in diverse ways. For example, increased particle size and decreased hardness and rupture force of hydrogel particles was observed by coating increasing molecular weight of chitosan. The better long-term storage stability of the ALG-COS sample was assumed to be a result from the improved mechanical property. However, no significant improvement was observed in all three samples with secondary layer of chitosan on improving the viability of encapsulated LGG during simulated GI digestion compared to the

plain ALG hydrogel particles. In other words, adding chitosan layer did not alter the disadvantage of ALG hydrogel as being instable under acidic conditions.

Therefore, another modification of ALG hydrogel by substituting partial ALG (10, 20, 30%) with LMP or KC to form the double-network hydrogel particles to improve the viability of the encapsulated LGG in simulated GI digestion was proposed. The findings were that LGG encapsulated hydrogel particles could be successfully fabricated using designed polysaccharide compositions via ionically cross-linking as confirmed by FTIR spectra and SEM images. The increased apparent viscosity provided by KC positively affected the spherical shape and size of hydrogel particles, though causing a huge viability loss of LGG in simulated GI digestion by altering the microstructure of the particles. On the other side, the cohesiveness of ALG–LMP group increased as the LMP concentration increases compared with plain ALG particles, which suggested that ALG–LMP double-network hydrogel particles was able to prevent the hydrogel particles from falling apart in simulated gastric digestion. The best protective effect on LGG was found in ALG–LMP (80:20). This was possibly resulted from the more uniformed morphological properties and the good shrinking-swelling profile during simulated GI digestion.

However, the overall performance of the double-network hydrogel particles did not achieve a great level as expected compared to the plain ALG hydrogel particles. Therefore, impact of complex coacervate powder as wall material with varied factors on viability of encapsulated LGG during simulated GI digestion were investigated, such as protein type (PPI or SC), protein to polysaccharide ratio (2:1 or 5:1), and drying method (spray-dry or freeze-dry). The results indicated that drying method critically affected the morphology of the microcapsules and hence, directly influenced the survivability of the encapsulated LGG. The spray-dried microcapsules presented a uniform spherical shape and intact, smooth surface, whereas the

freeze-dried ones were shattered, scale-like and porous. On the other hand, protein type also plays an important role on the properties of the microcapsules. For example, the spray-dried PPI−SBP microcapsules had a relatively smaller but widely distributed particle size compared with the SC-SBP sample. Taken all the parameters into consideration, the spray-dried PPI-SBP microcapsules showed the best protection on LGG and maintained an over 7.5 Log CFU/g viable cells after the simulated GI digestion, which was mainly attributed to the structural differences. Overall, complex coacervation is a promising encapsulation method to substantially protect the encapsulated LGG from digestion by the proper selection of protein and operation of drying, and plant-based protein shows a great potential as an encapsulation material.

## FUTURE WORKS

This project stated that the protective effects of ALG hydrogel particles on the viability of encapsulated compounds during storage could be improved by adding COS layer on the surface. However, this method showed little influence on the viability during in vitro digestion, which was possibly due to the properties were largely subjected to the inherent parameters of the hydrogel particles, such as the material type, concentration, $Ca^{2+}$ concentration and particle size etc. Therefore, the better and deeper understanding of how these dominant factors influence the relevant properties are of interest and needed to be studied.

On the other hand, improved viability of the encapsulated LGG to a desired level was achieved through complex coacervation combined with spray drying by using PPI, which showed a promising potential of application of plant proteins. Nevertheless, the role of the protein to polysaccharide ratio plays in this system was not completely elucidated yet, as well as the effects of this method on other probiotic strains. Therefore, the future works are highlighted below:

1) To construct a thoroughly designed hydrogel particles system by varying factor such as particle size, alginate concentration and $Ca^{2+}$ concentration, and at the meantime, the effects of involving other material (chitosan and pectin) and/or other processing such as spray drying or freeze drying on the relevant properties of the hydrogel particles and viability of the encapsulated bacteria should be investigated.

2) The correlations between the complex state, the formation mechanism and properties of complex coacervates and the protein to polysaccharide ratio, protein source, and more specifically, certain protein fractions will be studied to better understand the complex coacervates system and to further protect the encapsulated probiotics.

3) Furthermore, the universality of the complex coacervation method on protecting other commonly used probiotic strains and the industrial mixtures should be studied to facilitate the application of this method in food industry.

## REFERENCES


1. WHO, Health and nutritional properties of probiotics in food including powder milk with live lactic acid bacteria. 2001.
2. Ul Islam, S., Clinical Uses of Probiotics. *Medicine* **2016,** *95* (5), 1-5.
3. George, K. R.; Patra, J. K.; Gouda, S.; Park, Y.; Shin, H.-S.; Das, G., Benefaction of probiotics for human health: A review. *Journal of Food and Drug Analysis* **2018,** *26* (3), 927-939.
4. Awaisheh, S.; Obeidat, M.; Al-Tamimi, H.; Assaf, A.; El-Qudah, J.; Rahahleh, R., In vitro cytotoxic activity of probiotic bacterial cell extracts against Caco-2 and HRT-18 colorectal cancer cells. *Milk Science International-Milchwissenschaft* **2016,** *69* (7), 33-37.
5. Ross, R. P.; Desmond, C.; Fitzgerald, G. F.; Stanton, C., Overcoming the technological hurdles in the development of probiotic foods. *J Appl Microbiol* **2005,** *98* (6), 1410-1417.
6. Zhang, Z.; Law, D.; Lian, G., Characterization Methods of Encapsulates. In *Encapsulation Technologies for Active Food Ingredients and Food Processing*, Zuidam, N. J.; Nedovic, V., Eds. Springer New York: New York, NY, 2010; pp 101-125.
7. Liu, Y.; Sun, Y.; Sun, L.; Rizwan ur, R.; Wang, Y., In vitro and in vivo study of sodium polyacrylate grafted alginate as microcapsule matrix for live probiotic delivery. *Journal of Functional Foods* **2016,** *24*, 429-437.
8. Vidhya Hindu, S.; Thanigaivel, S.; Vijayakumar, S.; Chandrasekaran, N.; Mukherjee, A.; Thomas, J., Effect of microencapsulated probiotic Bacillus vireti 01-polysaccharide extract of Gracilaria folifera with alginate-chitosan on immunity, antioxidant activity and disease resistance of Macrobrachium rosenbergii against Aeromonas hydrophila infection. *Fish & Shellfish Immunology* **2018,** *73*, 112-120.
9. Trabelsi, I.; Bejar, W.; Ayadi, D.; Chouayekh, H.; Kammoun, R.; Bejar, S.; Ben Salah, R., Encapsulation in alginate and alginate coated-chitosan improved the survival of newly probiotic in oxgall and gastric juice. *International Journal of Biological Macromolecules* **2013,** *61*, 36-42.
10. Cook, M. T.; Tzortzis, G.; Charalampopoulos, D.; Khutoryanskiy, V. V., Production and Evaluation of Dry Alginate-Chitosan Microcapsules as an Enteric Delivery Vehicle for Probiotic Bacteria. *Biomacromolecules* **2011,** *12* (7), 2834-2840.
11. Yeung, T. W.; Üçok, E. F.; Tiani, K. A.; McClements, D. J.; Sela, D. A., Microencapsulation in alginate and chitosan microgels to enhance viability of Bifidobacterium longum for oral delivery. *Frontiers in microbiology* **2016,** *7*, 494.
12. Ghibaudo, F.; Gerbino, E.; Campo Dall' Orto, V.; Gómez-Zavaglia, A., Pectin-iron capsules: Novel system to stabilise and deliver lactic acid bacteria. *Journal of Functional Foods* **2017,** *39*, 299-305.
13. Li, M.; Jin, Y.; Wang, Y.; Meng, L.; Zhang, N.; Sun, Y.; Hao, J.; Fu, Q.; Sun, Q., Preparation of Bifidobacterium breve encapsulated in low methoxyl pectin beads and its effects on yogurt quality. *Journal of Dairy Science* **2019,** *102* (6), 4832-4843.
14. Singh, J.; Kaur, K.; Kumar, P., Optimizing microencapsulation of α-tocopherol with pectin and sodium alginate. *Journal of food science technology* **2018,** *55* (9), 3625-3631.
15. Zia, K. M.; Tabasum, S.; Nasif, M.; Sultan, N.; Aslam, N.; Noreen, A.; Zuber, M., A review on synthesis, properties and applications of natural polymer based carrageenan

blends and composites. *International Journal of Biological Macromolecules* **2017,** *96*, 282-301.
16. Dafe, A.; Etemadi, H.; Zarredar, H.; Mahdavinia, G. R., Development of novel carboxymethyl cellulose/k-carrageenan blends as an enteric delivery vehicle for probiotic bacteria. *International Journal of Biological Macromolecules* **2017,** *97*, 299-307.
17. Liu, S.; Li, L., Thermoreversible gelation and scaling behavior of Ca2+-induced κ-carrageenan hydrogels. *Food Hydrocolloids* **2016,** *61*, 793-800.
18. Timilsena, Y. P.; Wang, B.; Adhikari, R.; Adhikari, B., Advances in microencapsulation of polyunsaturated fatty acids (PUFAs)-rich plant oils using complex coacervation: A review. *Food Hydrocolloids* **2017,** *69*, 369-381.
19. Lan, Y.; Chen, B.; Rao, J., Pea protein isolate–high methoxyl pectin soluble complexes for improving pea protein functionality: Effect of pH, biopolymer ratio and concentrations. *Food Hydrocolloids* **2018,** *80*, 245-253.
20. Mao, L.; Pan, Q.; Yuan, F.; Gao, Y., Formation of soy protein isolate-carrageenan complex coacervates for improved viability of Bifidobacterium longum during pasteurization and in vitro digestion. *Food Chemistry* **2019,** *276*, 307-314.
21. Saravanan, M.; Rao, K. P., Pectin–gelatin and alginate–gelatin complex coacervation for controlled drug delivery: Influence of anionic polysaccharides and drugs being encapsulated on physicochemical properties of microcapsules. *Carbohydrate Polymers* **2010,** *80* (3), 808-816.
22. Oliveira, A. C.; Moretti, T. S.; Boschini, C.; Baliero, J. C.; Freitas, O.; Favaro-Trindade, C. S., Stability of microencapsulated B. lactis (BI 01) and L. acidophilus (LAC 4) by complex coacervation followed by spray drying. *Journal of Microencapsulation* **2007,** *24* (7), 673-81.
23. Tavares, L.; Noreña, C. P. Z., Encapsulation of garlic extract using complex coacervation with whey protein isolate and chitosan as wall materials followed by spray drying. *Food Hydrocolloids* **2019,** *89*, 360-369.
24. Zhao, M.; Huang, X.; Zhang, H.; Zhang, Y.; Gänzle, M.; Yang, N.; Nishinari, K.; Fang, Y., Probiotic encapsulation in water-in-water emulsion via heteroprotein complex coacervation of type-A gelatin/sodium caseinate. *Food Hydrocolloids* **2020,** *105*, 105790.
25. Liu, S.; Elmer, C.; Low, N. H.; Nickerson, M. T., Effect of pH on the functional behaviour of pea protein isolate–gum Arabic complexes. *Food Research International* **2010,** *43* (2), 489-495.
26. Lan, Y.; Ohm, J.-B.; Chen, B.; Rao, J., Phase behavior and complex coacervation of concentrated pea protein isolate-beet pectin solution. *Food Chemistry* **2020,** *307*, 125536.
27. Huang, S.; Vignolles, M.-L.; Chen, X. D.; Le Loir, Y.; Jan, G.; Schuck, P.; Jeantet, R., Spray drying of probiotics and other food-grade bacteria: A review. *Trends in Food Science & Technology* **2017,** *63*, 1-17.
28. Iaconelli, C.; Lemetais, G.; Kechaou, N.; Chain, F.; Bermúdez-Humarán, L. G.; Langella, P.; Gervais, P.; Beney, L., Drying process strongly affects probiotics viability and functionalities. *Journal of Biotechnology* **2015,** *214*, 17-26.
29. Marco, M. L.; Heeney, D.; Binda, S.; Cifelli, C. J.; Cotter, P. D.; Foligné, B.; Gänzle, M.; Kort, R.; Pasin, G.; Pihlanto, A., Health benefits of fermented foods: microbiota and beyond. *Current opinion in biotechnology* **2017,** *44*, 94-102.
30. Anal, A. K., Quality Ingredients and Safety Concerns for Traditional Fermented Foods and Beverages from Asia: A Review. *Fermentation* **2019,** *5* (1), 8.

31. Tejero-Sariñena, S.; Barlow, J.; Costabile, A.; Gibson, G. R.; Rowland, I., Antipathogenic activity of probiotics against Salmonella Typhimurium and Clostridium difficile in anaerobic batch culture systems: is it due to synergies in probiotic mixtures or the specificity of single strains? *Anaerobe* **2013,** *24*, 60-65.
32. Cammarota, G.; Pecere, S.; Ianiro, G.; Masucci, L.; Currò, D., Principles of DNA-Based Gut Microbiota Assessment and Therapeutic Efficacy of Fecal Microbiota Transplantation in Gastrointestinal Diseases. *Digestive Diseases* **2016,** *34* (3), 279-285.
33. Song, S.; Lee, S.-J.; Park, D.-J.; Oh, S.; Lim, K.-T., The anti-allergic activity of Lactobacillus plantarum L67 and its application to yogurt. *Journal of Dairy Science* **2016,** *99* (12), 9372-9382.
34. Takeda, S.; Hidaka, M.; Yoshida, H.; Takeshita, M.; Kikuchi, Y.; Tsend-Ayush, C.; Dashnyam, B.; Kawahara, S.; Muguruma, M.; Watanabe, W., Antiallergic activity of probiotics from Mongolian dairy products on type I allergy in mice and mode of antiallergic action. *Journal of Functional Foods* **2014,** *9*, 60-69.
35. Senok, A. C.; Ismaeel, A. Y.; Botta, G. A., Probiotics: facts and myths. *Clinical Microbiology and Infection* **2005,** *11* (12), 958-966.
36. Kechagia, M.; Basoulis, D.; Konstantopoulou, S.; Dimitriadi, D.; Gyftopoulou, K.; Skarmoutsou, N.; Fakiri, E. M., Health benefits of probiotics: a review. *International Scholarly Research Notices* **2013,** *2013*.
37. Mack, D. R.; Michail, S.; Wei, S.; McDougall, L.; Hollingsworth, M. A., Probiotics inhibit enteropathogenic E. coliadherence in vitro by inducing intestinal mucin gene expression. *American Journal of Physiology-Gastrointestinal and Liver Physiology* **1999,** *276* (4), G941-G950.
38. Perdigón, G.; Vintiñi, E.; Alvarez, S.; Medina, M.; Medici, M., Study of the Possible Mechanisms Involved in the Mucosal Immune System Activation by Lactic Acid Bacteria. *Journal of Dairy Science* **1999,** *82* (6), 1108-1114.
39. Eloe-Fadrosh, E. A.; Brady, A.; Crabtree, J.; Drabek, E. F.; Ma, B.; Mahurkar, A.; Ravel, J.; Haverkamp, M.; Fiorino, A.-M.; Botelho, C.; Andreyeva, I.; Hibberd, P. L.; Fraser, C. M., Functional Dynamics of the Gut Microbiome in Elderly People during Probiotic Consumption. *mBio* **2015,** *6* (2), e00231-15.
40. Metchnikoff, E., *The prolongation of life*. Putnam: 1908.
41. Annan, N. T.; Borza, A. D.; Hansen, L. T., Encapsulation in alginate-coated gelatin microspheres improves survival of the probiotic Bifidobacterium adolescentis 15703T during exposure to simulated gastro-intestinal conditions. *Food Research International* **2008,** *41* (2), 184-193.
42. Bielecka, M.; Biedrzycka, E.; Majkowska, A., Selection of probiotics and prebiotics for synbiotics and confirmation of their in vivo effectiveness. *Food Research International* **2002,** *35* (2), 125-131.
43. López-Rubio, A.; Sanchez, E.; Wilkanowicz, S.; Sanz, Y.; Lagaron, J. M., Electrospinning as a useful technique for the encapsulation of living bifidobacteria in food hydrocolloids. *Food Hydrocolloids* **2012,** *28* (1), 159-167.
44. Bernardeau, M.; Vernoux, J. P., Overview of differences between microbial feed additives and probiotics for food regarding regulation, growth promotion effects and health properties and consequences for extrapolation of farm animal results to humans. *Clinical Microbiology and Infection* **2013,** *19* (4), 321-330.

45. Syngai, G. G.; Gopi, R.; Bharali, R.; Dey, S.; Lakshmanan, G. M. A.; Ahmed, G., Probiotics - the versatile functional food ingredients. *Journal of Food Science and Technology* **2016,** *53* (2), 921-933.
46. Holzapfel, W. H.; Haberer, P.; Snel, J.; Schillinger, U.; Huis in't Veld, J. H. J., Overview of gut flora and probiotics. *International Journal of Food Microbiology* **1998,** *41* (2), 85-101.
47. O'Toole, P. W.; Marchesi, J. R.; Hill, C., Next-generation probiotics: the spectrum from probiotics to live biotherapeutics. *Nature Microbiology* **2017,** *2* (5), 17057.
48. Martín, R.; Miquel, S.; Benevides, L.; Bridonneau, C.; Robert, V.; Hudault, S.; Chain, F.; Berteau, O.; Azevedo, V.; Chatel, J. M.; Sokol, H.; Bermúdez-Humarán, L. G.; Thomas, M.; Langella, P., Functional Characterization of Novel Faecalibacterium prausnitzii Strains Isolated from Healthy Volunteers: A Step Forward in the Use of F. prausnitzii as a Next-Generation Probiotic. *Frontiers in Microbiology* **2017,** *8* (1226).
49. Zhai, Q.; Feng, S.; Arjan, N.; Chen, W., A next generation probiotic, Akkermansia muciniphila. *Critical Reviews in Food Science and Nutrition* **2019,** *59* (19), 3227-3236.
50. Bouchard, D. S.; Rault, L.; Berkova, N.; Le Loir, Y.; Even, S., Inhibition of Staphylococcus aureus Invasion into Bovine Mammary Epithelial Cells by Contact with Live Lactobacillus casei. *Applied and Environmental Microbiology* **2013,** *79* (3), 877.
51. Khan, R. U.; Naz, S., The applications of probiotics in poultry production. *World's Poultry Science Journal* **2013,** *69* (3), 621-632.
52. Maurya, P.; Mogra, R.; Bajpai, P., Probiotics: an approach towards health and disease. *Bioscience trends.* **2014,** *7* (20), 3107-3113.
53. Fontana, L.; Bermudez-Brito, M.; Plaza-Diaz, J.; Muñoz-Quezada, S.; Gil, A., Sources, isolation, characterisation and evaluation of probiotics. *British Journal of Nutrition* **2013,** *109* (S2), S35-S50.
54. Doleyres, Y.; Lacroix, C., Technologies with free and immobilised cells for probiotic bifidobacteria production and protection. *International Dairy Journal* **2005,** *15* (10), 973-988.
55. de Vos, P.; Faas, M. M.; Spasojevic, M.; Sikkema, J., Encapsulation for preservation of functionality and targeted delivery of bioactive food components. *International Dairy Journal* **2010,** *20* (4), 292-302.
56. Gitton, C.; Meyrand, M.; Wang, J.; Caron, C.; Trubuil, A.; Guillot, A.; Mistou, M.-Y., Proteomic signature of Lactococcus lactis NCDO763 cultivated in milk. *Applied and Environmental Microbiology* **2005,** *71* (11), 7152.
57. do Espírito Santo, A. P.; Cartolano, N. S.; Silva, T. F.; Soares, F. A. S. M.; Gioielli, L. A.; Perego, P.; Converti, A.; Oliveira, M. N., Fibers from fruit by-products enhance probiotic viability and fatty acid profile and increase CLA content in yoghurts. *International Journal of Food Microbiology* **2012,** *154* (3), 135-144.
58. Cleveland, J.; Montville, T. J.; Nes, I. F.; Chikindas, M. L., Bacteriocins: safe, natural antimicrobials for food preservation. *International Journal of Food Microbiology* **2001,** *71* (1), 1-20.
59. Shah, N. P.; Lankaputhra, W. E. V.; Britz, M. L.; Kyle, W. S. A., Survival of Lactobacillus acidophilus and Bifidobacterium bifidum in commercial yoghurt during refrigerated storage. *International Dairy Journal* **1995,** *5* (5), 515-521.

60. Amine, K. M.; Champagne, C. P.; Raymond, Y.; St-Gelais, D.; Britten, M.; Fustier, P.; Salmieri, S.; Lacroix, M., Survival of microencapsulated Bifidobacterium longum in Cheddar cheese during production and storage. *Food Control* **2014,** *37*, 193-199.
61. Ding, W.; Shah, N., Survival of free and microencapsulated probiotic bacteria in orange and apple juices. *International Food Research Journal* **2008,** *15* (2), 219-32.
62. Zhu, K.; Yu, D.; Chen, X. Y.; Song, G. L., Preparation, characterization and controlled-release property of Fe3+ crosslinked hydrogels based on peach gum polysaccharide. *Food Hydrocolloids* **2019,** *87*, 260-269.
63. Berger, B.; Moine, D.; Mansourian, R.; Arigoni, F., HspR mutations are naturally selected in Bifidobacterium longum when successive heat shock treatments are applied. *Journal of Bacteriology* **2010,** *192* (1), 256.
64. Corcoran, B. M.; Stanton, C.; Fitzgerald, G. F.; Ross, R. P., Survival of probiotic lactobacilli in acidic environments is enhanced in the presence of metabolizable sugars. *Applied and Environmental Microbiology* **2005,** *71* (6), 3060.
65. Jankovic, I.; Sybesma, W.; Phothirath, P.; Ananta, E.; Mercenier, A., Application of probiotics in food products—challenges and new approaches. *Current Opinion in Biotechnology* **2010,** *21* (2), 175-181.
66. Steenson, L. R.; Klaenhammer, T. R.; Swaisgood, H. E., Calcium alginate-immobilized cultures of Lactic Streptococci are protected from bacteriophages. *Journal of Dairy Science* **1987,** *70* (6), 1121-1127.
67. Prevost, H.; Divies, C.; Rousseau, E., Continuous yoghurt production with Lactobacillus bulgaricus and Streptococcus thermophilus entrapped in Ca-alginate. *Biotechnology Letters* **1985,** *7* (4), 247-252.
68. Roy, D.; Goulet, J.; Le Duy, A., Continuous production of lactic acid from whey perméate by free and calcium alginate entrapped Lactobacillus helveticus1. *Journal of Dairy Science* **1987,** *70* (3), 506-513.
69. Rinaudo, M., Main properties and current applications of some polysaccharides as biomaterials. *Polymer International* **2008,** *57* (3), 397-430.
70. Sheu, T. Y.; Marshall, R. T.; Heymann, H., Improving survival of culture bacteria in frozen desserts by microentrapment. *Journal of Dairy Science* **1993,** *76* (7), 1902-1907.
71. Sultana, K.; Godward, G.; Reynolds, N.; Arumugaswamy, R.; Peiris, P.; Kailasapathy, K., Encapsulation of probiotic bacteria with alginate–starch and evaluation of survival in simulated gastrointestinal conditions and in yoghurt. *International Journal of Food Microbiology* **2000,** *62* (1), 47-55.
72. Joye, I. J.; McClements, D. J., Biopolymer-based nanoparticles and microparticles: Fabrication, characterization, and application. *Current Opinion in Colloid & Interface Science* **2014,** *19* (5), 417-427.
73. Mladenovska, K.; Cruaud, O.; Richomme, P.; Belamie, E.; Raicki, R. S.; Venier-Julienne, M. C.; Popovski, E.; Benoit, J. P.; Goracinova, K., 5-ASA loaded chitosan–Ca–alginate microparticles: Preparation and physicochemical characterization. *International Journal of Pharmaceutics* **2007,** *345* (1), 59-69.
74. Ribeiro, A. J.; Silva, C.; Ferreira, D.; Veiga, F., Chitosan-reinforced alginate microspheres obtained through the emulsification/internal gelation technique. *European Journal of Pharmaceutical Sciences* **2005,** *25* (1), 31-40.

75. Lertsutthiwong, P.; Rojsitthisak, P., Chitosan-alginate nanocapsules for encapsulation of turmeric oil. *Die Pharmazie - An International Journal of Pharmaceutical Sciences* **2011,** *66* (12), 911-915.
76. Ribeiro, M. C. E.; Chaves, K. S.; Gebara, C.; Infante, F. N. S.; Grosso, C. R. F.; Gigante, M. L., Effect of microencapsulation of Lactobacillus acidophilus LA-5 on physicochemical, sensory and microbiological characteristics of stirred probiotic yoghurt. *Food Research International* **2014,** *66*, 424-431.
77. Heidebach, T.; Först, P.; Kulozik, U., Microencapsulation of probiotic cells by means of rennet-gelation of milk proteins. *Food Hydrocolloids* **2009,** *23* (7), 1670-1677.
78. Burgain, J.; Gaiani, C.; Cailliez-Grimal, C.; Jeandel, C.; Scher, J., Encapsulation of Lactobacillus rhamnosus GG in microparticles: Influence of casein to whey protein ratio on bacterial survival during digestion. *Innovative Food Science & Emerging Technologies* **2013,** *19*, 233-242.
79. Timilsena, Y. P.; Akanbi, T. O.; Khalid, N.; Adhikari, B.; Barrow, C. J., Complex coacervation: Principles, mechanisms and applications in microencapsulation. *International Journal of Biological Macromolecules* **2019,** *121*, 1276-1286.
80. Maltais, A.; Remondetto, G. E.; Gonzalez, R.; Subirade, M., Formation of soy protein isolate cold-set gels: Protein and salt effects. *Journal of Food Science* **2005,** *70* (1), C67-C73.
81. Adal, E.; Sadeghpour, A.; Connell, S.; Rappolt, M.; Ibanoglu, E.; Sarkar, A., Heteroprotein complex formation of bovine lactoferrin and pea protein isolate: A multiscale structural analysis. *Biomacromolecules* **2017,** *18* (2), 625-635.
82. Eratte, D.; Dowling, K.; Barrow, C. J.; Adhikari, B., Recent advances in the microencapsulation of omega-3 oil and probiotic bacteria through complex coacervation: A review. *Trends in Food Science & Technology* **2018,** *71*, 121-131.
83. Rathore, S.; Desai, P. M.; Liew, C. V.; Chan, L. W.; Heng, P. W. S., Microencapsulation of microbial cells. *Journal of Food Engineering* **2013,** *116* (2), 369-381.
84. Gerez, C. L.; Font de Valdez, G.; Gigante, M. L.; Grosso, C. R. F., Whey protein coating bead improves the survival of the probiotic Lactobacillus rhamnosus CRL 1505 to low pH. *Letters in Applied Microbiology* **2012,** *54* (6), 552-556.
85. Shoji, A. S.; Oliveira, A. C.; Balieiro, J. C. C.; Freitas, O.; Thomazini, M.; Heinemann, R. J. B.; Okuro, P. K.; Favaro-Trindade, C. S., Viability of L. acidophilus microcapsules and their application to buffalo milk yoghurt. *Food and Bioproducts Processing* **2013,** *91* (2), 83-88.
86. Eratte, D.; McKnight, S.; Gengenbach, T. R.; Dowling, K.; Barrow, C. J.; Adhikari, B. P., Co-encapsulation and characterisation of omega-3 fatty acids and probiotic bacteria in whey protein isolate–gum Arabic complex coacervates. *Journal of Functional Foods* **2015,** *19*, 882-892.
87. McClements, D. J., Encapsulation, protection, and release of hydrophilic active components: Potential and limitations of colloidal delivery systems. *Adv Colloid Interfac* **2015,** *219*, 27-53.
88. Krasaekoopt, W.; Bhandari, B.; Deeth, H., Evaluation of encapsulation techniques of probiotics for yoghurt. *International Dairy Journal* **2003,** *13* (1), 3-13.
89. Papagianni, M.; Anastasiadou, S., Encapsulation of Pediococcus acidilactici cells in corn and olive oil microcapsules emulsified by peptides and stabilized with xanthan in oil-in-

water emulsions: Studies on cell viability under gastro-intestinal simulating conditions. *Enzyme and Microbial Technology* **2009,** *45* (6-7), 514-522.
90. Rao, A. V.; Shiwnarain, N.; Maharaj, I., Survival of Microencapsulated Bifidobacterium pseudolongum in Simulated Gastric and Intestinal Juices. *Canadian Institute of Food Science and Technology Journal* **1989,** *22* (4), 345-349.
91. Fávaro-Trindade, C. S.; Grosso, C. R. F., Microencapsulation of L. acidophilus (La-05) and B. lactis (Bb-12) and evaluation of their survival at the pH values of the stomach and in bile. *Journal of Microencapsulation* **2002,** *19* (4), 485-494.
92. Shima, M.; Morita, Y.; Yamashita, M.; Adachi, S., Protection of Lactobacillus acidophilus from the low pH of a model gastric juice by incorporation in a W/O/W emulsion. *Food Hydrocolloids* **2006,** *20* (8), 1164-1169.
93. Shima, M.; Matsuo, T.; Yamashita, M.; Adachi, S., Protection of Lactobacillus acidophilus from bile salts in a model intestinal juice by incorporation into the inner-water phase of a W/O/W emulsion. *Food Hydrocolloids* **2009,** *23* (2), 281-285.
94. Frakolaki, G.; Katsouli, M.; Giannou, V.; Tzia, C., Novel encapsulation approach for Bifidobacterium subsp. lactis (BB-12) viability enhancement through its incorporation into a double emulsion prior to the extrusion process. *LWT* **2020,** *130*, 109671.
95. Feng, K.; Zhai, M.-Y.; Zhang, Y.; Linhardt, R. J.; Zong, M.-H.; Li, L.; Wu, H., Improved Viability and Thermal Stability of the Probiotics Encapsulated in a Novel Electrospun Fiber Mat. *Journal of Agricultural and Food Chemistry* **2018,** *66* (41), 10890-10897.
96. Feng, K.; Huang, R.-M.; Wu, R.-Q.; Wei, Y.-S.; Zong, M.-H.; Linhardt, R. J.; Wu, H., A novel route for double-layered encapsulation of probiotics with improved viability under adverse conditions. *Food Chemistry* **2020,** *310*, 125977.
97. Paz-Samaniego, R.; Rascon-Chu, A.; Brown-Bojorquez, F.; Carvajal-Millan, E.; Pedroza-Montero, M.; Silva-Campa, E.; Sotelo-Cruz, N.; Lopez-Franco, Y. L.; Lizardi-Mendoza, J., Electrospray-assisted fabrication of core-shell arabinoxylan gel particles for insulin and probiotics entrapment. *Journal of Applied Polymer Science* **2018,** *135* (26).
98. Zaeim, D.; Sarabi-Jamab, M.; Ghorani, B.; Kadkhodaee, R.; Tromp, R. H., Electrospray-assisted drying of live probiotics in acacia gum microparticles matrix. *Carbohydrate Polymers* **2018,** *183*, 183-191.
99. Fonseca, F.; Béal, C.; Corrieu, G., Method of quantifying the loss of acidification activity of lactic acid starters during freezing and frozen storage. *Journal of Dairy Research* **2000,** *67* (1), 83-90.
100. Xu, M.; Gagné-Bourque, F.; Dumont, M.-J.; Jabaji, S., Encapsulation of Lactobacillus casei ATCC 393 cells and evaluation of their survival after freeze-drying, storage and under gastrointestinal conditions. *Journal of Food Engineering* **2016,** *168*, 52-59.
101. Quintana, G.; Simoes, M. G.; Hugo, A.; Alves, P.; Ferreira, P.; Gerbino, E.; Simoes, P. N.; Gomez-Zavaglia, A., Layer-by-layer encapsulation of Lactobacillus delbrueckii subsp Bulgaricus using block-copolymers of poly(acrylic acid) and pluronic for safe release in gastro-intestinal conditions. *Journal of Functional Foods* **2017,** *35*, 408-417.
102. Sohail, A.; Turner, M. S.; Coombes, A.; Bhandari, B., The viability of Lactobacillus rhamnosus GG and Lactobacillus acidophilus NCFM following double encapsulation in alginate and maltodextrin. *Food and Bioprocess Technology* **2013,** *6* (10), 2763-2769.

103. Zayed, G.; Roos, Y. H., Influence of trehalose and moisture content on survival of Lactobacillus salivarius subjected to freeze-drying and storage. *Process Biochemistry* **2004,** *39* (9), 1081-1086.
104. Dimitrellou, D.; Kandylis, P.; Petrović, T.; Dimitrijević-Branković, S.; Lević, S.; Nedović, V.; Kourkoutas, Y., Survival of spray dried microencapsulated Lactobacillus casei ATCC 393 in simulated gastrointestinal conditions and fermented milk. *LWT - Food Science and Technology* **2016,** *71*, 169-174.
105. Arslan, S.; Erbas, M.; Tontul, I.; Topuz, A., Microencapsulation of probiotic Saccharomyces cerevisiae var. boulardii with different wall materials by spray drying. *LWT - Food Science and Technology* **2015,** *63* (1), 685-690.
106. Rajam, R.; Anandharamakrishnan, C., Microencapsulation of Lactobacillus plantarum (MTCC 5422) with fructooligosaccharide as wall material by spray drying. *LWT - Food Science and Technology* **2015,** *60* (2), 773-780.
107. Meng, X. C.; Stanton, C.; Fitzgerald, G. F.; Daly, C.; Ross, R. P., Anhydrobiotics: The challenges of drying probiotic cultures. *Food Chemistry* **2008,** *106* (4), 1406-1416.
108. Bustamante, M.; Villarroel, M.; Rubilar, M.; Shene, C., Lactobacillus acidophilus La-05 encapsulated by spray drying: Effect of mucilage and protein from flaxseed (Linum usitatissimum L.). *LWT - Food Science and Technology* **2015,** *62* (2), 1162-1168.
109. Gardiner, G. E.; Sullivan, E.; Kelly, J.; Auty, M. A. E.; Fitzgerald, G. F.; Collins, J. K.; Ross, R. P.; Stanton, C., Comparative Survival Rates of Human-Derived Probiotic<em>Lactobacillus paracasei</em> and <em>L. salivarius</em>Strains during Heat Treatment and Spray Drying. *Applied and Environmental Microbiology* **2000,** *66* (6), 2605.
110. Arepally, D.; Goswami, T. K., Effect of inlet air temperature and gum Arabic concentration on encapsulation of probiotics by spray drying. *LWT* **2019,** *99*, 583-593.
111. Ishwarya, S. P.; Anandharamakrishnan, C.; Stapley, A. G. F., Spray-freeze-drying: A novel process for the drying of foods and bioproducts. *Trends in Food Science & Technology* **2015,** *41* (2), 161-181.
112. Rajam, R.; Anandharamakrishnan, C., Spray freeze drying method for microencapsulation of Lactobacillus plantarum. *Journal of Food Engineering* **2015,** *166*, 95-103.
113. Semyonov, D.; Ramon, O.; Kaplun, Z.; Levin-Brener, L.; Gurevich, N.; Shimoni, E., Microencapsulation of Lactobacillus paracasei by spray freeze drying. *Food Research International* **2010,** *43* (1), 193-202.
114. Schell, D.; Beermann, C., Fluidized bed microencapsulation of Lactobacillus reuteri with sweet whey and shellac for improved acid resistance and in-vitro gastro-intestinal survival. *Food Research International* **2014,** *62*, 308-314.
115. Santivarangkna, C.; Kulozik, U.; Foerst, P., Alternative drying processes for the industrial preservation of lactic acid starter cultures. *Biotechnology Progress* **2007,** *23* (2), 302-315.
116. Zaeim, D.; Sarabi-Jamab, M.; Ghorani, B.; Kadkhodaee, R.; Tromp, R. H., Electrospray assisted fabrication of hydrogel microcapsules by single- and double-stage procedures for encapsulation of probiotics. *Food and Bioproducts Processing* **2017,** *102*, 250-259.
117. Atia, A.; Gomaa, A.; Fliss, I.; Beyssac, E.; Garrait, G.; Subirade, M., A prebiotic matrix for encapsulation of probiotics: physicochemical and microbiological study. *Journal of Microencapsulation* **2016,** *33* (1), 89-101.

118. Lan, Y.; Ohm, J.-B.; Chen, B.; Rao, J., Microencapsulation of hemp seed oil by pea protein isolate−sugar beet pectin complex coacervation: Influence of coacervation pH and wall/core ratio. *Food Hydrocolloids* **2021,** *113*, 106423.
119. Fischer, E. R.; Hansen, B. T.; Nair, V.; Hoyt, F. H.; Dorward, D. W., Scanning electron microscopy. *Curr Protoc Microbiol* **2012,** *Chapter 2*, Unit2B.2-2B.2.
120. Mu, R.-J.; Yuan, Y.; Wang, L.; Ni, Y.; Li, M.; Chen, H.; Pang, J., Microencapsulation of Lactobacillus acidophilus with konjac glucomannan hydrogel. *Food Hydrocolloids* **2018,** *76*, 42-48.
121. Gu, M.; Zhang, Z.; Pan, C.; Goulette, T. R.; Zhang, R.; Hendricks, G.; McClements, D. J.; Xiao, H., Encapsulation of Bifidobacterium pseudocatenulatum G7 in gastroprotective microgels: Improvement of the bacterial viability under simulated gastrointestinal conditions. *Food Hydrocolloids* **2019,** *91*, 283-289.
122. Sousa, S.; Gomes, A. M.; Pintado, M. M.; Silva, J. P.; Costa, P.; Amaral, M. H.; Duarte, A. C.; Rodrigues, D.; Rocha-Santos, T. A. P.; Freitas, A. C., Characterization of freezing effect upon stability of, probiotic loaded, calcium-alginate microparticles. *Food and Bioproducts Processing* **2015,** *93*, 90-97.
123. Muthukumarasamy, P.; Allan‐Wojtas, P.; Holley, R. A., Stability of Lactobacillus reuteri in different types of microcapsules. *Journal of Food Science* **2006,** *71* (1), M20-M24.
124. Allan-Wojtas, P.; Truelstrup Hansen, L.; Paulson, A. T., Microstructural studies of probiotic bacteria-loaded alginate microcapsules using standard electron microscopy techniques and anhydrous fixation. *LWT - Food Science and Technology* **2008,** *41* (1), 101-108.
125. Lamprecht, A.; Schäfer, U.; Lehr, C.-M., Structural analysis of microparticles by confocal laser scanning microscopy. *AAPS PharmSciTech* **2000,** *1* (3), 10-19.
126. Doherty, S. B.; Gee, V. L.; Ross, R. P.; Stanton, C.; Fitzgerald, G. F.; Brodkorb, A., Efficacy of whey protein gel networks as potential viability-enhancing scaffolds for cell immobilization of Lactobacillus rhamnosus GG. *Journal of Microbiological Methods* **2010,** *80* (3), 231-241.
127. Yao, M.; Li, B.; Ye, H.; Huang, W.; Luo, Q.; Xiao, H.; McClements, D. J.; Li, L., Enhanced viability of probiotics (Pediococcus pentosaceus Li05) by encapsulation in microgels doped with inorganic nanoparticles. *Food Hydrocolloids* **2018,** *83*, 246-252.
128. Picone, C. S. F.; Bueno, A. C.; Michelon, M.; Cunha, R. L., Development of a probiotic delivery system based on gelation of water-in-oil emulsions. *LWT* **2017,** *86*, 62-68.
129. Yan, W.; Jia, X.; Zhang, Q.; Chen, H.; Zhu, Q.; Yin, L., Interpenetrating polymer network hydrogels of soy protein isolate and sugar beet pectin as a potential carrier for probiotics. *Food Hydrocolloids* **2021,** *113*, 106453.
130. Franck, A., *Viscoelasticity and dynamic mechanical testing*. 1993.
131. Qin, X.-S.; Luo, Z.-G.; Li, X.-L., An enhanced pH-sensitive carrier based on alginate-Ca-EDTA in a set-type W1/O/W2 double emulsion model stabilized with WPI-EGCG covalent conjugates for probiotics colon-targeted release. *Food Hydrocolloids* **2021,** *113*, 106460.
132. Bosnea, L.; Moschakis, T.; Biliaderis, C., Microencapsulated cells of Lactobacillus paracasei subsp. paracasei in biopolymer complex coacervates and their function in a yogurt matrix. *Food Function* **2017,** *8* (2), 554-562.

133. Vaziri, A. S.; Alemzadeh, I.; Vossoughi, M.; Khorasani, A. C., Co-microencapsulation of Lactobacillus plantarum and DHA fatty acid in alginate-pectin-gelatin biocomposites. *Carbohydrate Polymers* **2018,** *199*, 266-275.
134. Lan, Y.; Ohm, J.-B.; Chen, B.; Rao, J., Phase behavior, thermodynamic and microstructure of concentrated pea protein isolate-pectin mixture: Effect of pH, biopolymer ratio and pectin charge density. *Food Hydrocolloids* **2020,** *101*, 105556.
135. Huang, G.-Q.; Sun, Y.-T.; Xiao, J.-X.; Yang, J., Complex coacervation of soybean protein isolate and chitosan. *Food Chemistry* **2012,** *135* (2), 534-539.
136. Ashwar, B. A.; Gani, A.; Gani, A.; Shah, A.; Masoodi, F. A., Production of RS4 from rice starch and its utilization as an encapsulating agent for targeted delivery of probiotics. *Food Chemistry* **2018,** *239*, 287-294.
137. Bosnea, L. A.; Moschakis, T.; Biliaderis, C. G., Complex coacervation as a novel microencapsulation technique to improve viability of probiotics under different stresses. *Food Bioprocess Technology* **2014,** *7* (10), 2767-2781.
138. Zhao, M.; Wang, Y.; Huang, X.; Gaenzle, M.; Wu, Z.; Nishinari, K.; Yang, N.; Fang, Y., Ambient storage of microencapsulated Lactobacillus plantarum ST-III by complex coacervation of type-A gelatin and gum arabic. *Food Function* **2018,** *9* (2), 1000-1008.
139. Lim, P. Y., Microbiological procedure: Aerobic plate count. In *Laboratory Manual on Analytical Methods and Procedures for Fish and Fish Products*, Marine Fisheries Research Department, Southeast Asian Fisheries Development: 1992; pp E-2.1-E-2.5.
140. Glasson, J. H.; Guthrie, L. H.; Nielsen, D. J.; Bethell, F. A., Evaluation of an Automated Instrument for Inoculating and Spreading Samples onto Agar Plates. *Journal of Clinical Microbiology* **2008,** *46* (4), 1281.
141. Maruyama, A.; Sunamura, M., Simultaneous direct counting of total and specific microbial cells in seawater, using a deep-sea microbe as target. *Applied and Environmental Microbiology* **2000,** *66* (5), 2211.
142. Lee, J.; Deininger, R. A., Detection of E. coli in beach water within 1 hour using immunomagnetic separation and ATP bioluminescence. *Luminescence* **2004,** *19* (1), 31-36.
143. Nakajima, K.; Nonaka, K.; Yamamoto, K.; Yamaguchi, N.; Tani, K.; Nasu, M., Rapid monitoring of microbial contamination on herbal medicines by fluorescent staining method. *Letters in Applied Microbiology* **2005,** *40* (2), 128-132.
144. Klein, S., The Use of Biorelevant Dissolution Media to Forecast the In Vivo Performance of a Drug. *The AAPS Journal* **2010,** *12* (3), 397-406.
145. Matalanis, A.; McClements, D. J., Impact of encapsulation within hydrogel microspheres on lipid digestion: An in vitro study. *Food Biophysics* **2012,** *7* (2), 145-154.
146. Krasaekoopt, W.; Bhandari, B.; Deeth, H., The influence of coating materials on some properties of alginate beads and survivability of microencapsulated probiotic bacteria. *International Dairy Journal* **2004,** *14* (8), 737-743.
147. Sun, W.; Griffiths, M. W., Survival of bifidobacteria in yogurt and simulated gastric juice following immobilization in gellan–xanthan beads. *International Journal of Food Microbiology* **2000,** *61* (1), 17-25.
148. And, C. I.; Kailasapathy, K., Effect of Co-encapsulation of Probiotics with Prebiotics on Increasing the Viability of Encapsulated Bacteria under In Vitro Acidic and Bile Salt Conditions and in Yogurt. *Journal of Food Science* **2005,** *70* (1), M18-M23.

149. Fu, T.-J.; Abbott, U. R.; Hatzos, C., Digestibility of Food Allergens and Nonallergenic Proteins in Simulated Gastric Fluid and Simulated Intestinal FluidA Comparative Study. *Journal of Agricultural and Food Chemistry* **2002,** *50* (24), 7154-7160.
150. Roger, E.; Lagarce, F.; Benoit, J. P., The gastrointestinal stability of lipid nanocapsules. *International Journal of Pharmaceutics* **2009,** *379* (2), 260-265.
151. Bhagat, N. B., A review on development of biorelevant dissolution medium. *Journal of Drug Delivery Therapeutics* **2014,** *4* (2), 140-148.
152. Qian, C.; Decker, E. A.; Xiao, H.; McClements, D. J., Nanoemulsion delivery systems: Influence of carrier oil on β-carotene bioaccessibility. *Food Chemistry* **2012,** *135* (3), 1440-1447.
153. Sandoval-Castilla, O.; Lobato-Calleros, C.; García-Galindo, H. S.; Alvarez-Ramírez, J.; Vernon-Carter, E. J., Textural properties of alginate–pectin beads and survivability of entrapped Lb. casei in simulated gastrointestinal conditions and in yoghurt. *Food Research International* **2010,** *43* (1), 111-117.
154. Chávarri, M.; Marañón, I.; Ares, R.; Ibáñez, F. C.; Marzo, F.; Villarán, M. d. C., Microencapsulation of a probiotic and prebiotic in alginate-chitosan capsules improves survival in simulated gastro-intestinal conditions. *International Journal of Food Microbiology* **2010,** *142* (1), 185-189.
155. García-Ceja, A.; Mani-López, E.; Palou, E.; López-Malo, A., Viability during refrigerated storage in selected food products and during simulated gastrointestinal conditions of individual and combined lactobacilli encapsulated in alginate or alginate-chitosan. *LWT - Food Science and Technology* **2015,** *63* (1), 482-489.
156. Liu, H.; Gong, J.; Chabot, D.; Miller, S. S.; Cui, S. W.; Ma, J.; Zhong, F.; Wang, Q., Incorporation of polysaccharides into sodium caseinate-low melting point fat microparticles improves probiotic bacterial survival during simulated gastrointestinal digestion and storage. *Food Hydrocolloids* **2016,** *54*, 328-337.
157. Kararli, T. T., Comparison of the gastrointestinal anatomy, physiology, and biochemistry of humans and commonly used laboratory animals. *Biopharmaceutics & Drug Disposition* **1995,** *16* (5), 351-380.
158. Masco, L.; Vanhoutte, T.; Temmerman, R.; Swings, J.; Huys, G., Evaluation of real-time PCR targeting the 16S rRNA and recA genes for the enumeration of bifidobacteria in probiotic products. *International Journal of Food Microbiology* **2007,** *113* (3), 351-357.
159. Maré, L.; Wolfaardt, G. M.; Dicks, L. M. T., Adhesion of Lactobacillus plantarum 423 and Lactobacillus salivarius 241 to the intestinal tract of piglets, as recorded with fluorescent in situ hybridization (FISH), and production of plantaricin 423 by cells colonized to the ileum. *J Appl Microbiol* **2006,** *100* (4), 838-845.
160. Guglielmotti, D. M.; Marcó, M. B.; Golowczyc, M.; Reinheimer, J. A.; Quiberoni, A. d. L., Probiotic potential of Lactobacillus delbrueckii strains and their phage resistant mutants. *International Dairy Journal* **2007,** *17* (8), 916-925.
161. Mokhtari, S.; Jafari, S. M.; Khomeiri, M.; Maghsoudlou, Y.; Ghorbani, M., The cell wall compound of Saccharomyces cerevisiae as a novel wall material for encapsulation of probiotics. *Food Research International* **2017,** *96*, 19-26.
162. Camino, N. A.; Pérez, O. E.; Pilosof, A. M. R., Molecular and functional modification of hydroxypropylmethylcellulose by high-intensity ultrasound. *Food Hydrocolloids* **2009,** *23* (4), 1089-1095.

163. Puppo, C.; Chapleau, N.; Speroni, F.; de Lamballerie-Anton, M.; Michel, F.; Añón, C.; Anton, M., Physicochemical modifications of high-pressure-treated soybean protein isolates. *Journal of Agricultural and Food Chemistry* **2004,** *52* (6), 1564-1571.
164. Mirmoghtadaie, L.; Shojaee Aliabadi, S.; Hosseini, S. M., Recent approaches in physical modification of protein functionality. *Food Chemistry* **2016,** *199*, 619-627.
165. Jambrak, A. R.; Lelas, V.; Mason, T. J.; Krešić, G.; Badanjak, M., Physical properties of ultrasound treated soy proteins. *Journal of Food Engineering* **2009,** *93* (4), 386-393.
166. Calligaris, S.; Plazzotta, S.; Bot, F.; Grasselli, S.; Malchiodi, A.; Anese, M., Nanoemulsion preparation by combining high pressure homogenization and high power ultrasound at low energy densities. *Food Research International* **2016,** *83*, 25-30.
167. Saier, M. H.; Mansour, N. M., Probiotics and prebiotics in human health. *Journal of Molecular Microbiology and Biotechnology* **2005,** *10* (1), 22-25.
168. Mach, T., Clinical usefulness of probiotics in inflammatory bowel diseases. *Journal of Physiology and Pharmacology* **2006,** *57*, 23-33.
169. Ouwehand, A. C.; Salminen, S. J., The health effects of cultured milk products with viable and non-viable bacteria. *International Dairy Journal* **1998,** *8* (9), 749-758.
170. Liu, H.; Gong, J.; Chabot, D.; Miller, S. S.; Cui, S. W.; Zhong, F.; Wang, Q., Improved survival of Lactobacillus zeae LB1 in a spray dried alginate-protein matrix. *Food Hydrocolloids* **2018,** *78*, 100-108.
171. Saarela, M.; Virkajärvi, I.; Alakomi, H.-L.; Sigvart-Mattila, P.; Mättö, J., Stability and functionality of freeze-dried probiotic Bifidobacterium cells during storage in juice and milk. *International Dairy Journal* **2006,** *16* (12), 1477-1482.
172. Laličić-Petronijević, J.; Popov-Raljić, J.; Obradović, D.; Radulović, Z.; Paunović, D.; Petrušić, M.; Pezo, L., Viability of probiotic strains Lactobacillus acidophilus NCFM® and Bifidobacterium lactis HN019 and their impact on sensory and rheological properties of milk and dark chocolates during storage for 180 days. *Journal of Functional Foods* **2015,** *15*, 541-550.
173. Pinto, S. S.; Fritzen-Freire, C. B.; Benedetti, S.; Murakami, F. S.; Petrus, J. C. C.; Prudêncio, E. S.; Amboni, R. D. M. C., Potential use of whey concentrate and prebiotics as carrier agents to protect Bifidobacterium-BB-12 microencapsulated by spray drying. *Food Research International* **2015,** *67*, 400-408.
174. Cook, M. T.; Tzortzis, G.; Charalampopoulos, D.; Khutoryanskiy, V. V., Microencapsulation of probiotics for gastrointestinal delivery. *Journal of Controlled Release* **2012,** *162* (1), 56-67.
175. Martin, M. J.; Lara-Villoslada, F.; Ruiz, M. A.; Morales, M. E., Microencapsulation of bacteria: A review of different technologies and their impact on the probiotic effects. *Innovative Food Science & Emerging Technologies* **2015,** *27*, 15-25.
176. Burgain, J.; Gaiani, C.; Linder, M.; Scher, J., Encapsulation of probiotic living cells: From laboratory scale to industrial applications. *Journal of Food Engineering* **2011,** *104* (4), 467-483.
177. Dong, Q.-Y.; Chen, M.-Y.; Xin, Y.; Qin, X.-Y.; Cheng, Z.; Shi, L.-E.; Tang, Z.-X., Alginate-based and protein-based materials for probiotics encapsulation: a review. **2013,** *48* (7), 1339-1351.
178. Anal, A. K.; Singh, H., Recent advances in microencapsulation of probiotics for industrial applications and targeted delivery. *Trends in Food Science & Technology* **2007,** *18* (5), 240-251.

179. Strand, B. L.; Morch, Y. A.; Skjak-Braek, G., Alginate as immobilization matrix for cells. *Minerva Biotechnol.* **2000,** *12* (4), 223-233.
180. Donthidi, A. R.; Tester, R. F.; Aidoo, K. E., Effect of lecithin and starch on alginate-encapsulated probiotic bacteria. *Journal of Microencapsulation* **2010,** *27* (1), 67-77.
181. Nualkaekul, S.; Lenton, D.; Cook, M. T.; Khutoryanskiy, V. V.; Charalampopoulos, D., Chitosan coated alginate beads for the survival of microencapsulated Lactobacillus plantarum in pomegranate juice. *Carbohydrate Polymers* **2012,** *90* (3), 1281-1287.
182. Shamekhi, F.; Tamjid, E.; Khajeh, K., Development of chitosan coated calcium-alginate nanocapsules for oral delivery of liraglutide to diabetic patients. *International Journal of Biological Macromolecules* **2018,** *120*, 460-467.
183. Lee, D. W.; Lim, C.; Israelachvili, J. N.; Hwang, D. S., Strong adhesion and cohesion of chitosan in aqueous solutions. *Langmuir* **2013,** *29* (46), 14222-14229.
184. Zhou, Y.; Martins, E.; Groboillot, A.; Champagne, C. P.; Neufeld, P. C., Spectrophotometric quantification of lactic bacteria in alginate and control of cell release with chitosan coating. *J Appl Microbiol* **1998,** *84* (3), 342-348.
185. Bourne, M., *Food texture and viscosity: concept and measurement*. Elsevier: 2002.
186. Lan, Y.; Xu, M.; Ohm, J.-B.; Chen, B.; Rao, J., Solid dispersion-based spray-drying improves solubility and mitigates beany flavour of pea protein isolate. *Food Chemistry* **2019,** *278*, 665-673.
187. Wang, Y.; Khan, A.; Liu, Y.; Feng, J.; Dai, L.; Wang, G.; Alam, N.; Tong, L.; Ni, Y., Chitosan oligosaccharide-based dual pH responsive nano-micelles for targeted delivery of hydrophobic drugs. *Carbohydrate Polymers* **2019,** *223*, 115061.
188. Muanprasat, C.; Chatsudthipong, V., Chitosan oligosaccharide: Biological activities and potential therapeutic applications. *Pharmacology & Therapeutics* **2017,** *170*, 80-97.
189. Lee, H.-W.; Park, Y.-S.; Jung, J.-S.; Shin, W.-S., Chitosan oligosaccharides, dp 2–8, have prebiotic effect on the Bifidobacterium bifidium and Lactobacillus sp. *Anaerobe* **2002,** *8* (6), 319-324.
190. Rabelo, R. S.; Oliveira, I. F.; da Silva, V. M.; Prata, A. S.; Hubinger, M. D., Chitosan coated nanostructured lipid carriers (NLCs) for loading Vitamin D: A physical stability study. *International Journal of Biological Macromolecules* **2018,** *119*, 902-912.
191. Luo, Q.; Zhao, J.; Zhang, X.; Pan, W., Nanostructured lipid carrier (NLC) coated with Chitosan Oligosaccharides and its potential use in ocular drug delivery system. *International Journal of Pharmaceutics* **2011,** *403* (1), 185-191.
192. Einbu, A.; Grasdalen, H.; Vårum, K. M., Kinetics of hydrolysis of chitin/chitosan oligomers in concentrated hydrochloric acid. *Carbohydrate Research* **2007,** *342* (8), 1055-1062.
193. Ramos, P. E.; Silva, P.; Alario, M. M.; Pastrana, L. M.; Teixeira, J. A.; Cerqueira, M. A.; Vicente, A. A., Effect of alginate molecular weight and M/G ratio in beads properties foreseeing the protection of probiotics. *Food Hydrocolloids* **2018,** *77*, 8-16.
194. Koo, S. M.; Cho, Y. H.; Huh, C. S.; Baek, Y. J.; Park, J., Improvement of the stability of Lactobacillus casei YIT 9018 by microencapsulation using alginate and chitosan. *J. Microbiol. Biotechnol.* **2001,** *11* (3), 376-383.
195. Zhao, Q.; Mutukumira, A.; Lee, S. J.; Maddox, I.; Shu, Q., Functional properties of free and encapsulated Lactobacillus reuteri DPC16 during and after passage through a simulated gastrointestinal tract. *World Journal of Microbiology and Biotechnology* **2012,** *28* (1), 61-70.

196. Lee, J.; Cha, D.; Park, H. J., Survival of freeze-dried Lactobacillus bulgaricus KFRI 673 in chitosan-coated calcium alginate microparticles. *Journal of agricultural food chemistry* **2004,** *52* (24), 7300-7305.
197. Smidsrød, O.; Skja˚k-Br┤k, G., Alginate as immobilization matrix for cells. *Trends in Biotechnology* **1990,** *8*, 71-78.
198. Stokke, B. T.; Draget, K. I.; Smidsrød, O.; Yuguchi, Y.; Urakawa, H.; Kajiwara, K., Small-Angle X-ray scattering and rheological characterization of alginate gels. 1. Ca−alginate gels. *Macromolecules* **2000,** *33* (5), 1853-1863.
199. Sabitha, P.; Ratna, J. V.; Reddy, K. R., Design and evaluation of controlled release chitosan-calcium alginate microcapsules of antitubercular drugs for oral use. *International Journal of ChemTech Research* **2010,** *2* (1), 88-98.
200. Melo-Silveira, R. F.; Fidelis, G. P.; Costa, M. S. S. P.; Telles, C. B. S.; Dantas-Santos, N.; Elias, S. d. O.; Ribeiro, V. B.; Barth, A. L.; Macedo, A. J.; Leite, E. L.; Rocha, H. A. O., In vitro antioxidant, anticoagulant and antimicrobial activity and in inhibition of cancer cell proliferation by xylan extracted from corn cobs. *International Journal of Molecular Sciences* **2012,** *13* (1).
201. Silva, F. R. F.; Dore, C. M. P. G.; Marques, C. T.; Nascimento, M. S.; Benevides, N. M. B.; Rocha, H. A. O.; Chavante, S. F.; Leite, E. L., Anticoagulant activity, paw edema and pleurisy induced carrageenan: Action of major types of commercial carrageenans. *Carbohydrate Polymers* **2010,** *79* (1), 26-33.
202. Vino, A. B.; Ramasamy, P.; Shanmugam, V.; Shanmugam, A., Extraction, characterization and in vitro antioxidative potential of chitosan and sulfated chitosan from Cuttlebone of Sepia aculeata Orbigny, 1848. *Asian Pacific Journal of Tropical Biomedicine* **2012,** *2* (1, Supplement), S334-S341.
203. Song, C.; Yu, H.; Zhang, M.; Yang, Y.; Zhang, G., Physicochemical properties and antioxidant activity of chitosan from the blowfly Chrysomya megacephala larvae. *International Journal of Biological Macromolecules* **2013,** *60*, 347-354.
204. Smitha, B.; Sridhar, S.; Khan, A. A., Chitosan–sodium alginate polyion complexes as fuel cell membranes. *European Polymer Journal* **2005,** *41* (8), 1859-1866.
205. Belščak-Cvitanović, A.; Komes, D.; Karlović, S.; Djaković, S.; Špoljarić, I.; Mršić, G.; Ježek, D., Improving the controlled delivery formulations of caffeine in alginate hydrogel beads combined with pectin, carrageenan, chitosan and psyllium. *Food Chemistry* **2015,** *167*, 378-386.
206. Tripathi, M. K.; Giri, S. K., Probiotic functional foods: Survival of probiotics during processing and storage. *Journal of Functional Foods* **2014,** *9*, 225-241.
207. Mussatto, S. I.; Mancilha, I. M., Non-digestible oligosaccharides: A review. *Carbohydrate Polymers* **2007,** *68* (3), 587-597.
208. Doherty, S. B.; Auty, M. A.; Stanton, C.; Ross, R. P.; Fitzgerald, G. F.; Brodkorb, A., Survival of entrapped Lactobacillus rhamnosus GG in whey protein micro-beads during simulated ex vivo gastro-intestinal transit. *International Dairy Journal* **2012,** *22* (1), 31-43.
209. Li, R.; Zhang, Y.; Polk, D. B.; Tomasula, P. M.; Yan, F.; Liu, L., Preserving viability of Lactobacillus rhamnosus GG in vitro and in vivo by a new encapsulation system. *Journal of Controlled Release* **2016,** *230*, 79-87.
210. Cook, M. T.; Tzortzis, G.; Khutoryanskiy, V. V.; Charalampopoulos, D., Layer-by-layer coating of alginate matrices with chitosan–alginate for the improved survival and targeted

delivery of probiotic bacteria after oral administration. *Journal of Materials Chemistry B* **2013,** *1* (1), 52-60.
211. Abbaszadeh, S.; Gandomi, H.; Misaghi, A.; Bokaei, S.; Noori, N., The effect of alginate and chitosan concentrations on some properties of chitosan‐coated alginate beads and survivability of encapsulated Lactobacillus rhamnosus in simulated gastrointestinal conditions and during heat processing. *Journal of the Science of Food Agriculture* **2014,** *94* (11), 2210-2216.
212. Saez-Lara, M. J.; Gomez-Llorente, C.; Plaza-Diaz, J.; Gil, A., The role of probiotic lactic acid bacteria and bifidobacteria in the prevention and treatment of inflammatory bowel disease and other related diseases: a systematic review of randomized human clinical trials. *BioMed Research International* **2015,** *2015*.
213. Schwabe, R. F.; Jobin, C., The microbiome and cancer. *Nature Reviews Cancer* **2013,** *13* (11), 800-812.
214. Stanton, C.; Gardiner, G.; Meehan, H.; Collins, K.; Fitzgerald, G.; Lynch, P. B.; Ross, R. P., Market potential for probiotics. *The American journal of clinical nutrition* **2001,** *73* (2), 476s-483s.
215. Robinson, R. K., *Therapeutic properties of fermented milks*. Elsevier Applied Science: 1991.
216. Matalanis, A.; Jones, O. G.; McClements, D. J., Structured biopolymer-based delivery systems for encapsulation, protection, and release of lipophilic compounds. *Food Hydrocolloids* **2011,** *25* (8), 1865-1880.
217. Arifin, D. Y.; Lee, L. Y.; Wang, C.-H., Mathematical modeling and simulation of drug release from microspheres: Implications to drug delivery systems. *Advanced Drug Delivery Reviews* **2006,** *58* (12), 1274-1325.
218. Qi, X.; Simsek, S.; Ohm, J.-B.; Chen, B.; Rao, J., Viability of Lactobacillus rhamnosus GG microencapsulated in alginate/chitosan hydrogel particles during storage and simulated gastrointestinal digestion: role of chitosan molecular weight. *Soft Matter* **2020,** *16* (7), 1877-1887.
219. Chakraborty, S., Carrageenan for encapsulation and immobilization of flavor, fragrance, probiotics, and enzymes: A review. *Journal of Carbohydrate Chemistry* **2017,** *36* (1), 1-19.
220. Assifaoui, A.; Chambin, O.; Cayot, P., Drug release from calcium and zinc pectinate beads: Impact of dissolution medium composition. *Carbohydrate Polymers* **2011,** *85* (2), 388-393.
221. Das, S.; Ng, K. Y., Colon-specific delivery of resveratrol: Optimization of multi-particulate calcium-pectinate carrier. *International Journal of Pharmaceutics* **2010,** *385* (1-2), 20-28.
222. Voo, W.-P.; Ravindra, P.; Tey, B.-T.; Chan, E.-S., Comparison of alginate and pectin based beads for production of poultry probiotic cells. *Journal of Bioscience and Bioengineering* **2011,** *111* (3), 294-299.
223. Shi, L.-E.; Li, Z.-H.; Li, D.-T.; Xu, M.; Chen, H.-Y.; Zhang, Z.-L.; Tang, Z.-X., Encapsulation of probiotic Lactobacillus bulgaricus in alginate–milk microspheres and evaluation of the survival in simulated gastrointestinal conditions. *Journal of Food Engineering* **2013,** *117* (1), 99-104.

224. Curto, A. L.; Pitino, I.; Mandalari, G.; Dainty, J. R.; Faulks, R. M.; Wickham, M. S. J., Survival of probiotic lactobacilli in the upper gastrointestinal tract using an in vitro gastric model of digestion. *Food Microbiol.* **2011,** *28* (7), 1359-1366.
225. Coghetto, C. C.; Brinques, G. B.; Siqueira, N. M.; Pletsch, J.; Soares, R. M. D.; Ayub, M. A. Z., Electrospraying microencapsulation of Lactobacillus plantarum enhances cell viability under refrigeration storage and simulated gastric and intestinal fluids. *Journal of Functional Foods* **2016,** *24*, 316-326.
226. Brinques, G. B.; Ayub, M. A. Z., Effect of microencapsulation on survival of Lactobacillus plantarum in simulated gastrointestinal conditions, refrigeration, and yogurt. *Journal of Food Engineering* **2011,** *103* (2), 123-128.
227. Davarcı, F.; Turan, D.; Ozcelik, B.; Poncelet, D., The influence of solution viscosities and surface tension on calcium-alginate microbead formation using dripping technique. *Food Hydrocolloids* **2017,** *62*, 119-127.
228. Klokk, T.; Melvik, J., Controlling the size of alginate gel beads by use of a high electrostatic potential. *Journal of Microencapsulation* **2002,** *19* (4), 415-424.
229. Moghadam, H.; Samimi, M.; Samimi, A.; Khorram, M., Electro-spray of high viscous liquids for producing mono-sized spherical alginate beads. *Particuology* **2008,** *6* (4), 271-275.
230. Mohamadnia, Z.; Zohuriaan-Mehr, M.; Kabiri, K.; Jamshidi, A.; Mobedi, H., Ionically cross-linked carrageenan-alginate hydrogel beads. *Journal of Biomaterials Science, Polymer Edition* **2008,** *19* (1), 47-59.
231. Park, S.-J.; Shin, Y.-S.; Lee, J.-R., Preparation and characterization of microcapsules containing lemon oil. *Journal of Colloid Interface Science* **2001,** *241* (2), 502-508.
232. Díaz-Rojas, E.; Pacheco-Aguilar, R.; Lizardi, J.; Argüelles-Monal, W.; Valdez, M.; Rinaudo, M.; Goycoolea, F., Linseed pectin: gelling properties and performance as an encapsulation matrix for shark liver oil. *Food Hydrocolloids* **2004,** *18* (2), 293-304.
233. Chen, F.; Zhang, Z.; Deng, Z.; Zhang, R.; Fan, G.; Ma, D.; McClements, D. J., Controlled-release of antacids from biopolymer microgels under simulated gastric conditions: Impact of bead dimensions, pore size, and alginate/pectin ratio. *Food Research International* **2018,** *106*, 745-751.
234. Li; Zhao, J.; Sun, Y.; Yu, F.; Ma, J., Ionically cross-linked sodium alginate/κ-carrageenan double-network gel beads with low-swelling, enhanced mechanical properties, and excellent adsorption performance. *Chemical Engineering Journal* **2019,** *372*, 1091-1103.
235. Totosaus, A.; de Jesús Ariza-Ortega, T., Lactic acid bacteria microencapsulation in sodium alginate and other gelling hydrocolloids mixtures. *Journal of Food and Nutrition Research* **2013,** *52* (2), 107-120.
236. Pillay, V.; Fassihi, R., In vitro release modulation from crosslinked pellets for site-specific drug delivery to the gastrointestinal tract: II. Physicochemical characterization of calcium–alginate, calcium–pectinate and calcium–alginate–pectinate pellets. *Journal of Controlled Release* **1999,** *59* (2), 243-256.
237. Cao, L.; Lu, W.; Mata, A.; Nishinari, K.; Fang, Y., Egg-box model-based gelation of alginate and pectin: A review. *Carbohydrate Polymers* **2020**, 116389.
238. Hurler, J.; Engesland, A.; Poorahmary Kermany, B.; Škalko‐Basnet, N., Improved texture analysis for hydrogel characterization: gel cohesiveness, adhesiveness, and hardness. *Journal of Applied Polymer Science* **2012,** *125* (1), 180-188.

239. Stroumpoulis, D.; Guillen, K. H. Hair-like shaped hydrogels for soft tissue augmentation. 2010.
240. Krop, E. M.; Hetherington, M. M.; Holmes, M.; Miquel, S.; Sarkar, A., On relating rheology and oral tribology to sensory properties in hydrogels. *Food Hydrocolloids* **2019,** *88*, 101-113.
241. Smrdel, P.; Bogataj, M.; Mrhar, A., The influence of selected parameters on the size and shape of alginate beads prepared by ionotropic gelation. *Scientia Pharmaceutica* **2008,** *76* (1), 77-90.
242. Arriola, N. D. A.; Chater, P. I.; Wilcox, M.; Lucini, L.; Rocchetti, G.; Dalmina, M.; Pearson, J. P.; de Mello Castanho Amboni, R. D., Encapsulation of stevia rebaudiana Bertoni aqueous crude extracts by ionic gelation – Effects of alginate blends and gelling solutions on the polyphenolic profile. *Food Chemistry* **2019,** *275*, 123-134.
243. Kim, J. H.; Park, S.; Kim, H.; Kim, H. J.; Yang, Y.-H.; Kim, Y. H.; Jung, S.-K.; Kan, E.; Lee, S. H., Alginate/bacterial cellulose nanocomposite beads prepared using Gluconacetobacter xylinus and their application in lipase immobilization. *Carbohydrate Polymers* **2017,** *157*, 137-145.
244. Zhang, J.-Y.; Tian, X.; He, T.; Zaman, S.; Miao, M.; Yan, Y.; Qi, K.; Dong, Z.; Liu, H.; Xia, B. Y., In situ formation of Ni 3 Se 4 nanorod arrays as versatile electrocatalysts for electrochemical oxidation reactions in hybrid water electrolysis. *Journal of Materials Chemistry A* **2018,** *6* (32), 15653-15658.
245. Mohamadnia, Z.; Zohuriaan-Mehr, M.; Kabiri, K.; Jamshidi, A.; Mobedi, H., pH-sensitive IPN hydrogel beads of carrageenan-alginate for controlled drug delivery. *Journal of Bioactive Compatible Polymers* **2007,** *22* (3), 342-356.
246. Csernatoni, F.; Pop, R. M.; Romaciuc, F.; Fetea, F.; Pop, O.; Socaciu, C., Sea buckthorn juice, tomato juice and pumpkin oil microcapsules/microspheres with health benefit on prostate disease–obtaining process, characterization and testing properties. *Romanian Biotechnological Letters* **2018,** *23* (1), 13214-13224.
247. Fareez, I. M.; Lim, S. M.; Mishra, R. K.; Ramasamy, K., Chitosan coated alginate–xanthan gum bead enhanced pH and thermotolerance of Lactobacillus plantarum LAB12. *International Journal of Biological Macromolecules* **2015,** *72*, 1419-1428.
248. Singh, R.; Singh, D., Radiation synthesis of PVP/alginate hydrogel containing nanosilver as wound dressing. *Journal of Materials Science: Materials in Medicine* **2012,** *23* (11), 2649-2658.
249. Shi, J.; Alves, N. M.; Mano, J. F., Chitosan coated alginate beads containing poly (N‐isopropylacrylamide) for dual‐stimuli‐responsive drug release. *Journal of Biomedical Materials Research Part B: Applied Biomaterials: An Official Journal of The Society for Biomaterials, The Japanese Society for Biomaterials, and The Australian Society for Biomaterials and the Korean Society for Biomaterials* **2008,** *84* (2), 595-603.
250. Mahdavinia, G. R.; Rahmani, Z.; Karami, S.; Pourjavadi, A., Magnetic/pH-sensitive κ-carrageenan/sodium alginate hydrogel nanocomposite beads: preparation, swelling behavior, and drug delivery. *Journal of Biomaterials Science, Polymer Edition* **2014,** *25* (17), 1891-1906.
251. Cao, J.; Wang, Y.; Wang, L.; Yu, F.; Ma, J., Na3V2(PO4)3@C asfaradaic electrodes in capacitive deionization for high-performance desalination. *Nano Letters* **2019,** *19* (2), 823-828.

252. Zhang, Z.; Zhang, R.; Chen, L.; Tong, Q.; McClements, D. J., Designing hydrogel particles for controlled or targeted release of lipophilic bioactive agents in the gastrointestinal tract. *European Polymer Journal* **2015,** *72*, 698-716.
253. Celus, M.; Kyomugasho, C.; Van Loey, A. M.; Grauwet, T.; Hendrickx, M. E., Influence of pectin structural properties on interactions with divalent cations and its associated functionalities. *Comprehensive Reviews in Food Science and Food Safety* **2018,** *17* (6), 1576-1594.
254. Sadeghi, M., Synthesis of a biocopolymer carrageenan-g-poly (AAm-co-IA)/montmorilonite superabsorbent hydrogel composite. *Brazilian Journal of Chemical Engineering* **2012,** *29* (2), 295-305.
255. Cammarota, G.; Ianiro, G.; Cianci, R.; Bibbò, S.; Gasbarrini, A.; Currò, D., The involvement of gut microbiota in inflammatory bowel disease pathogenesis: Potential for therapy. *Pharmacology & Therapeutics* **2015,** *149*, 191-212.
256. Sanders, M.; Merenstein, D.; Merrifield, C.; Hutkins, R., Probiotics for human use. *Nutrition bulletin* **2018,** *43* (3), 212-225.
257. Warnakulasuriya, S. N.; Nickerson, M. T., Review on plant protein–polysaccharide complex coacervation, and the functionality and applicability of formed complexes. *Journal of the Science of Food Agriculture* **2018,** *98* (15), 5559-5571.
258. Zuanon, L. A. C.; Malacrida, C. R.; Telis, V. R. N., Production of turmeric oleoresin microcapsules by complex coacervation with gelatin–gum Arabic. *Journal of Food Process Engineering* **2013,** *36* (3), 364-373.
259. Abd El-Salam, M. H.; El-Shibiny, S., Preparation and properties of milk proteins-based encapsulated probiotics: a review. *Dairy Science & Technology* **2015,** *95* (4), 393-412.
260. Liu, S.; Low, N. H.; Nickerson, M. T., Effect of pH, salt, and biopolymer ratio on the formation of pea protein isolate− gum Arabic complexes. *Journal of Agricultural Food Chemistry* **2009,** *57* (4), 1521-1526.
261. Qi, X.; Simsek, S.; Chen, B.; Rao, J., Alginate-based double-network hydrogel improves the viability of encapsulated probiotics during simulated sequential gastrointestinal digestion: Effect of biopolymer type and concentrations. *International Journal of Biological Macromolecules* **2020,** *165*, 1675-1685.
262. Stone, A. K.; Teymurova, A.; Chang, C.; Cheung, L.; Nickerson, M. T., Formation and functionality of canola protein isolate with both high- and low-methoxyl pectin under associative conditions. *Food Science and Biotechnology* **2015,** *24* (4), 1209-1218.
263. Moschakis, T.; Biliaderis, C. G., Biopolymer-based coacervates: Structures, functionality and applications in food products. *Current Opinion in Colloid & Interface Science* **2017,** *28*, 96-109.
264. Pillai, P. K. S.; Stone, A. K.; Guo, Q.; Guo, Q.; Wang, Q.; Nickerson, M. T., Effect of alkaline de-esterified pectin on the complex coacervation with pea protein isolate under different mixing conditions. *Food Chemistry* **2019,** *284*, 227-235.
265. Thakur, D.; Jain, A.; Ghoshal, G.; Shivhare, U. S.; Katare, O. P., Microencapsulation of β-carotene based on casein/guar gum blend using zeta potential-yield stress phenomenon: an approach to enhance photo-stability and retention of functionality. *AAPS PharmSciTech* **2017,** *18* (5), 1447-1459.
266. Liu, J.; Shim, Y. Y.; Shen, J.; Wang, Y.; Reaney, M. J. T., Whey protein isolate and flaxseed (Linum usitatissimum L.) gum electrostatic coacervates: Turbidity and rheology. *Food Hydrocolloids* **2017,** *64*, 18-27.

267. Raei, M.; Rafe, A.; Shahidi, F., Rheological and structural characteristics of whey protein-pectin complex coacervates. *Journal of Food Engineering* **2018,** *228*, 25-31.
268. Espinosa-Andrews, H.; Sandoval-Castilla, O.; Vázquez-Torres, H.; Vernon-Carter, E. J.; Lobato-Calleros, C., Determination of the gum Arabic–chitosan interactions by Fourier Transform Infrared Spectroscopy and characterization of the microstructure and rheological features of their coacervates. *Carbohydrate Polymers* **2010,** *79* (3), 541-546.
269. Li, X.; Fang, Y.; Phillips, G. O.; Al-Assaf, S., Improved sugar beet pectin-stabilized emulsions through complexation with sodium caseinate. *Journal of Agricultural and Food Chemistry* **2013,** *61* (6), 1388-1396.
270. Matia-Merino, L.; Lau, K.; Dickinson, E., Effects of low-methoxyl amidated pectin and ionic calcium on rheology and microstructure of acid-induced sodium caseinate gels. *Food Hydrocolloids* **2004,** *18* (2), 271-281.
271. Curley, D. M.; Kumosinski, T. F.; Unruh, J. J.; Farrell, H. M., Changes in the secondary structure of bovine casein by fourier transform infrared spectroscopy: Effects of calcium and temperature. *Journal of Dairy Science* **1998,** *81* (12), 3154-3162.
272. Synytsya, A.; Čopíková, J.; Matějka, P.; Machovič, V., Fourier transform Raman and infrared spectroscopy of pectins. *Carbohydrate Polymers* **2003,** *54* (1), 97-106.
273. Posé, S.; Kirby, A. R.; Mercado, J. A.; Morris, V. J.; Quesada, M. A., Structural characterization of cell wall pectin fractions in ripe strawberry fruits using AFM. *Carbohydrate Polymers* **2012,** *88* (3), 882-890.
274. Li, Y.; Zhang, X.; Zhao, Y.; Ding, J.; Lin, S., Investigation on complex coacervation between fish skin gelatin from cold-water fish and gum arabic: Phase behavior, thermodynamic, and structural properties. *Food Research International* **2018,** *107*, 596-604.
275. Souza, C. J. F.; Garcia-Rojas, E. E., Interpolymeric complexing between egg white proteins and xanthan gum: Effect of salt and protein/polysaccharide ratio. *Food Hydrocolloids* **2017,** *66*, 268-275.
276. Yuan, Y.; Wan, Z.-L.; Yang, X.-Q.; Yin, S.-W., Associative interactions between chitosan and soy protein fractions: Effects of pH, mixing ratio, heat treatment and ionic strength. *Food Research International* **2014,** *55*, 207-214.
277. Kanha, N.; Regenstein, J. M.; Surawang, S.; Pitchakarn, P.; Laokuldilok, T., Properties and kinetics of the in vitro release of anthocyanin-rich microcapsules produced through spray and freeze-drying complex coacervated double emulsions. *Food Chemistry* **2021,** *340*, 127950.
278. Costa, A. M. M.; Nunes, J. C.; Lima, B. N. B.; Pedrosa, C.; Calado, V.; Torres, A. G.; Pierucci, A. P. T. R., Effective stabilization of CLA by microencapsulation in pea protein. *Food Chemistry* **2015,** *168*, 157-166.
279. Subtil, S. F.; Rocha-Selmi, G. A.; Thomazini, M.; Trindade, M. A.; Netto, F. M.; Favaro-Trindade, C. S., Effect of spray drying on the sensory and physical properties of hydrolysed casein using gum arabic as the carrier. *Journal of Food Science and Technology* **2014,** *51* (9), 2014-2021.
280. Tao, T.; Ding, Z.; Hou, D.; Prakash, S.; Zhao, Y.; Fan, Z.; Zhang, D.; Wang, Z.; Liu, M.; Han, J., Influence of polysaccharide as co-encapsulant on powder characteristics, survival and viability of microencapsulated Lactobacillus paracasei Lpc-37 by spray drying. *Journal of Food Engineering* **2019,** *252*, 10-17.

281. Rajam, R.; Karthik, P.; Parthasarathi, S.; Joseph, G. S.; Anandharamakrishnan, C., Effect of whey protein – alginate wall systems on survival of microencapsulated Lactobacillus plantarum in simulated gastrointestinal conditions. *Journal of Functional Foods* **2012,** *4* (4), 891-898.
282. Kalita, D.; Saikia, S.; Gautam, G.; Mukhopadhyay, R.; Mahanta, C. L., Characteristics of synbiotic spray dried powder of litchi juice with Lactobacillus plantarum and different carrier materials. *LWT* **2018,** *87*, 351-360.

## APPENDIX

**Table A-1.** The change of viable *Lactobacillus rhamnosus* GG (LGG) cells in microcapsules during the simulated sequential gastrointestinal digestion.

| Code of sample | Viable LGG cells (Log CFU/g) | | | | |
|---|---|---|---|---|---|
| | **0h** | **1h** | **2h** | **3h** | **4.5h** |
| **C5-S** | 9.19 ± 0.49 A | 8.82 ± 0.55 A | 8.49 ± 0.88 A | 7.60 ± 0.87 A | 7.00 ± 0.61 A |
| **C2-S** | 9.10 ± 0.53 A | 8.39 ± 0.79 A | 8.23 ± 1.29 A | 7.48 ± 0.71 A | 6.31 ± 1.05 AB |
| **P5-S** | 9.55 ± 0.47 A | 9.06 ± 0.21 A | 8.59 ± 0.08 A | 7.97 ± 0.06 A | 7.79 ± 0.28 A |
| **P2-S** | 9.09 ± 0.90 A | 8.68 ± 0.18 A | 8.45 ± 0.45 A | 7.86 ± 0.46 A | 7.54 ± 0.19 A |
| **C5-F** | 9.81 ± 0.26 A | 8.96 ± 0.34 A | 8.70 ± 0.31 A | 6.63 ± 0.65 A | 6.08 ± 0.94 ABC |
| **C2-F** | 9.72 ± 0.24 A | 8.71 ± 0.41 A | 8.56 ± 0.51 A | 6.99 ± 0.41 A | 6.75 ± 0.17 A |
| **P5-F** | 8.63 ± 0.84 A | 6.46 ± 0.20 B | 5.47 ± 0.09 B | 4.61 ± 0.33 B | 4.10 ± 0.66 C |
| **P2-F** | 8.30 ± 0.93 A | 6.08 ± 0.18 B | 4.88 ± 0.38 B | 4.33 ± 0.33 B | 4.15 ± 0.86 BC |

The values with different superscript letters within the same column are significantly different ($p < 0.05$).